IMPERIAL COLLEGE OF SCIENCE TECHNOLOGY AND MEDICINE

University of London

DISBOND DETECTION IN ADHESIVE JOINTS USING LOW-FREQUENCY ULTRASOUND

by

Jonathan Mark Allin

A thesis submitted to the University of London for the degree of

Doctor of Philosophy

May 2002

Department of Mechanical Engineering

Imperial College of Science Technology and Medicine

London

SW7 2BX

Abstract

Adhesive use in the automotive industry is limited by a lack of suitable non-destructive testing methods. Ultrasonic methods have been used successfully in some applications. However, current techniques cannot be used in the automotive industry due to large variations in the thickness of the attenuative adhesive and the need for couplant-free testing.

This thesis details the development of a novel ultrasonic technique for the detection of disbonds in the automotive industry, based on the fundamental through-thickness resonance (mode 1) frequency of the joint. For a specified range of adhesive thickness in a bonded joint, a corresponding range of mode 1 frequencies can be predicted. Where the joint is disbonded these frequencies are much higher. During testing, the mode 1 resonance is excited in the joint and the received signal is windowed, leaving the ringing of the first mode. If the frequency of this resonance falls into the range known for bonded joints, then the bond integrity is confirmed. Further investigation has shown that narrow beads of adhesive and tapered adhesive layers, which commonly occur in practice, do not affect the reliability of this technique.

In order to make spot measurements of the bond condition, a novel dry-contact dabber probe was developed. This comprises a low loss rubber delay line with a highly attenuative rubber bonded to the side walls to eliminate side wall reflections. This allowed results to be successfully collected in the factory.

Testing a wide range of adhesive thicknesses requires a very wide band, well damped, low frequency transducer. Such devices are not commercially available, which led to the development of a novel non-resonant transducer. The device is constructed from small undamped piezo-electric elements bonded to a thin membrane. It operates below the first resonance mode and provides an operating frequency range of 200-500kHz.

Acknowledgements

Firstly, I would like to offer my sincere gratitude to my supervisors, Professor Peter Cawley and Dr. Mike Lowe, for their help and guidance, and for their support and patience.

My thanks extends to everyone involved with the project from Nottingham University, Bristol University, and NDT Solutions Ltd. for their input and help with this work. I would also like to thank Satish Chauhan, Jeff Kapp, and Roger Davies for their contributions, especially providing the industrial samples and a view of automotive manufacturing from the inside.

I am also indebted to my colleagues in the NDT group at Imperial College for their help and advice.

Lastly, I would like to thank my family for their encouragement and infinite patience, and in particular my wife, Jules, for her strength and reassurance.

This work was funded by the EPSRC, Alcan, British Aerospace, and a major UK automotive manufacturer.

Table of contents

List of figures

List of tables

Nomenclature & Terminology

A	Attenuation
a	Contact area
c	Compression wave velocity
D	Transducer diameter
E	Young's modulus
$E´$	Apparent modulus
F	Force
$K´´$	Specific stiffness
k	Spring stiffness
λ	Wavelength
m	Mass
N	Extent of near field
ν	Poisson's ratio
$\ddot{p}$	Peak amplitude
P	Contact pressure
P_0	Maximum contact pressure
R	Reflection coefficient
r	Radius
ρ	Density
Q	Quality factor
T_f	Time between front face reflections
T_w	Maximum window length
T_e	Time for response of transducer to die away
t	Layer thickness
W	Half width of soundfield beam
ω_n	Fundamental thickness resonance frequency
x	Displacement
Z	Impedance

Subscript a	Adhesive layer
Subscript m	Metal adherend
Front adherend	Adherend nearest to transducer
Rear adherend	Adherend furthest from transducer
Full disbond	No contact between front adherend and adhesive
Partial disbond	No contact between rear adherend and adhesive
Disbond	General term for fully disbonded or partially disbonded joint
Bondline	Adhesive layer
Front bondline	Interface between adhesive layer and front adherend
Rear bondline	Interface between adhesive layer and rear adherend
Acoustic thickness	Time taken for wave to propagate through a layer
F1,F2	First and second front face reflections
FB_n	n^{th} reflection from front bondline
RB_n	n^{th} reflection from rear bondline

Chapter 1

Introduction and industrial background

Adhesive use in the automotive industry now extends to structural joints and a robust bond inspection system is required. This chapter provides some background to automotive adhesive use and applications, and discusses the requirements for an automotive non-destructive testing (NDT) system.

1.1. Adhesives in the automotive industry

Automotive body shells have been made almost exclusively from steel for many years. Recently, growing environmental pressures to reduce fuel consumption and exhaust emissions have led automotive manufacturers to shift from steel to aluminium for body shell construction in order to reduce vehicle weight [1]. Several challenges have been faced with this change of material, not least finding a suitable method to join the panels.

1.1.1 Techniques for joining aluminium

In conventional body shell construction pressed steel sheet body panels are joined using resistance spot-welding. This gives a fast, versatile, and effective means of joining the panels and is well suited to automated high volume production environments. Welding aluminium is more difficult than steel due to the natural surface oxide layer which has a much higher melting point than the parent metal and must be broken down during welding [2]. Spot-welding aluminium [3] requires currents and electrode clamping forces to be approximately twice as large as for steel in order to rapidly breakdown this oxide layer. This results in higher capital equipment costs, bulkier weld guns, more frequent electrode tip dressing, and is therefore much less attractive than spot-welding steel. Liquid welding techniques, such as MIG (Metal Inert Gas), TIG (Tungsten Inert Gas) and laser welding, are also less attractive for aluminium than steel, but are nevertheless used by some manufacturers producing body shells based on an extruded spaceframe approach, rather than the conventional monocoque structure; the arc-welding techniques are more prone to weld cracking, thermally induced distortion, and a large heat affected zone; although laser welding offers significant improvements [4], it attracts a high capital cost. Recently, techniques

such as solid state friction stir welding have been developed to overcome these problems but are not currently viable for automotive applications. Most manufacturers are therefore beginning to use adhesives to join the panels [5, 6].

Adhesives are now common-place in non-structural applications [7], for example in fixing windscreens, trim, and vibration damping panels. They offer many advantages [1] over mechanical fastenings and welding which they are beginning to replace, notably:

- More uniform stress distribution over the length of the joint.
- Improved fatigue and impact performance.
- Increased joint stiffness.
- Increased vibration damping.
- Sealing to prevent water ingress and galvanic corrosion of dissimilar metals.
- Fixings not visible on surface and distortion from high temperatures inherent with welding is avoided.
- Allows complex shapes and dissimilar materials to be joined with ease.
- Low cost joining method, although dispensing equipment and maintenance costs can be high.

The increase in torsional stiffness gained through adhesive bonding is particularly attractive for the automotive industry [8] and manufacturers of conventional steel body shells are now adding adhesives (through which spot welds can be made) into the joints for just this reason.

Whilst they offer many advantages over welding, there are concerns about the effect of environmental degradation on the long term performance of adhesives; this in an on-going area of research [9]. Their major drawback, however, is inherently low peel strength compared to mechanical fastenings and welding. Although peel stresses can be minimised through careful design and by using lap shear joints which minimise stress concentrations at the ends of joints, a lack of confidence within the industry and uncertainty about their long term performance are responsible for reluctance to use adhesives as the sole joining method in structural applications. As a result, fastenings such as rivets or spot-welds are used in conjunction with the adhesive. The unique advantages of adhesive bonding can then be utilised with an increased peel strength and safety factor.

1.1.2 Adhesive use in the automotive industry

Before aluminium can be bonded successfully, the natural surface oxide must be removed or modified by pre-treating the surface [10]. This increases surface wetting and adhesion. Pre-treatments range from surface abrasion to anodising, and increase in cost and complexity with the effectiveness of the treatment. Chromic acid anodising, for example, provides an excellent surface for bonding and increases resistance to environmental attack which helps prevent premature joint failure, but is a lengthy and costly process. Most pre-treatments have a limited shelf life, and any contaminants must usually be removed prior to bonding. This is not practical for the automotive industry, so special pre-treatments have been developed. For example, Alcan [8, 11] have developed a process where a chemical etch is applied to the coiled aluminium sheet after rolling, followed by a specially developed press forming lubricant; the surface treatment remains stable for up to one year.

Adhesives have been developed which are compatible with the press forming lubricant, absorbing limited amounts, and can therefore be applied directly to the panels without degreasing. Studies have shown that adhesive lap shear strength is unaffected by the lubricant, even when applied in excess [8].

Typically, single part epoxy adhesives [7] are used for body shell construction in the automotive industry, and are applied to the joint as a uniform bead either manually or robotically [12]. The adhesive is placed so that none is visible on the outer edge of the joint when formed. The desired placement of adhesive after a typical joint is formed is shown in figure 1·1.

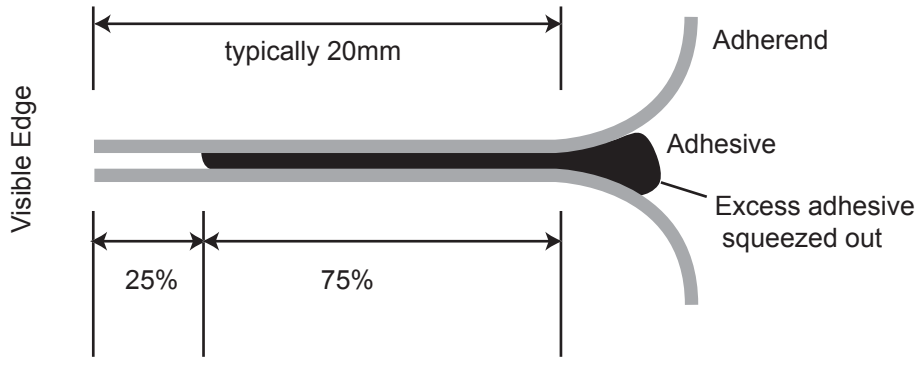

Figure 1·1 Cross-section through joint flanges showing optimum adhesive placement.

Significant variation in adhesive layer, or 'bondline' thickness can result from variability in the fit of panels and local distortion of the aluminium around the rivets. This variation depends on the geometry of the mating panels, manufacturing tolerances and the assembly process. An example of the distortion of two mating flanges around the rivets causing considerable bondline thickness variation is shown in figure 1·2.

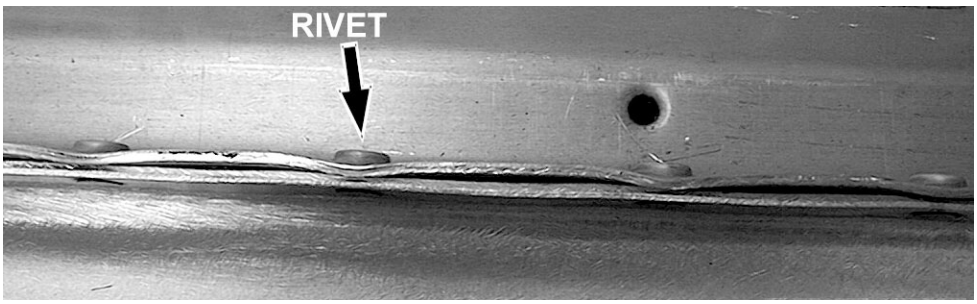

Figure 1·2 An example of panel distortion around rivets.

The use of rivets in conjunction with bonding ('riv-bonding') not only increases joint strength, but holds the structure together before cure. Self-piercing rivets and clinch joints [13] are used in the majority of joints where there is access to both sides of the joint, providing a fast, low cost, reliable fixing. Where access is limited to one side, self drilling rivets and pop-rivets can be used. In situations where rivets would otherwise be visible, adhesive bonded clinch flanges are often used, for example in fixing door skins [14]; the adhesive is applied prior to the flange being formed and is induction cured (steel doors), or a two-part room temperature adhesive is used (aluminium doors) to prevent slipping during assembly.

After application, the adhesive must remain in the joint throughout the assembly and paint preparation processes, and must remain slump resistant even at cure temperatures. The curing process takes place in paint ovens after the completed body shell has been degreased and primed. A typical cure cycle is 180°C for 30 minutes.

1.1.3 Adhesively bonded joint defects

Defects in adhesive joints [15] occur either at the adherend-adhesive interface, or within the adhesive layer itself. A summary of these defects is shown in figure 1·3.

The adhesive ('interfacial') strength at the interface between the adhesive and adherend layers is critical to the overall joint strength, but is difficult to measure non-destructively. A lack of adhesion can generally be attributed to poor preparation of the adherend surface. Suitable pre-treatments, appropriate for the service conditions and

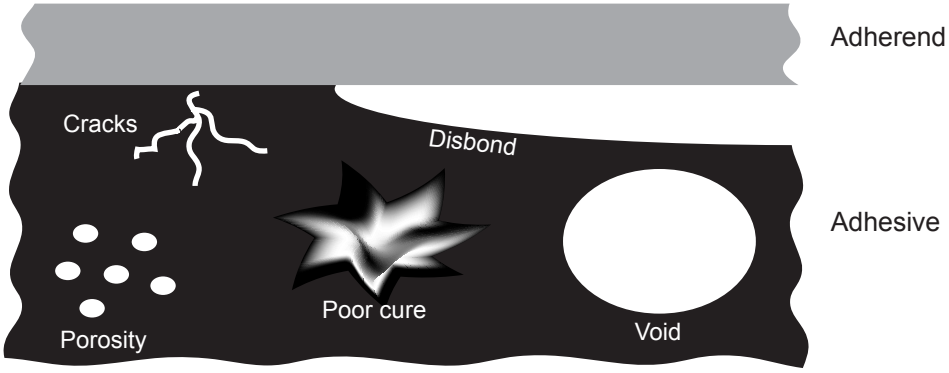

Figure 1·3 Common defects in adhesive joints (after Adams [15]).

which are compatible with the adhesive, give improved adhesion and are particularly important for bonding aluminium. However, any surface contamination, such as grease, remaining after cleaning and pre-treating will usually result in poor adhesion. For automotive use, pre-treatments and adhesives have been designed for compatibility and to tolerate pressing oil, and so provided there are no other sources of contamination and the panels are bonded before the shelf life of the pre-treatment expires, adhesion should be good.

Although deterioration (leading to the formation of disbonds in service) at the interface can result from environmental degradation, accelerated aging tests have shown that excellent performance is obtained with the latest generation of automotive pre-treatments and adhesives, without degreasing prior to adhesive application [8]. In practice, any degradation through water ingress into the joint is held back by application of sealants and paint to critical joints.

Within the adhesive layer, large defects such as gross voids and disbonds can occur where insufficient adhesive has been applied, or where it is placed incorrectly trapping air in the joint. Low joint strength can result where a narrow bead of adhesive along the joint has been dispensed. Excessive amounts of surface contamination, or the formation of a skin on uncured adhesive which as been left for excessive amounts of time before bonding, can also result in disbonds. Where there is no physical gap between the adhesive and adherend, but little or no strength in the bond, zero-volume disbonds or 'kissing bonds' [16, 17]] are formed. These are generally caused by contamination, resulting in very low adhesion.

Defects which occur principally during the cure cycle can lead to a reduction in the cohesive strength of the adhesive layer. The cure state is a major factor and significantly affects the strength of the bulk material; under cured or over cured adhesive will have reduced cohesive strength. Air introduced when mixing and contaminants present during cure may vaporise leading to porosity and voids, but this does not seem to be a problem with the viscous one-part epoxies. Rapid fluctuations in temperature or thermal shock may lead to cracks, as could a mechanical shock loading, although again this is unlikely with the toughened epoxies used in the automotive industry. Finally, incorrect mixing (where applicable) and storage of the adhesive can also lead to a reduction in cohesive strength.

1.1.4 Terminology used in this thesis relating to bond condition

It is appropriate at this point to define the terms used throughout this thesis, which can be found to have different meaning in the literature. The general term ‘disbond’ refers to fully disbonded and partially disbonded joints. The term ‘full disbond’ is used where there is a complete lack of adhesive on the front adherend in the region under test (i.e. top adherend only). ‘Front adherend’ and ‘rear adherend’ refer to the adherends closest and furthest from the transducer respectively. The term ‘partial bond’ is used where there is no contact between the adhesive and rear adherend, so that adhesive is bonded to the front adherend only. This should not be confused with a weak interface as is sometimes termed in the literature. Throughout the thesis, the term ‘bondline’ is used interchangeably for the adhesive layer, and the terms front bondline and rear bondline refer to the interface between adhesive and the front and rear adherends respectively.

1.1.5 Quality assurance of bonded joints: Current practices in the automotive and aerospace industries.

With adhesives being used in safety critical applications, quality assurance (QA) to determine the integrity of the joint is essential. Currently, automotive QA is achieved in two ways: destructive testing of a random sample of completed body shells, and the production of test samples (‘coupons’) which are produced alongside a body shell and destructively tested providing a simple check on the production processes. Testing of the coupons is less expensive, but does not provide a direct indication of the condition of joints in the body shell. Clearly, there is a real need for a suitable NDT technique to assess the bond condition.

Adhesive bonding of structural components is commonplace in the aerospace industry for example, where considerable experience in their use has been built up. There are, however, significant differences between the aerospace and automotive industries which limits the degree of synergy possible between the two sectors. In aerospace, bond quality is ensured through tight process control [18]; complex surface pre-treatments, such as phosphoric acid anodising, are used to increase resistance to environmental attack and increase adhesion, but this is an expensive, time consuming and environmentally unfriendly process which has a short shelf-life prior to bonding. Adhesive application is also significantly different: high performance epoxies and phenolics have been developed for aerospace applications which are applied in film form and contain scrims to control the bondline thickness and flow during cure. Joints are heat cured under pressure in a carefully controlled cure cycle. Some NDT is also carried out depending on the application (see chapter 2). Various techniques which have proved reliable in the aerospace industry [19, 20] include bond testers, C-scans using ultrasonic time domain methods, holography/shearography, and thermography. The effectiveness of this rigorous quality control has been borne out by exposure in harsh environments for many years, without any serious disbonding problems. Unfortunately this level of process control is unsuited and too expensive to be employed by the automotive sector which instead has tried to develop adhesives to fit in with existing production processes. In the next section, the automotive requirements are set out.

1.1.6 Automotive non-destructive testing requirements

The development of suitable pre-treatments and the use of adhesives which absorb oil has reduced the likelihood of interfacial defects in the automotive industry. The primary areas of concern are therefore the detection of disbonds, and achieving the optimum cure state in joints throughout the vehicle. Disbonds and narrow beads of adhesive are most likely to occur through incorrect adhesive application, or movement after application. This can be caused by human error where adhesive is applied manually, or by clogged dispensing equipment, for example, when applied by robot. Concern about adhesive curing arises from the non-uniform heating of joints in different parts of the oven. An insight into the cure state of different joints is best achieved by in-process cure monitoring inside the paint oven; this is the subject of other research [21]. These measurements would be made at different stage in the

production process and it is not appropriate to attempt to combine an NDT system for cure monitoring and disbond detection. Thus the work in this thesis focuses on the development of a robust technique for the detection of disbonds.

An NDT technique capable of meeting the QA requirement must obviously be well suited to the demanding technical and production requirements of the automotive industry. A suitable NDT system must be able to detect and give a positive identification that the joint is fully bonded; it is not sufficient just to look for diagnostic signals produced where a joint is disbonded. Testing is required when the adhesive has been cured after the body shell primer paint bake cycle. In order to prevent contamination of the paint film prior to topcoat painting, no couplants or water can be used for the NDT. Access can be limited, especially where two panels are at right angles, and the majority of the joints requiring testing can only be accessed easily from one side (e.g. around the floorpan area). In order to enable integration into a high volume production environment, testing must be rapid, and offer the flexibility for automation. In the body shells studied, 'Henrob' rivets have been used which are flush on one side of the joint. This is advantageous since a device could be used to scan across the joint surface, if required, without becoming fouled on the rivet heads. Low cost, both in terms capital expenditure and day-to-day operation, is also an important factor in the selection of a NDT system for the automotive industry which operates to relatively low margins. Techniques requiring costly safety measures or highly skilled operators would therefore be undesirable.

The majority of bonded joints in automotive structures are 3 layer (metal-adhesive-metal) and have therefore been selected as the focus for this work. The geometry of the joints can be quite complex and often includes curved sections. Automotive joints have relatively thin sheet metal adherends, with thicknesses generally ranging from 0.7mm to 1.5mm in steel body shells, and 1.0 to 3.0mm in aluminium structures. Perhaps the most common panel thicknesses are 0.9mm and 2.0mm for steel and aluminium respectively. The variability of fit between the pressed body panels discussed in section 1.1.2 can result in bondline thicknesses up to 3.0mm and down to 0.1mm, especially close to the mechanical fastenings which pinch the panels tightly together. In critical structural joints, the maximum permissible bondline thickness range is relatively small since the cohesive strength of the joint is reduced at thick bondlines, and has been specified as 0.1-0.4mm by the manufacturers. An example of an automotive joint which requires testing is shown in figure 1·4.

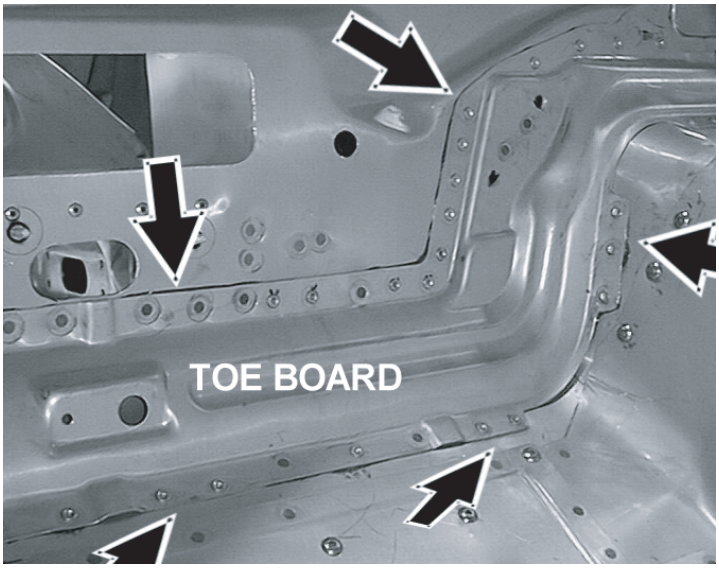

Figure 1·4 Example of a bonded joint in an automotive structure. Bonded joints indicated with arrows.

1.2. Project aims

The objective of this work is to develop an NDT system to provide a fast, cheap, reliable way to check the quality of automotive bonded joints in-process. This will replace the destructive random sampling currently carried out, resulting in cost savings whilst increasing the quality of the product. The system will have the capability to map out the bond condition (detecting 'disbonds') and bondline thickness along a joint and hence also provide a means to optimise the bonding and assembly processes to achieve optimum quantity and placement of adhesive. This will lead to reduced in-process testing in the longer term.

The motivation and requirements for this work have been provided by a major automotive maufacturer, and the primary aim is to develop a suitable system to the point where it is ready for implementation in the factory. Consideration will also be given to making the system as generic as possible for testing adhesively bonded structures.

1.3. Outline of thesis

The complex geometries and variable thickness bondlines typically found on automotive structures, in conjunction with the requirement for robust, low cost, couplant free testing are primarily responsible for precluding the use of any existing NDT techniques. Current adhesive bond testing techniques are reviewed in chapter 2,

and their suitability for automotive testing is discussed. Ultrasonic testing using the first through-thickness mode (mode 1) resonance was identified as the most attractive method for further development.

The viability of using mode 1 for automotive bond testing is assessed in chapter 3. The parameters which can be used to determine the bond condition are identified using a one-dimensional model. A signal processing algorithm is developed to extract the necessary data from the ultrasound signals, and the results of the modelling are validated using laboratory prepared joint samples.

The validity of the one-dimensional modelling used in chapter 3 for real automotive joint geometries is investigated in chapter 4. The effect of testing joints which are not one-dimensional is quantified using Finite Element analysis, and the implications for the proposed test are discussed. Transducer misalignment is also considered.

In order to make spot measurements of the bond condition on automotive structures without couplant, a novel dry contact dabber probe has been developed for use at low frequency, which is detailed in chapter 5.

Test results from a variety of prepared and real structures are presented in chapter 6. These structures do not have a wide bondline variation and can be tested with a commercially available transducer fixed to the dabber probe. Results have been correlated with independent bondline thickness measurements.

The wide variation in bondline thickness which is found in some joints requires a low frequency, wideband transducer. The absence of suitable commercially available devices has led to the development of a novel non-resonant piezoelectric transducer to meet the demanding testing requirements. Development and test results are presented in chapter 7.

In chapter 8, conclusions of the work are presented and the overall success of the project is evaluated, with consideration also given to suggestions for further development work. Lastly, the main contributions of the thesis are summarised.

Chapter 2

NDT technique suitability for automotive testing

The use of adhesives in structural applications became established over 50 years ago. Since then, many research laboratory solutions and commercial instruments have been produced to non-destructively test the quality of bonded joints. The various techniques have been the subject of numerous reviews [22-31]. In this chapter, testing techniques and their suitability for use in the automotive industry are discussed. This is not an exhaustive list, but focuses on techniques used commercially for characterisation of adhesive bonds, or which have received a large research effort. Of all the techniques presented, ultrasonics is perhaps best suited for characterising adhesive defects and is most widely used; the various ultrasonic techniques are discussed separately.

2.1. Non-ultrasonic techniques

2.1.1 Low frequency (sonic) vibration

A family of NDT techniques operating at sonic frequencies are used to detect defects in bonded structures [23, 32]. The principle of operation is common, namely that a defect in the adhesive layer will alter the local stiffness, and hence the local impedance which is measured at each test point. The techniques [33-35] include the coin-tap test, mechanical impedance method, membrane resonance and velocimetric method. These methods are attractive for use in the field because testing can be carried out quickly, and since they operate at low frequency (less than 20kHz) can be dry coupled. Each technique has its own merits, but in general they are most sensitive to large defects close to the surface where the base structure is relatively stiff, and are therefore popular for testing thin-skinned honeycomb composite aircraft structures, for example. Many commercially available bond testers are based on these techniques, for example the Acoustic Flaw detector (Model AD-42 1M – JME Ltd.) and Sonic BondMaster (Model 1000 – Staveley NDT Ltd.). However, the techniques are not sufficiently sensitive to detect defects in the adhesive layer of 3 layer automotive joints with thick adherends [32, 34, 35].

2.1.2 Optical techniques

There is a family of optical techniques which can be used to detect defects in bonded joints. In operation, the test structure is illuminated with coherent light from a laser and images are produced with the structure in the stressed and unstressed states; when

combined, an image with interference fringes is generated. In general, the displacement in the stressed state will be greatest around a defect and the fringes will be closer together. In holography, the fringes are a measure of relative surface displacement before and after deformation, but whilst very small deformations can be detected, any rigid body motion or vibration can destroy the image. Electronic speckle interferometry [36] is another technique which also measures surface displacement, but being a speckle method, larger amounts of rigid body motion can be tolerated. Shearography uses a laser based interferometer to detect displacement gradient when the structure is stressed. It is easier to set up than holography, and it is less sensitive to rigid body motion [37].

Optical techniques have advanced in recent years particularly with the ability to record images electronically, and are used for a variety of applications including disbond detection in bonded aircraft structures [38, 39]. They are particularly well suited for testing large relatively flat surfaces quickly. However, automotive joints have complex geometries with limited access, and the high cost of the equipment and facilities to stress the structure is prohibitive. Further, the sensitivity of all the methods is dependent on defect size/depth ratio which can make defects at the rear bondline interface difficult to find.

2.1.3 Thermography

Two thermographic techniques can be used to detect defects in structures by monitoring the surface temperature with an infra-red thermal imaging camera after exposure to a heat source. In transient thermography (thermal wave imaging), the structure is thermally pulsed with a heat source, such as a camera flash [37]. Defects can be identified by anomalous cooling behaviour due to a reduction in thermal diffusivity, over a disbond for example. Provided the heat input is fast enough, materials with a high thermal diffusivity such as aluminium can be tested. The technique is used successfully in the aerospace industry for disbond and corrosion detection of aluminium and composite structures [40, 41].

Steady-state thermography requires heat flow through the structure by heating on one side. Disbonds and voids have a higher thermal resistance than the surrounding material, and this will affect the steady-state surface temperature on the opposite side. Temperature differences around defects are much smaller with steady-state

thermography which makes them very difficult to detect, but there has been a suggestion that with recent advances in image processing, this technique could be suitable for automotive applications during a cooling-down period [42].

Whilst these techniques are suitable for detecting complete voids in the adhesive layer, the low thermal diffusivity of the adhesive layer would prevent rear adherend disbond detection. The capital costs and data processing requirements, especially for transient thermography, also make these techniques unattractive for automotive use.

2.1.4 Radiography

X-radiography [24, 43] is a commonly used method of NDT in which an X-ray source is placed on one side of a joint, and X-ray sensitive film or an electronic detector on the other side. Defects will affect the transmission of X-rays and will show up on the detected image. However, X-ray absorption in the aluminium adherends is much higher than the adhesive layer, and any disbonds will have negligible effect on the overall absorption. In addition, the technique is least sensitive to defects, such as disbonds, which run parallel to the surface under test.

2.1.5 Magnetic resonance imaging

This technique makes use of the magnetic properties of the nuclei of certain elements which behave like spinning bar magnets. The interaction between these nuclei and a large externally applied oscillating magnetic field then produces measurable signals which can be used to characterise the materials. This technique can provide insight into the state and composition of an adhesive layer. However, it cannot be used with metallic bonded structures [44, 45].

2.1.6 Dielectric measurements

The adhesive and surface oxide layers in an adhesively bonded joint behave as a dielectric between the conducting aluminium adherends. Application of a high frequency voltage to the adherends will cause waves to propagate along the dielectric layer and be reflected from the end of the joint. Analysis of the received waveforms in the time and frequency domains can reveal hydration of the interface layer due water ingress [46-48]. Identification of voids within the adhesive layer and measurements of the cure state [49] have also been made using this technique. Progress is being made in this field, but the technique is not commercially available, and it is unlikely that measurements can be made on the complex automotive joints, especially with the inclusion of mechanical fastenings along the joint.

2.2. Ultrasonic methods

2.2.1 Time domain bulk wave measurements

The most widely used technique for the detection of defects in structures is ultrasonic time domain measurements using compression waves at normal incidence to the structure. In a basic set-up, compression waves are generated by a transducer connected to a pulser which delivers a short duration pulse. The transducer, positioned normal to the surface, is coupled to the structure under test with a couplant, commonly gel or water. The propagation of waves within the structure can be detected in two ways, namely 'pulse-echo' or 'through-transmission' [50, 51].

2.2.1.1 Through-transmission

Through-transmission is used where both sides of a structure or joint are accessible; a receiving transducer is placed directly opposite to the transmitting transducer, on the other side of the structure. A received signal of low amplitude indicates the presence of a defect between the contact regions of the transducers. Whilst this technique can provide a simple, effective means of disbond detection in bonded joints, most automotive joints cannot easily be accessed from both sides simultaneously. Through-transmission ultrasound is therefore unsuitable for this work.

2.2.1.2 Reflections from multi-layered structures at normal incidence

Where testing is to be carried out from only one side of the structure, the pulse-echo arrangement can be used. A transducer is connected to a pulser or waveform generator, which switches to receive mode after the excitation signal has been transmitted. The output from the receiver amplifier can be connected to an oscilloscope which shows the amplitude of the reflections in the structure with time. Where sound waves pass from one medium to another, at the boundary, part of the wave is reflected and part is transmitted, as shown in figure 2·1. The amplitude of the reflected signal can be quantified [52] by the reflection coefficient (R) from material 2 to 1:

$$R_{21} = \frac{Z_1 - Z_2}{Z_1 + Z_2} \qquad (2{\cdot}1)$$

where Z_i is the acoustic impedance of the medium i, and is given by:

$$Z = \rho c \qquad (2{\cdot}2)$$

where ρ is the density and c is the bulk compression wave velocity.

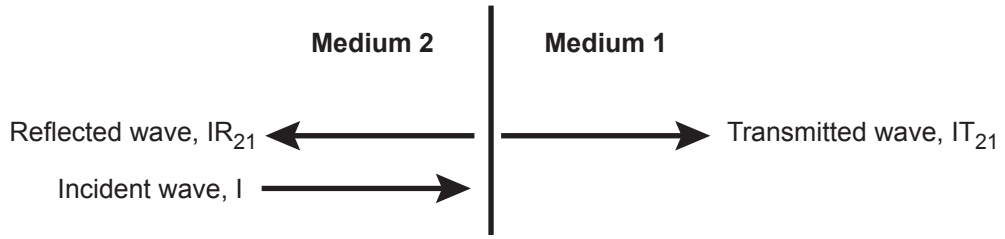

Figure 2·1 Transmission and reflection from the interface between two media.

In a simple case where a thick sheet of metal in air is being tested, defects can be easily detected. Compression waves propagate into the sheet from the transducer through the coupling medium. At the rear face, there will be a large reflection due to the large impedance mismatch between air and metal. At the front face, there is a relatively large impedance mismatch between the coupled transducer and the metal, hence the wave will again be reflected. In the absence of any well matched attenuative material, reverberations will continue for some time in the sheet. A defect, such as a crack or void, is filled with air and will introduce a large reflection, but this will occur before the first rear face reflection, indicating the presence and depth of the defect. Flaw detection carried out in this manner is dependent on the resolution of the system; individual reflections from flaws and the back face of the material must be clearly separated in time. In thin materials, a high frequency, short duration pulse is therefore required.

Time domain analysis of multilayer systems, such as adhesive joints, can be more difficult. It is convenient at this point to define the term ‘acoustic thickness’, which is the time taken for a wave to propagate across the layer (i.e. t/c). A system comprising a transducer coupled to a three layer aluminium-adhesive-aluminium joint is depicted in figure 2·2(a). The adhesive layer is 0.5mm thick and has a bulk compression wave velocity of 2300m/s. This layer is several times thinner than the 2.0mm aluminium adherends which have a velocity of 6330m/s. The ratio of acoustic thickness in the adhesive to the adherend is therefore less than unity in this case.

The transducer (omitted from the figure for clarity) is coupled to the front adherend at normal incidence and the system can be considered one-dimensional. Wave propagation through the different layers in the joint is shown varying with time (i.e. at oblique incidence) in order to illustrate the source of reflections which would be received by the transducer. Figure 2·2(b) shows the time domain waveform which would be received by a 10MHz transducer. This plot has been generated using

ultrasonic simulation software (Imagine 3D – Utex Scientific Instruments Inc.) and has the same time scale as figure 2·2(a) so that the reflections in the two figures correspond.

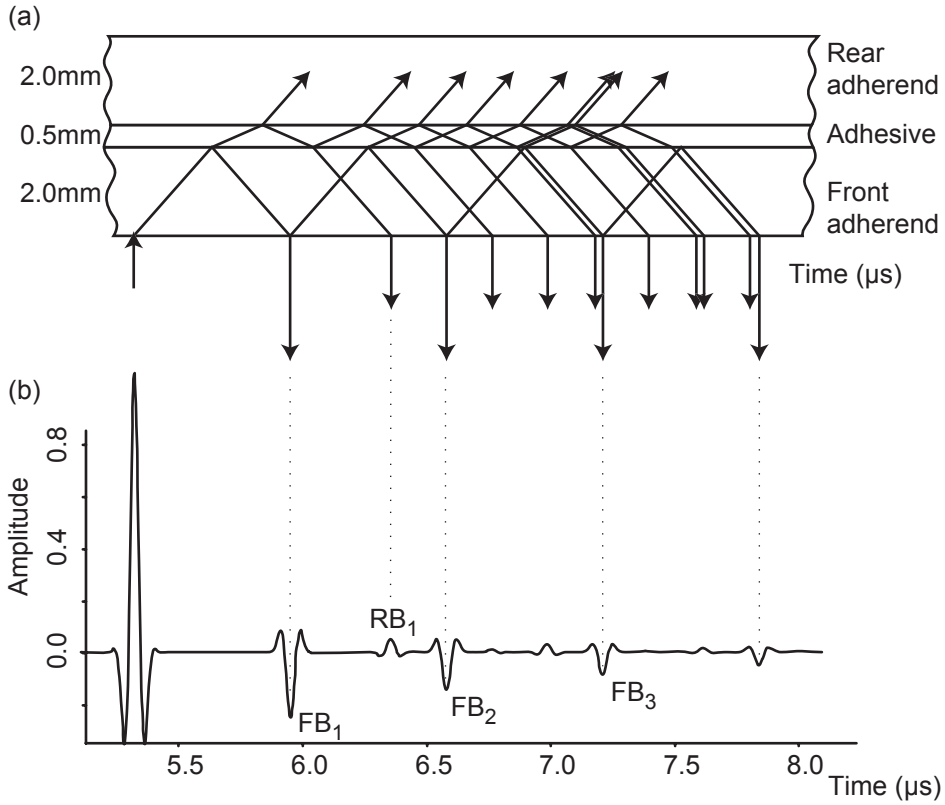

Figure 2·2 (a) Wave propagation in a 3 layer joint (rays drawn at oblique incidence for clarity) and (b) corresponding time domain waveform.

In this joint, the first rear bondline reflection (RB_1) occurs between the first two front adherend reverberations (FB_1 and FB_2), which are 0.65μs apart. In order to resolve the rear bondline echo from the front adherend reverberations, a short pulse of 10MHz was used. Figure 2·2(b) also shows the amplitudes of the various reflections. The impedance of the adhesive is 3.0MRayl, which is much lower than aluminium which has an impedance of 17.8MRayl. Using equation 2·1, only 29% of the amplitude at the aluminium-adhesive interface is transmitted into the adhesive layer. At the rear adhesive-adherend interface, 71% of the amplitude will be reflected, but after further transmission loss into the front aluminium layer, the resulting amplitude of this rear adhesive layer reflection is only 21% or -13.6dB. This value excludes the effect of attenuation in the adhesive layer. This is high in automotive adhesives; for the adhesive used in this work, which is a typical structural adhesive, a compression wave attenuation of 0.51dB/mm/MHz was measured (see appendix A). At 10MHz, the

attenuation of a signal transmitted twice through the adhesive layer is 5.1dB. Although the rear bondline reflection is low amplitude, it is detectable in this particular joint, and its presence indicates that the front adherend and adhesive layer are bonded.

Detection of the reflection from the rear of the rear adherend (furthest interface from the transducer) to confirm the presence of the rear adherend, however, is unrealistic. The amplitude of the reflection would be very small, and it would occur after the rear bondline reflection. Hence it is likely to be masked by reverberations in the other layers. Instead, the rear bond condition can be determined from the phase of the rear bondline reflection, given by the sign of the reflection coefficient in equation 2·1. At the interface between two media, the reflection is phase reversed where the impedance of the furthest layer is higher; where the wave passes from high to low impedance, the sign of the impedance is not reversed. Figure 2·3 shows a simulated time trace, similar to figure 2·2(a), but from a joint where the rear adherend is disbonded (i.e. the rear of the adhesive contacts air rather than aluminium). The phase of the rear bondline

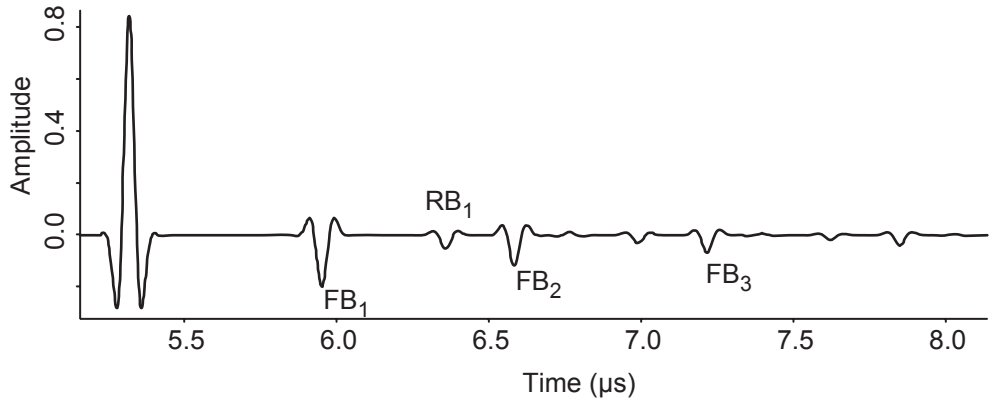

Figure 2·3 Time domain waveform of partially bonded joint showing rear bondline reflection without phase reversal.

reflection is the same as the front adherend reverberations, whereas it was reversed in figure 2·2. The amplitude of the reflection in both cases is not very different whether air or metal contacts the rear adherend. In this joint, detection of the phase of a rear bondline echo provides an effective means of identifying that the joint is fully bonded.

Unfortunately, this time domain method is only reliable within a very limited range of adhesive thickness. Two problems are encountered when the adhesive thickness is increased. First, when the ratio of acoustic thickness of the adhesive to adherend layers is close to unity (just how close depends on the pulse width, hence transducer centre frequency) the small rear bondline reflection becomes masked by the second front

adherend reverberation (FB_2). In this example, this occurs where the bondline thickness is around 0.7mm, but in steel automotive structures where adherends can be 0.7mm thin, the acoustic thickness ratio will become unity at a much smaller adhesive thickness. If the adhesive thickness is known, or relatively constant, and the acoustic thickness ratio is between 1 and 2, it may be possible to test thicker bondlines; the rear bondline reflection would then lie between the second and third front adherend reverberations. Where the adhesive thickness could be any value in a wide range, as in the automotive industry, an acoustic thickness ratio close to unity limits the maximum thickness which can be tested reliably. Secondly, at a given frequency, attenuation is proportional to adhesive thickness. At 3mm, the upper end of the adhesive thickness specification for example, the rear bondline reflection is attenuated by 30.6dB at 10MHz in the adhesive layer alone, which would render the reflection undetectable.

2.2.1.3 Adhesive presence testing

Conventional time domain analysis to detect a bonded joint is too limited for general automotive use. However, there are some non-structural applications in the automotive industry where testing for adhesive presence on the front adherend is sufficient. For example, the application of adhesive in a specific non-continuous pattern between bonnet skins and the stiffening structure has been found to eliminate flutter at high road speeds. Here NDT is required to verify that the adhesive has been applied in the correct pattern. The joint is not safety critical and the detection of voids or rear face disbonds is not required since they are less likely to occur than incorrect application. A solution to this NDT problem has been developed and implemented by Freemantle and other workers [53-56] based on the principle that the decay rate of reverberations in a metal sheet is sensitive to the impedance of the material on the rear face. At the rear face of the front adherend, where there is air present, all of the energy is reflected giving rise to a relatively low decay rate for the reverberations; if adhesive is present, some energy is transmitted into the adhesive, damping the adherend reverberations. Figure 2·4 shows the reverberations in a 2mm aluminium adherend (neglecting attenuation) with and without a thick adhesive layer. This was generated using ultrasonic simulation software (Imagine 3D – Utex Scientific Instruments Inc.) and only the adherend reverberations have been shown for clarity. The method developed by Freemantle uses an adaptive filtering technique which identifies the poles of the resonance in the metal sheet, and determines a decay parameter which is the product of the reflection

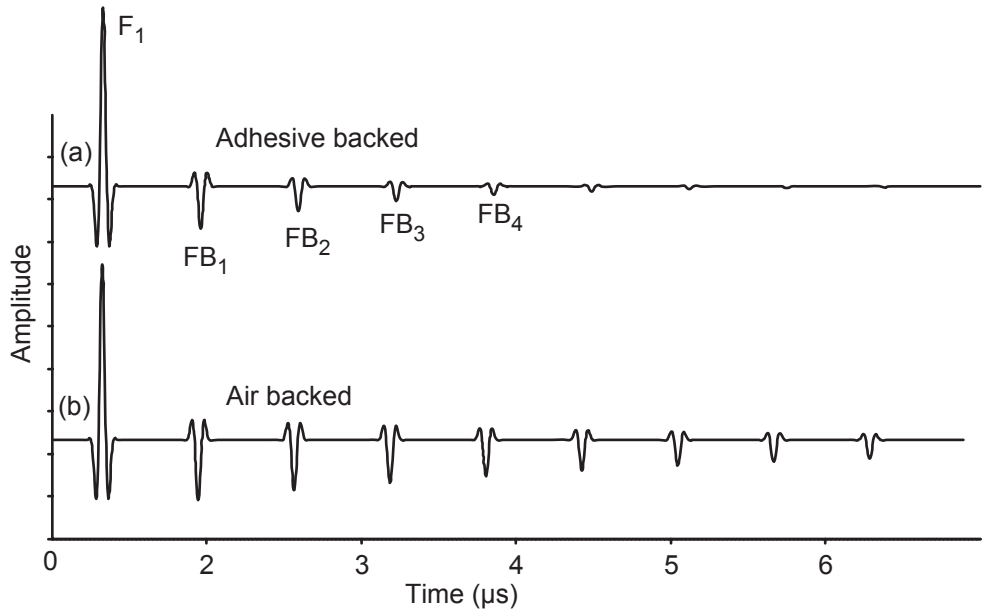

Figure 2·4 Time domain waveforms showing reverberations in a 2mm aluminium adherend with (a) adhesive and (b) air on the rear face

coefficients at the front and rear faces of the adherend. Typical decay parameter values for a steel sheet backed with air and cured adhesive are 0.75 and 0.54 respectively. This technique has proved successful in testing automotive structures in the field, and has been implemented in commercially available equipment (Automated Bond Inspection System (ABIS) – NDT Solutions Ltd.).

2.2.1.4 Enhanced detection of rear bondline interface reflections

Despite the success of this technique, the main QA requirement for this work is to ensure that joints are fully bonded. It has been demonstrated that standard pulse-echo techniques are unreliable for rear disbond detection where the acoustic thickness of the adhesive can be greater than that of the adherend. Various techniques to improve the resolution of echoes in the time domain in multilayer systems are reviewed by Freemantle [57] who concludes that these techniques are either too computationally demanding for rapid, robust testing, or introduce noise which can itself mask the diagnostic bondline echo. An alternative method has been developed [53], using an adaptive filtering technique. Based on the decay rate, the top adherend reverberations are filtered from the received signal. The resulting signal then contains only the bondline echoes, which can be analysed in the time domain in the conventional manner. Figure 2·5 shows an example of a time domain signal before and after filtering. A 1.0mm steel adherend was used, hence the front adherend reverberations are much closer together than in previous examples. The rear bondline reflection (RB_1)

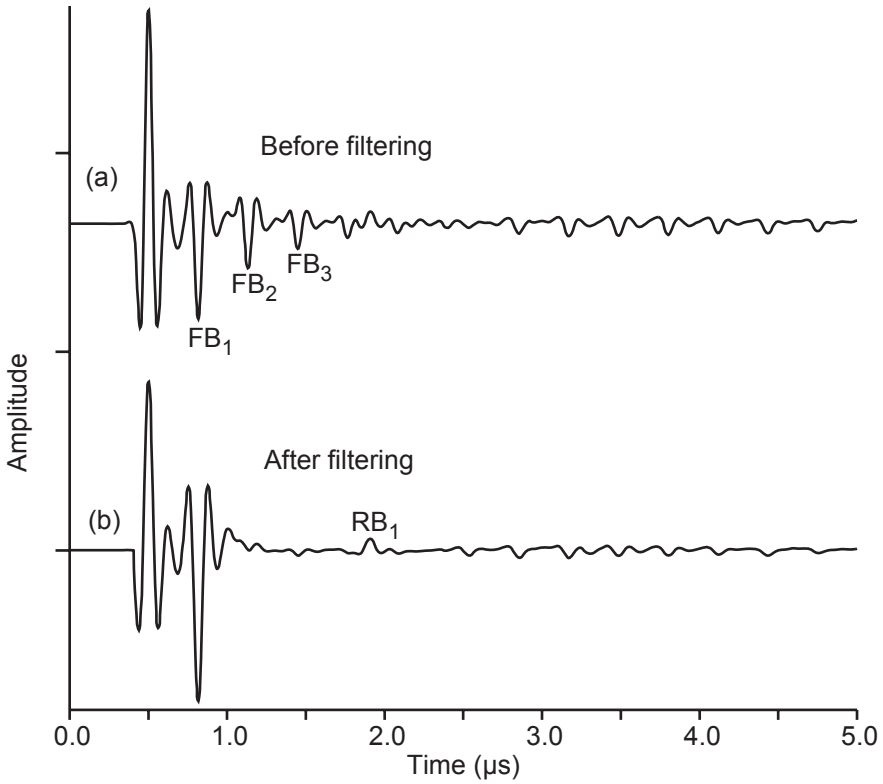

Figure 2·5 Time domain waveforms from a bonded joint with a 1.0mm steel adherend and 1.2mm bondline (a) before and (b) after adaptive filtering (reproduced from Challis et al. [53]).

is clearly visible after filtering, but is very difficult to identify in the unfiltered waveform. This technique does boast a significant improvement in the range of adhesive layer thickness which can be tested using pulse-echo, but is still limited by the attenuation of the rear bondline reflection. To date, automatic detection of this rear bondline reflection has not been implemented since robust detection is difficult with such a small reflection. The limits of testability for aluminium and steel joints with various combinations of adherend and adhesive thickness are reproduced in tables 2·1 and 2·2. This data, whilst suggesting that a wide range of adhesive thicknesses can be tested in joints with 2mm aluminium adherends, for example, does not cover the 0.1-0.4mm bondline thickness range. This would require a higher frequency transducer, which would reduce the rear bondline reflection amplitude in joints with thick adhesive layers due to the increased attenuation.

2.2.1.5 Interfacial defect detection

The application of high frequency ultrasound in the time domain to detect the presence of a rear adherend is limited due to the high attenuation in the adhesive layer. However, high frequency time domain techniques can be used to inspect the thin adherend-

Adherend thickness (mm)	Adhesive thickness (mm)						
	0.50	0.75	1.00	1.50	2.00	2.50	3.00
2.00	**Good**	**Good**	**Good**	**Good**	**Good**	**Good**	**Good**
1.50	**Good**	**Good**	**Good**	**Good**	**Good**	**Good**	**Good**
1.00	**Good**	**Good**	**Good**	**Good**	**Good**	Poor	Poor
0.75	**Good**	**Good**	**Good**	**Good**	**Good**	Poor	Poor
0.50	Poor	Poor	Poor	No	No	No	No

Table 2·1 Limits of testability for a rear adherend disbond in aluminium joints [54].

Adherend thickness (mm)	Adhesive thickness (mm)						
	0.50	0.75	1.00	1.50	2.00	2.50	3.00
2.00	**Good**	**Good**	**Good**	**Good**	**Good**	**Good**	Poor
1.50	**Good**	**Good**	**Good**	**Good**	**Good**	Poor	Poor
1.00	**Good**	**Good**	**Good**	**Good**	Poor	Poor	No
0.75	**Good**	Poor	Poor	Poor	No	No	No
0.50	No	No	No	No	No	No	No

Table 2·2 Limits of testability for a rear adherend disbond in steel joints [54].

adhesive interface. Various models of the different types of defect which can exist at the interface are reviewed by Nagy [58]. This section considers inspection of the interface using time domain techniques whilst frequency domain techniques, which have been the focus of a large part of bond inspection work, are discussed in section 2.2.2.

Environmental degradation at the interface has been studied by Vine [59] by scanning joints in an immersion tank at normal incidence using a 50MHz focused transducer. The results of testing showed that degradation could be identified, but the technique was of limited use since some joints had lost 50% of their toughness without showing any visible change in the ultrasound scans.

Improved sensitivity would be expected using oblique incidence measurements generating only shear waves. The interface is commonly considered as a thin layer between the adherend and the adhesive, and can be modelled as a thin viscous layer [60-62], for example. The reflection coefficient from a rigid (or 'welded') interface is lower than for a slip (or 'smooth') condition. This value is dependent on the frequency-thickness product of the layer, the angle of incidence and the properties

of the interface layer. Thus by testing at a particular frequency and incidence angle, the reflection coefficient is sensitive to the interfacial properties. This approach has been used by many workers to characterise the interface based on time domain data [60, 63-66]. Whilst the technique is attractive since it is sensitive to the condition of the interface at the test point, amplitude measurements are difficult to make reliably and accurate setup is required to make the measurements. Interfacial characterisation using frequency domain measurements is discussed in section 2.2.2.4.

2.2.2 Spectroscopy

Ultrasonic spectroscopy involves the analysis in the frequency domain of resonances in a structure. Early work in the field of spectroscopy was in the form of bond testers. Later, the advent of frequency analysers and computers able to capture waveform data and transform it to the frequency domain using Fast Fourier Transform (FFT) routines increased interest in spectroscopy, since it can reveal frequency dependent features which are not evident in the time domain, and does not require echoes from different layers in a joint to be resolved. Resonances can be seen experimentally in an amplitude spectrum which can be obtained by exciting an ultrasonic transducer, which is coupled to the joint via a liquid or solid delay line, in pulse-echo with a broadband pulse. Any resonances within the frequency range input into the structure will be excited and will destructively interfere with the reflection from the front face of the structure, appearing as minima in the frequency domain spectrum. A more detailed discussion of this method is given in chapter 3, section 3.4.2.1.

2.2.2.1 Bond testers

Since the 1950s, when adhesive use on aircraft structures started to become more widespread, various bond testing instruments have been developed to detect defects in bonded joints. Many of the devices operated in the sonic frequency range (see section 2.1.1) but were unsuitable for some applications since they were not able to detect small enough defects. As a result, instruments were developed which operated in the ultrasonic frequency range working on the principle that the presence of disbonds in a joint alters the through-thickness resonance characteristics; by monitoring the resonances, defects could then be detected. Early on, the first through thickness mode of vibration (mode 1) of a three layer bonded joint was identified to be suitable for testing [67] since its resonance frequency is sensitive to adhesive thickness and modulus. This first mode can be represented simply by a one-dimensional mass-

spring-mass model where the metal adherends behave as rigid masses, and the adhesive as a massless spring. This mode is discussed in more detail in chapter 3, section 3.2.1. Mode 1 frequency predictions made using this mass-spring-mass model had been found to correlate well with experiments on three layer joints [67], but variations in the adhesive sheet thickness and cohesive 'quality' resulted in a very wide range of possible frequencies which could not be monitored by the devices at the time. The Fokker Mk 2 bond tester [68-70] (Models 67 onwards – Fokker aircraft, Netherlands) overcame this problem by coupling a probe to the joint and measuring the resonance of the combined probe-joint system. This limits the resonance frequency range, but at the cost of decreasing the sensitivity to joint properties.

The Fokker bond tester uses a probe [71] consisting of a piezoelectric crystal (which is coupled to the structure) connected electrically in series with a resistor. The impedance of the system comprising the probe coupled to the joint reaches a minimum at resonance. The instrument operates by sweeping the driving frequency across a chosen range in which the resonance is expected, and displays the resonant frequency shift from a reference value and the impedance (amplitude). The reference is obtained by tuning to the resonance of the probe coupled to the top adherend only. In use, the response will change when the probe is over a bonded region and the operator uses the shift in frequency and amplitude to diagnose the bond condition. The shift in frequency is related to the specific stiffness of the adhesive layer, K'', which is defined as:

$$K'' = \frac{E'}{t} \qquad (2\cdot3)$$

where E' is the apparent modulus (see chapter 3, section 3.2.1), and t is the layer thickness. (Note that this is the stiffness of the adhesive layer and not the stiffness of the adherend-adhesive interface.) Correlation curves provided by the manufacturer have attempted to use the readings given by the instrument to measure the cohesive strength. Such measurements have since been shown to be unreliable unless the adhesive has a low specific stiffness and the bond line thickness is monitored independently [72]. The instrument has proved, however, to be more reliable for disbond detection; a front adherend disbond is indicated where there is no shift in the resonance frequency. The instrument has been widely used in this way, but is limited to defects with diameter greater than the probe diameter; the maximum joint thickness is also limited by the probe diameter. For example, a 20mm diameter probe is needed to test joints 3.5mm thick. These instruments work well for disbond detection in

relatively large, flat aircraft structures, but for automotive joint testing this presents several problems. Thick aluminium adherends (1.0-3.0mm) are used which would require a probe of larger diameter than the joint width in many cases. More importantly, the requirement for couplant free testing precludes the use of such bond testers in the automotive industry.

2.2.2.2 Disbond detection

Owing to the limitations of bond testers, analysis of the bond condition to identify disbonds and adhesive thickness has been investigated through the analysis of the frequency spectra from joints by several workers. Hutchins et al. [73] used a multilayer wave propagation model to study reflection coefficient spectra from bonded joints using longitudinal and shear waves, and plotted frequency and amplitude variation of the modes up to 10MHz with varying adhesive thicknesses for an aluminium bonded joint. Based on the predicted frequencies of the resonance modes, two dimensional scans of a bonded joint with a known defect were made. Results were presented showing spatial variation of resonance frequency and amplitude in a frequency window centred around the expected second through-thickness mode. The amplitude and frequency were seen to change rapidly around the defect, but no further analysis was provided. This work assumed that the bondline thickness remained roughly constant. Challis et al. [53] have also studied the variation of resonance frequency with adhesive thickness for an aluminium bonded joint at different states of adhesive cure, and for bonded and disbonded cases. They concluded that if the adhesive thickness is known a priori, then the reflection coefficient spectra can be used to detect front and rear disbonds; in the absence of a bondline thickness measurement, their time domain technique (see chapter 2, section 2.2.1) would be required.

Weise [74] carried forward the work of Challis and Freemantle by evaluating their time domain technique, and also studied the viability of using spectroscopy to determine the bond condition. The frequency domain analysis focused on the first mode since it is significantly lower than other modes where a joint is bonded, and could therefore easily be identified. Weise [74] proposed tracking the lowest resonance of the system to form the basis of a diagnostic system for the non-destructive testing of adhesive joints. A multilayer wave propagation model [54] was used to predict the resonance frequencies for the bond conditions: fully bonded, rear adherend disbonded, front adherend disbonded. A 1MHz transducer was used for the experimental validation and

was coupled to the structure with gel via a large diameter Perspex delay line. The received signal consisted of the reflection from the delay line-joint interface, followed by the echo train from resonances in the joint. This was zero padded and transformed to the frequency domain using an FFT. A signal processing algorithm was used which searched for the first minimum in the resulting amplitude spectrum. Unfortunately, the transducer had very little energy below 250kHz and most of the first mode resonances from the joints tested fell into this frequency range, and were barely detectable as a result. In the absence of a rear adherend, the frequency of the first mode was found to be higher and this could be detected with the transducer used. It was concluded that spectroscopy could be used to detect the presence of adhesive (i.e. contact between front adherend and adhesive) and determine the thickness of the front adherend, and if the lowest system resonance could be found then the presence of a rear adherend and the adhesive layer thickness could be determined. However, the implementation of the technique had limited success due to the poor low frequency performance of the transducer and an unreliable signal processing algorithm. This appeared to be a promising technique, but had not proved to be a robust test suitable for automotive application, and the effect of wide ranging variations in adhesive thickness had not been considered.

Since bond testers and time domain ultrasonics, as well as other non-ultrasonic methods, are able to reliably detect disbonds in bonded aerospace structures, other research efforts have largely been directed towards determining the adhesive and cohesive ‘quality’ of the bonds.

2.2.2.3 Cohesive property determination

The cohesive properties of an adhesive layer can vary, depending primarily on the cure state and composition. It is therefore attractive to be able to determine the cohesive properties after curing.

Several workers have investigated the resonances of adhesive joints over a wide frequency band in an attempt to determine the cohesive strength. Early work, for example by Flynn et al. [75, 76], correlated adhesive stiffness with velocity, and cohesive strength with attenuation coefficient (or amplitude ratio and resonance depth) assuming the geometry of the bond remained constant. Cawley and Hodson [77] refined a previous technique [78] allowing adhesive modulus to be measured to within 6.5%, and bondline thickness to micrometer accuracy. It has been shown that the

frequency variation with specific stiffness (see equation 2·3 for definition) of higher order modes, unlike mode 1, is not coincident for adhesives of different moduli. The technique therefore used the frequency of the first mode to determine the specific stiffness of the joint, and accordingly selected three suitable higher order modes from which to calculate the modulus and bondline thickness. This technique has enabled a more reliable check to be made on the cohesive properties of an adhesive layer than the Fokker bond tester, but does have disadvantages. Two transducers are required to cover the required frequency range, and whilst the higher order modes can be identified relatively easily in the lab, robust automatic detection in the field is more difficult. Dewen [79] has also found that the technique is sensitive to small measurement errors.

Much work has been done to solve the 'inverse problem' and determine the acoustic properties (thickness, density, wave velocity and attenuation) from ultrasonic data. From this, the mechanical properties of the adhesive layer can be obtained. Lavrentyev and Rokhlin [80] have used a spectroscopic technique to solve the inverse problem and determine the acoustic properties of the adhesive layer from ultrasonic data. They calculate these from six non-dimensional parameters, three obtained from each of the normal and oblique incidence measurements. The technique has been shown to be stable, but assumes a perfect interface and known adherend properties. Kinra and Iyer [81, 82] have developed a technique to identify the acoustic properties of the adhesive from a through thickness ultrasonic measurement. This technique makes use of the entire spectrum, rather than using just the frequency of the resonance peaks as many other techniques have done. These techniques have proved suitable to determine cohesive properties in a controlled laboratory set-up. Unfortunately, measurements in the field, particularly on automotive structures, are likely to be much less reliable.

2.2.2.4 Interfacial property determination

The task of characterising the interfacial properties is more difficult than the cohesive properties. Numerous approaches have been taken using time domain and guided waves, and many also rely on frequency domain analysis, which is the focus of this section. A review of early work in the 1970s is provided by Thompson [83], and some of the later work is reviewed by Light [22]. More recently, a variety of approaches have been used to model a weak interface layer and characterise it using ultrasound. Wang and Rokhlin [61, 62] have modelled the interface as an anisotropic thin viscoelastic layer and confirmed that the frequency of some minima in the reflection coefficient

spectrum are sensitive to interfacial properties, whilst some are independent of the interface properties. From this data, they suggest that the thickness and viscoelastic properties of the interface can be reconstructed. The spectra depend on adhesive thickness, bulk properties and interface quality. In order to separate the effect of variations in the bulk adhesive properties and thickness from the interfacial properties, Rokhlin [84] used the difference in frequency between minima from the spectra obtained at normal incidence and oblique incidence to measure the degradation at the interface. Modelling the layer as adhesive with an array of micro-disbonds filled with a viscoelastic liquid, also predicts a shift in the frequency of the minima when the interface is degraded [85]. The interface can also be modelled as springs [86]. In this case, the reflection from the interface is a function of the impedances of the two contacting surfaces and the interfacial stiffness. In their work, the effect of mismatched impedance in a real joint has been removed by using two identical materials with rough contacting surfaces. Again, an increasing shift in the minima is observed with a decreasing interface stiffness, and this can provide a measure of adhesion quality.

Whilst these techniques can be used to distinguish between a good and poor interface in the lab, none are able to provide an absolute measure of the interfacial strength. Testing in the field using these techniques, which require accurate set-up, would be extremely impractical and time consuming.

2.2.3 Guided waves

There are a family of guided or travelling waves which propagate in-plane, such as Raleigh, Lamb, and interface waves. They are attractive for testing because they can propagate over long distances, allowing a line rather than a point to be interrogated. Guided wave modes have been studied by many workers in the context of characterising the cohesive and adhesive properties of bonded joints [65, 87-90]. Plate ('Lamb') waves have been shown [89] to be relatively insensitive to adhesive and interfacial properties. This is because Lamb modes are modes of the whole joint, and the properties are dominated by the adherends. Guided modes propagating only in the adhesive layer are more attractive since the properties of the wave are dependent on the conditions at the adhesive-adherend interface. The disadvantage is that they cannot be excited through the adherends which precludes them as a practical testing technique. However, leaky guided modes (which leak energy into the surrounding media) propagating in the adhesive layer can be excited through the adherends and are

therefore viable for testing [27, 65]. It is also possible to generate interface waves along the interface itself, and these have been used to measure adhesive and cohesive properties [24].

In situations where a joint cannot be accessed, Lamb modes have been used to propagate along one adherend, through the adhesive, and into the other adherend, in order to asses the adhesive dimensions (width and thickness) [87, 90]. The received signals are complicated, but prepared lap joint samples have been correlated to joint dimensions using Artificial Neural Network techniques [90]. This can be a benefit if a joint is completely inaccessible and the joint geometry is suitable for testing, such as a T-joint. Where the joint is accessible this technique does not offer any advantages over direct inspection techniques, and it is more complicated to set-up and analyse the data. Further, all the automotive joints in the body shell considered are accessible from one side.

Propagation of a wave along the length of the bondline, rather than across the width, would be more attractive since it would enable a long length of adhesive to be interrogated from a single measurement. However, recent work [88] has shown that waves cannot be propagated over long distances from one adherend into the other through the bondline. Further, the rivets and spot welds which are placed regularly along the joint would preclude the use of any long range inspection techniques.

2.3. Conclusions

A variety of NDT techniques are available which can be used for testing adhesive bonds, but no single technique is able to detect all three of the main classes of defect found in adhesive joints, namely voids/disbonds in the adhesive layer, poor cohesion and poor adhesion.

Through careful process control and some use of thermography, optical methods, bond testers and time domain ultrasonics, the requirements for disbond detection, notably in the aerospace industry, have largely been met. Research efforts have therefore focused mainly on determining the cohesive and interfacial quality of bonds. Several techniques have been established to provide cohesive bond quality measurements from ultrasonic data. However, these require relatively accurate experimental set-up and are not well suited to field testing. Characterisation of the interfacial properties has provided more of a challenge. Normal and oblique incidence bulk and guided wave measurements have been used to identify variation in interfacial properties. Several

models of the interface have been proposed which account for the observed changes in ultrasonic data when an interface degrades. The main problem with the development of these techniques for field use is the careful set-up required to collect the ultrasonic data.

The remainder of this section considers the applicability of the techniques discussed in this chapter to the automotive industry for disbond detection. Of all the adhesive joint defects, the reliable detection of voids and disbonds in automotive joints is of primary concern for this work. It is important that the method developed is robust and can be applied reliably in the industrial setting, and not just used as a laboratory technique.

Non-ultrasonic techniques are attractive since they do not require couplant, but are generally insufficiently sensitive to detect defects in automotive joints. Ultrasonic techniques are more promising, and a time domain technique using an adaptive reverberation filter has been used successfully in the industry, but its use is limited by the attenuative bondline which can vary considerably in thickness. Bond testers have been used with much success in the aerospace industry, but require the probe to be coupled directly to the structure, making them unsuitable for this application. Other ultrasonic techniques are aimed at cohesive and adhesive strength measurements and are not appropriate for detecting disbonds. Guided waves can offer inspection across the width of a joint with a transmitter and receiver placed remotely from the bonded region, and would therefore be useful where joints are inaccessible. However, this is not a requirement for the structures considered in this thesis; it was felt early on that because of the increased complexity in generation and analysis of guided waves, further development would not be pursued in preference to simpler point measurements which were more likely to be robust. A summary of the automotive testing requirement and the principal reasons for the unsuitability of existing techniques is given in table 2·3.

Previous work has shown that by using ultrasonic spectroscopy to determine the frequency of the fundamental thickness mode, disbonds in three layer joints can be identified. Bond testers using this mode have used a probe coupled to the joint to limit the wide range of mode 1 frequencies which result from variations in bondline thickness. Weise [74] showed that the frequency of the first mode of a joint could be

Automotive industry requirement	Non-ultrasonic						Ultrasonic				
	Sonic	Optical	Thermography	Radiography	MRI	Dielectric	Through-transmission	Pulse-echo	Oblique incidence	Guided waves	Bond testers
High volume production environment						X			X		
Couplant free											X
Single side access							X				
Confirm rear adherend presence	X							X	X		
Thin adherends & variable bondline								X			
Small defects/ high sensitivity	X										X
Test on line (no dedicated test facilities)		X	X	X	X						
Metal adherends				X	X						
Complex joint layout	X					X				X	
Robust and rapid test						X			X		
Low cost		X	X	X	X						

Table 2·3 NDT technique rejection chart showing principal reasons for unsuitability. 'X' indicates unsuitability.

used to determine the presence of adhesive and a rear adherend, but results were hampered by the poor low frequency performance of the transducer used and the signal processing, which resulted in unreliable detection of this mode.

With the principal automotive requirement being for disbond detection, it was decided to focus on the development of a suitable robust ultrasonic technique for disbond detection which could be used to test automotive type joints. Such a system would be a valuable contribution to the field of NDT and industry. Mode 1 was seen as an attractive option. However, it has not previously been possible to test joints of such varying adhesive thickness from one side using a couplant-free system which can interrogate a small area and confirm rear adhesive presence (see table 2·3 for a complete summary of requirements). It was therefore decided to re-assess the viability of using mode 1 and attempt to develop an approach which would meet the demanding requirements and overcome the obstacles encountered by previous workers.

Chapter 3

Viability of mode 1 for disbond detection in automotive joints

Bond testers using low frequency through thickness resonance to identify disbonds in joints have limitations which prevents their wider use. Previous work has suggested that mode 1 could be used in a technique for more general purpose disbond detection which could be used in the automotive industry, for example. In this chapter, the viability of using mode 1 for joints with a wide range of adhesive thickness is assessed through modelling and experimental validation. The suitability of signal processing techniques for detection of this mode are then discussed. It will be shown how mode 1 can be used in a novel technique to provide a robust means of disbond detection and also considers the extent of the range of joints which can be tested.

3.1. Material properties

Before modelling of bonded joints can be carried out, the acoustic properties of the materials must be known. No data was available for the adhesive used throughout this work (XD4600-Betamate) and hence its properties have been measured experimentally. Various techniques can be used to calculate the compression wave velocity and attenuation of ultrasound in a material. Previous workers have reported success using the amplitude and normalised amplitude spectrum methods [66, 88]. These techniques are particularly well suited for characterising the material properties in thin attenuative materials since they do not require individual echoes to be resolved in the time domain; values can be obtained over a wide range of frequencies with a single measurement and they do not require a purpose made test rig. The theory and practical application of these techniques are well documented, hence only a summary of the methods is provided in appendix A. The measured acoustic properties for the XD4600 adhesive and published data [91] for aluminium and steel are presented in table 3·1. The density of the cured adhesive was provided by the manufacturers, and confirmed experimentally.

Material	Density (kg/m^3)	Compression wave velocity (m/s)	Compression wave attenuation (Np/λ)
Aluminium	2820	6330	-
Steel	7700	6100	-
XD4600	1310[a]	2463[a]	0.145[a]

Table 3·1 Material properties for joint materials.

a.Note: Values given are from experimental measurements (see appendix A). Variation in cure state can result in differences in material properties from the values given.

3.2. Analysis

The three layer metal-adhesive-metal joints found in automotive structures have been modelled to determine how the response of the first through-thickness resonance mode (mode 1) varies with adhesive thickness for joints with adherends of different thickness and material. The motivation for the work in this thesis was provided by the need to test aluminium bonded structures, and the majority of the modelling and experimental work has been carried out on aluminium joints, although a comparison with steel joints is made in section 3.3.4 of this chapter. Aluminium adherends usually range from 1.0 to 3.0mm thick, the majority being around 2.0mm. The predictions in this chapter are therefore shown at 2.0mm, and where appropriate are also given over the likely range of adherend thickness. All of the modelling has been done with front and rear adherends of the same thickness, but the techniques are equally applicable to joints with different adherend thicknesses. Three possible bond conditions have been modelled (see Nomenclature for definitions):

- Bonded (rear adherend present)
- Partially bonded (rear adherend disbonded)
- Fully disbonded (front adherend only)

3.2.1 One-dimensional mass-spring-mass model

The first thickness mode of a bonded joint can be approximated by a simple mass-spring-mass model, as mentioned in chapter 2, section 2.2.2. This system has a resonance frequency given by:

$$\omega_n = \frac{1}{2\pi}\sqrt{\frac{2k}{m}} = \frac{1}{2\pi}\sqrt{\frac{2K''_a}{\rho_m t_m}} \qquad (3{\cdot}1)$$

where ρ and t are the layer density and thickness. The subscripts m and a refer to the metal adherend and adhesive respectively. The specific stiffness K'', is the ratio of the apparent modulus to bondline thickness and defines the stiffness of the adhesive layer (see equation 2·3). The apparent modulus E', is defined as [92]:

$$E' = \frac{E(1-\nu)}{(1-2\nu)(\nu+1)} \qquad (3{\cdot}2)$$

where ν is the Poissons ratio and E is the Young's Modulus. It can be calculated from the compression wave velocity and density by:

$$E' = c^2 \rho \qquad (3{\cdot}3)$$

The apparent modulus is higher than the Young's modulus. This is because when ultrasonic testing is carried out, the area of the material under test is smaller than the bulk material and is constrained at the edges by the surrounding material. The apparent moduli for adherend and adhesive materials are given in table 3·2.

Material	Apparent Modulus (GPa)
Steel	287
Aluminium	113
XD4600	7.9[a]

Table 3·2 Apparent moduli of joint materials.

a.Note: variation in cure state can result in differences in material properties from the value given.

Mass-spring-mass models have been used by several workers [20, 67, 72, 93] to predict the frequency of the first thickness mode. Good correlation between measured and predicted values has been reported, but these results were obtained with early adhesives which had a lower modulus than those used today. Equation 3·1 shows that the model does not account for strain in the adherends and assumes the adhesive is perfectly elastic and massless. At realistic bondline thicknesses (e.g. 0.2mm) the specific stiffness of the early adhesives was low enough for there to be little adherend strain and the mass-spring-mass approximation was valid. However, with the high modulus epoxies used today, the strain in the adherends is low only where the bondline is relatively thick. This can be seen by inspection of the mode shapes.

Figures 3·1a and b show the displacement mode shapes for mode 1 of a bonded joint with adhesive thicknesses 0.2mm and 3.0mm respectively. These show the relative normal displacements through the thickness of the joint (obtained using Disperse software [94]). The strain is given by the rate of change of displacement with distance. Where the adhesive is very thin, it is likely to have a higher specific stiffness than the adherend. Consequently, there will be significant strain in the adherend as shown in figure 3·1(a). Their stiffness being lower, the adherends then dominate the resonance frequency. Indeed, as the adhesive thickness tends to zero, the mode shape approaches that of a plain plate with the same overall thickness as the joint.

In the case of a plain plate, the mode 1 frequency, ω_n, is given by:

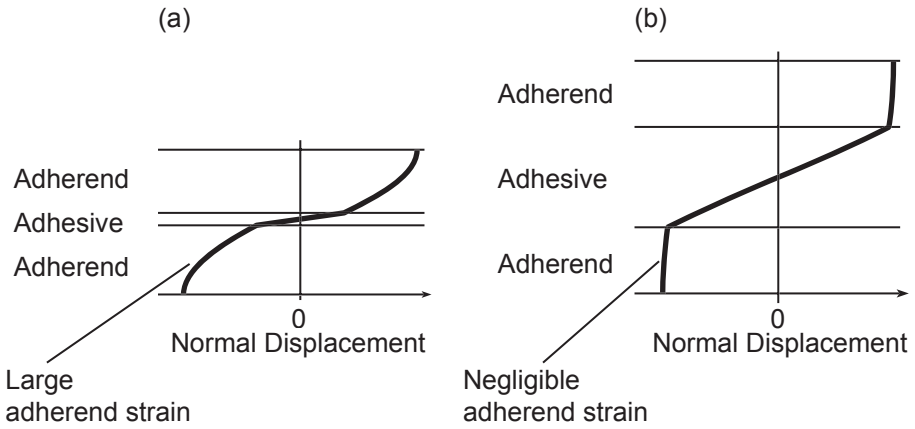

Figure 3·1 Mode shapes for a bonded joint with 2mm aluminium adherends and (a)0.2mm and (b)3.0mm adhesive layers.

$$\omega_n = \frac{\sqrt{E'/\rho}}{t} \qquad (3\cdot4)$$

where t is the total thickness (i.e. twice the adherend thickness in the absence of adhesive).

If the specific stiffness of the adhesive is now reduced to be much less than that of the adherends, either by holding the modulus constant and increasing the thickness, or by decreasing the modulus with a constant thickness, then the strain in the adherends will be small and they will behave more like rigid masses. Thus at thick bondlines the system behaves like a mass-spring-mass system. This is confirmed by the mode shape in figure 3·1(b) which shows negligible adherend strain.

The mass-spring-mass model cannot therefore be used for thin adhesive layers, and will only provide a solution for the first mode of a bonded joint. More accurate results have been obtained by modelling a joint as three solid cylinders (adherend-adhesive-adherend) in axial vibration joined end-on [72]. The lengths of the cylinders correspond to the thickness of the appropriate layer in the joint. Receptance analysis [95] is used to calculate the natural frequencies of the system. This model does account for strain in the adherends and good agreement between predicted and measured values has been reported across a wide range of adhesive thicknesses. This model can also be used to predict the mode 1 frequencies for partially bonded joints and higher order modes.

An alternative approach, used by many workers [53, 54, 66, 73], is a multi-layer wave propagation model. The work presented here made use of a computer program (DGLOBAL) which has undergone extensive testing and validation, developed by

Pialucha [66, 96] employing a global matrix solution technique. This overcomes numerical instability problems which can occur with the transfer matrix techniques first formulated by Thompson and Haskell [97]. This general purpose tool was used in preference to the receptance model for convenience since it was already available. It is also more versatile, allowing many layers to be modelled with excitation at any angle of incidence.

The material properties for the layers used in the model are given in table 3·1. These values are assumed constant with frequency except for the attenuation which is assumed proportional to frequency (see appendix A). The adhesive attenuation of $0.145\text{Np}/\lambda$ means that the amplitude of a wave is attenuated by $e^{-0.145}$ per wavelength, which is equivalent to 0.51dB/mm/MHz. The model is one-dimensional, hence only layer thicknesses are specified. The joint was loaded with a water half-space on one side (closest to the excitation) and an air half-space on the other side. This represents real testing conditions where the joint is surrounded by air but dry coupled to a rubber delay line (as would be used in a dabber probe - see chapter 5). The use of water in the model to represent the rubber delay line is valid since the impedances of the two materials are very close. A plane wave source (infinite transducer) has been used at normal incidence which makes the system one-dimensional. This excites the structure over a chosen frequency range which is discretised and the reflection coefficient calculated at each frequency. This then outputs a reflection coefficient spectrum, an example of which is shown in figure 3·2.

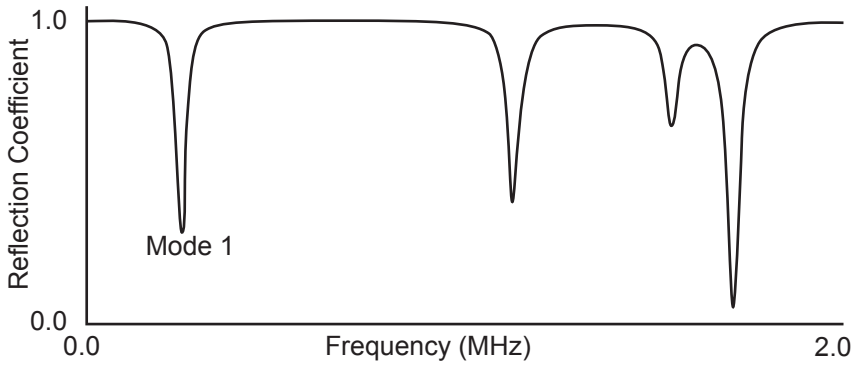

Figure 3·2 Example of reflection coefficient spectrum.

Compression waves are used in the model, so only through thickness resonances are present. In the model, it is assumed that there are no shear components. Interference between the reverberations in the joint and the reflection from the front surface of the

joint at resonance gives rise to the minima in the reflection coefficient spectrum. The first of these minima occurs at the mode 1 frequency. The depth of the minimum is an indication of the strength of the resonance.

A comparison of mode 1 frequencies of a bonded joint predicted with the multilayer wave propagation model and the mass-spring-mass model is given in figure 3·3. The comparison is made for 2mm aluminium adherends with bondline thickness ranging from 0.1-3.0mm. As confirmed by the analysis provided earlier, the mass-spring-mass model offers a reasonable approximation where the bondline is thick, but is seen to break down at thin bondline thickness where the adherend stiffness dominates the resonance frequency.

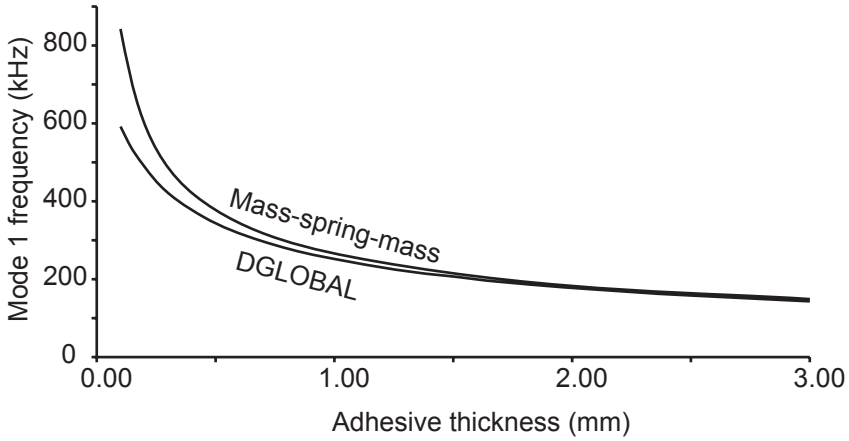

Figure 3·3 Comparison of mode 1 frequencies predicted by the mass-spring-mass model and DGLOBAL for a bonded joint with 2mm aluminium adherends.

3.3. Predictions

3.3.1 Mode 1 frequency variation: small bondline thickness range

The front and rear adherend thicknesses of joints are known prior to testing. Although variation in thickness of the adhesive layer is likely, its thickness at any point should fall within a specified range; for the structural joints investigated in this work this is 0.1-0.4mm, whilst in other applications (such as stiffeners on bonnets and boot lids) the range can extend up to 3.0mm. Based on the bondline thickness limits, mode 1 frequency ranges have been predicted for the three possible bond conditions. The variation of mode 1 frequency with bondline thickness for the structural bondline specification (0.1-0.4mm) is shown for a joint with 2mm aluminium adherends in figure 3·4. Figure 3·5 shows the same data across the adherend thickness range of 1-3mm.

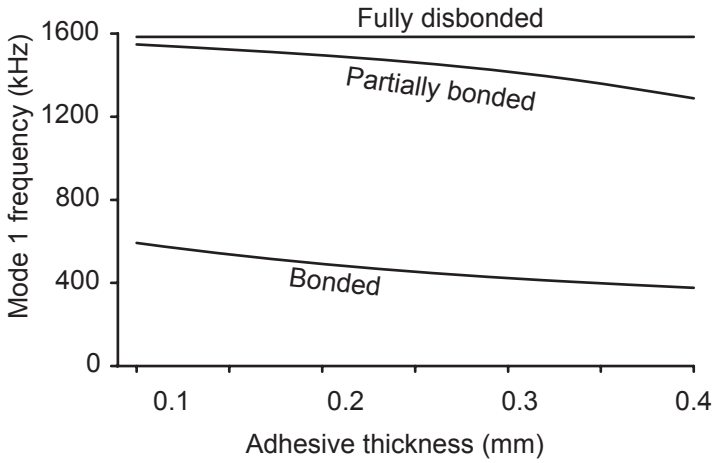

Figure 3·4 *Mode 1 frequency variation with adhesive thickness for joints with 2.0mm aluminium adherends for the bonded, partially bonded and fully disbonded conditions with an adhesive thickness range of 0.1-0.4mm.*

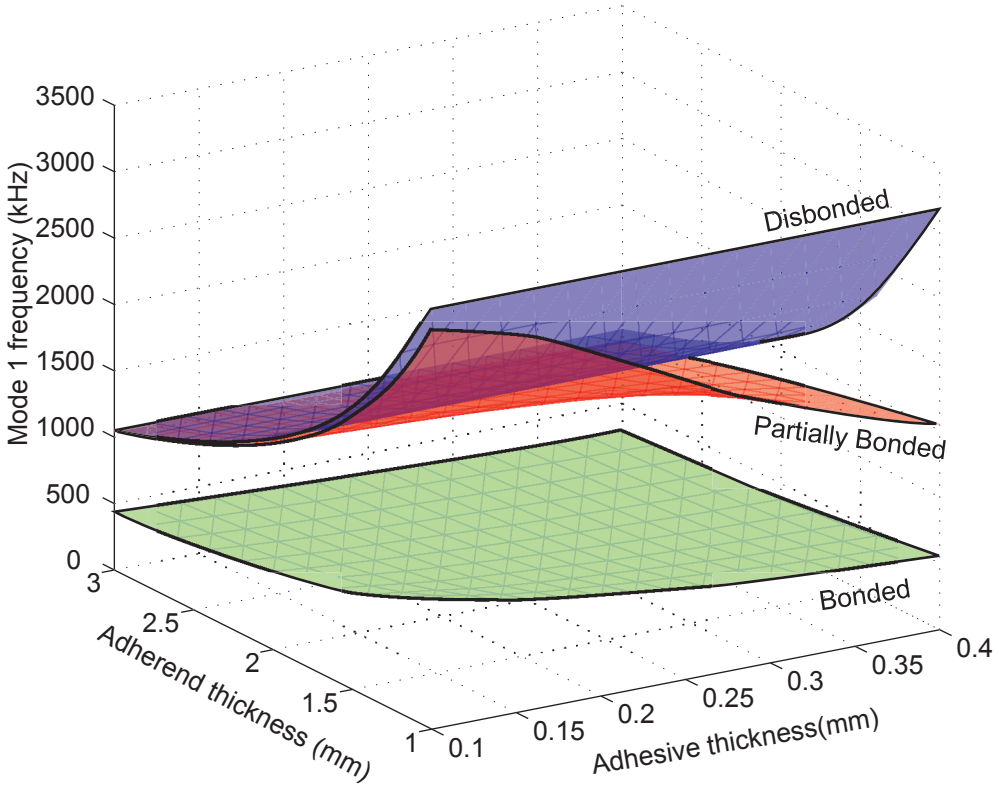

Figure 3·5 *Mode 1 frequency variation with adhesive thickness for joints with 1-3mm aluminium adherends for the bonded, partially bonded and fully disbonded conditions with an adhesive thickness range of 0.1-0.4mm.*

The mode 1 frequency of a bonded joint is dependent on the specific stiffness of the adhesive layer to some degree, even at thin bondlines. Hence as the adhesive thickness increases, the specific stiffness and mode 1 frequency decrease. As mentioned

previously, where the adhesive layer is thin, the resonance is dominated by the adherend stiffness. This is clearly visible in figure 3·5 by comparing the bonded joint mode 1 frequency variation at adhesive thicknesses of 0.1mm and 0.4mm. For a plain plate, the mode 1 frequency varies as a function of $1/t_m$, where t_m is the metal adherend thickness. In contrast, the bonded mode 1 frequency for a joint with a thick bondline (i.e. mass-spring-mass approximation valid) varies as a function of $1/\sqrt{t_m}$. At 0.1mm, the frequency variation with adherend thickness tends towards the fully disbonded case (i.e. plain plate) rising more quickly as the adherend thickness decreases; obviously the bonded mode 1 frequency approaches half that of the fully disbonded case since there are two adherends sandwiched together. At 0.4mm bondline, the bonded mode 1 frequency increases more slowly with decreasing adherend thickness, as expected.

The variation in mode 1 frequency with thick and thin adhesive layers is even more noticeable with the partially bonded case in figure 3·5. At 0.1mm bondline, the mode 1 frequency is dominated by the adherend stiffness and the response of the joint follows closely that of the fully disbonded adherend. As the adhesive thickness increases, the mode quickly becomes dominated by the lower specific stiffness of the adhesive layer, deviating more from the fully disbonded case.

This again can be explained by inspection of the mode shapes. Figure 3·6 shows mode shapes for a partially bonded 2mm aluminium adherend with 0.2mm and 3.0mm adhesive layers. There is significant strain in the adherend at thin bondlines, but it behaves like a rigid mass when the adhesive stiffness is low. In the fully disbonded case, obviously the adhesive layer is absent and has no effect.

Figure 3·5 clearly shows that at a given adherend thickness, with an adhesive variation of 0.1-0.4mm, the frequency ranges for bonded, fully and partially disbonded joints are well separated in frequency. When testing a joint with 2mm aluminium adherends, for example, a measured resonance in the bonded frequency range (approximately 375-590kHz) can therefore only be attributable to the response from a fully bonded joint.

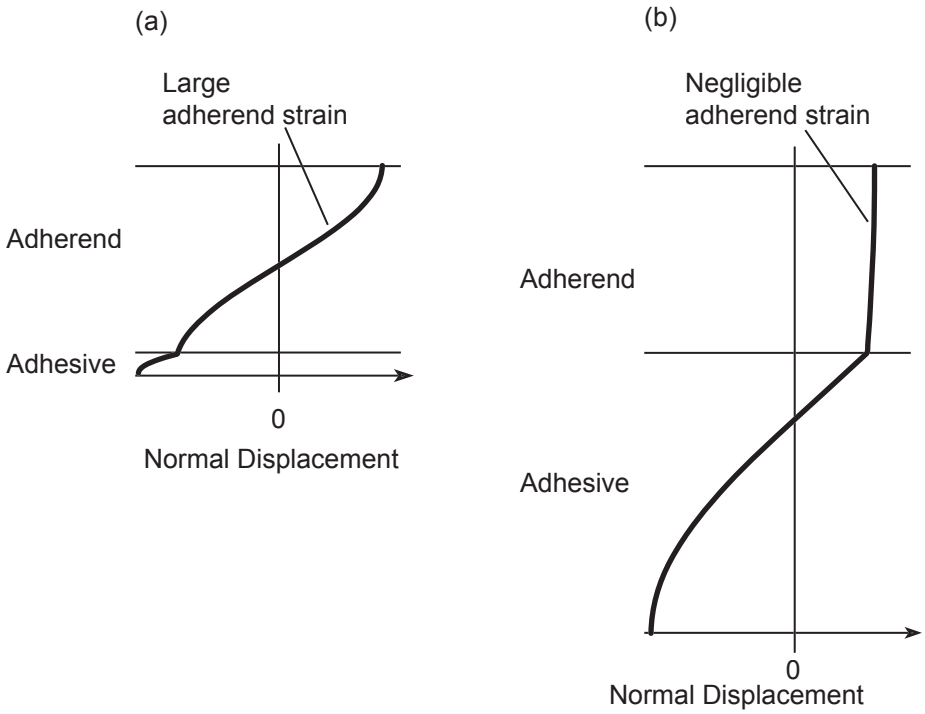

Figure 3·6 Mode shapes for a partially bonded joint with 2mm aluminium adherends and (a)0.2mm and (b)3.0mm adhesive layers.

3.3.2 Mode 1 frequency variation: large bondline thickness range

For the structural bondline thickness range (0.1-0.4mm) used in figures 3·4 and 3·5, the bond condition can be determined from a single measurement of the mode 1 frequency. Figures 3·7 and 3·8 show the mode 1 frequency variation for the same joints, but with a wider bondline thickness, ranging from 0.1-3.0mm. The fully disbonded case, since it does not change with adhesive thickness, has been omitted for clarity.

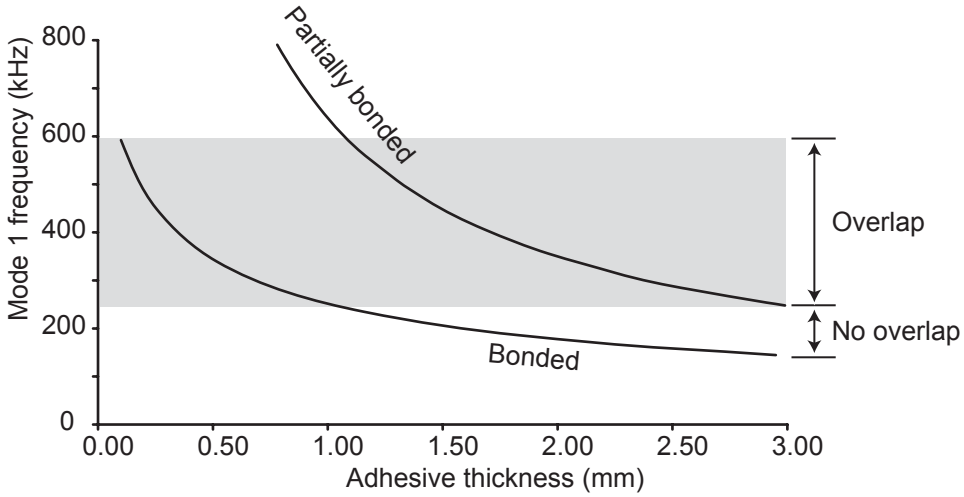

Figure 3·7 Mode 1 frequency variation with adhesive thickness for joints with 2mm aluminium adherends for the bonded and partially bonded conditions with an adhesive thickness range of 0.1-3.0mm.

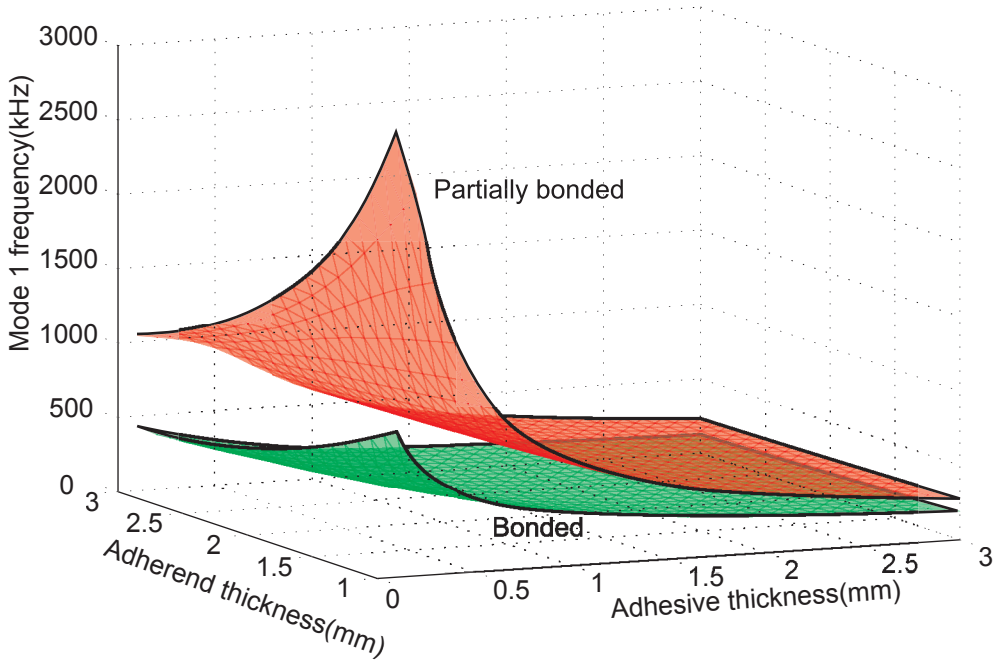

Figure 3·8 *Mode 1 frequency variation with adhesive thickness for joints with 1-3mm aluminium adherends for the bonded and partially bonded conditions with an adhesive thickness range of 0.1-3.0mm.*

In these figures, the effect of the varying adhesive stiffness is more pronounced. Where the bondline is thin, the mode 1 frequency is dominated by the *adherend* stiffness. With a thin bondline (0.1mm, for example) the mode 1 frequency varies approximately as a function of $1/t_m$; a relatively large increase in mode 1 frequency is observed with a decreasing adherend thickness. (Note that in the bonded case, the total adherend thickness is twice that of the partially bonded case, and hence has a lower mode 1 frequency.) As the bondline thickness increases, the mode 1 frequency becomes dominated by the *adhesive* stiffness. This is evident at thick bondlines (3.0mm, for example); here the mode 1 frequency varies as a function of $1/\sqrt{t_m}$ (in the bonded case), and indeed the variation in mode 1 frequency with adherend thickness is relatively small.

Since relatively large variations in frequency occur as a result of adhesive thickness changes, it is important to note that mode 1 cannot be used to predict the adhesive modulus alone. This is the reason that the Fokker bond tester became unreliable for cohesive property measurements.

It is also evident that the bonded and partially bonded frequency ranges are no longer separated in frequency. The overlap between the two frequency ranges is highlighted in figure 3·7. In this case, the mode 1 frequency of a partially bonded joint with a bondline in excess of 1.2mm falls into the range for bonded joints. The surface plots of figure 3·8 show that this overlap is greater where the adherends are thinner.

The degree of overlap is clearly affected by the bondline thickness range. An increase in the minimum adhesive thickness will reduce the extent of the overlap, as illustrated in figure 3·9. Here, the same data is shown as in figure 3·7 (0.1-3.0mm bondline), but for a reduced adhesive thickness range of 0.5-2.5mm; the reduction in overlap is clearly visible. Since the mode 1 frequency–bondline thickness variation is greater where the bondline is thin, an increase in the minimum adhesive thickness will reduce the overlap more than the same reduction in maximum thickness. Figure 3·10 shows a graph from which the maximum adhesive thickness to avoid frequency range overlap can be determined, given the minimum adhesive thickness. Such data is not available in the literature. In the figure, data is plotted for joints with 2mm aluminium adherends.

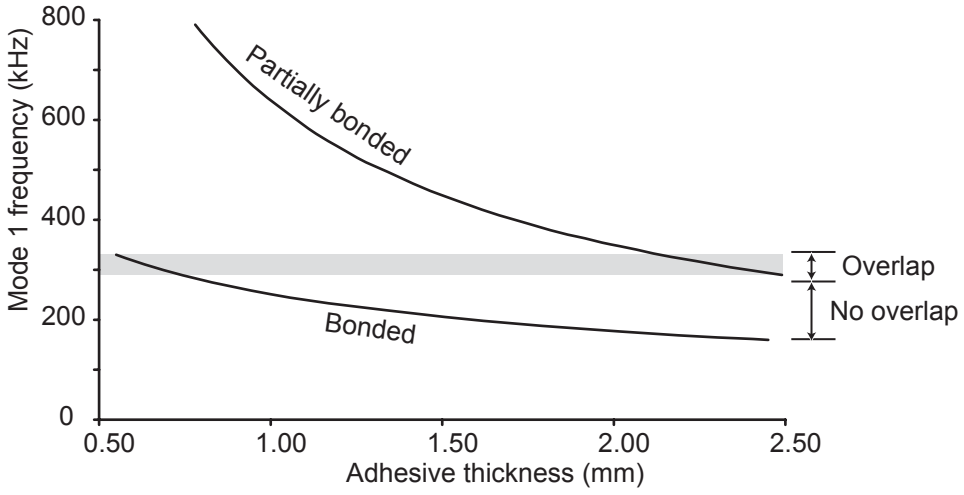

Figure 3·9 *Mode 1 frequency variation with adhesive thickness for joints with 2mm aluminium adherends for the bonded and partially bonded conditions with an adhesive thickness range of 0.5-2.5mm.*

The existence of an overlap between frequency ranges for bonded and partially bonded joints is detrimental for the test. There now become two frequency ranges which must be considered when testing whether a joint is fully bonded; a measurement giving a mode 1 frequency below the overlap region indicates the bonded condition; a reading with a mode 1 frequency in the overlap region can be either from a bonded joint with a thin bondline, or a partially bonded joint with a thick bondline. There are two possible

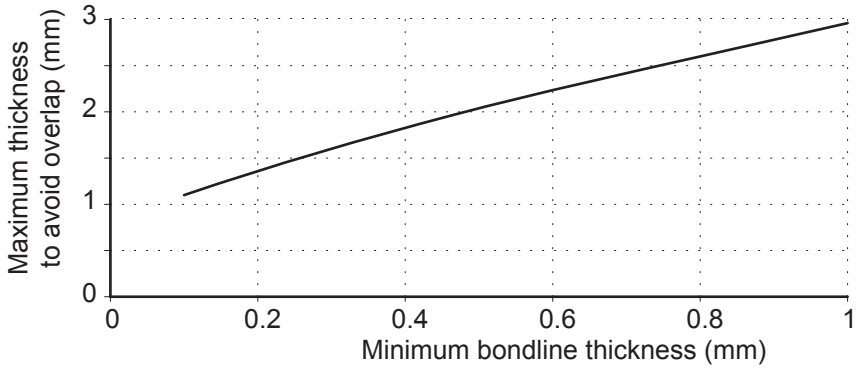

Figure 3·10 Variation of maximum adhesive thickness to avoid overlap with minimum thickness for joints with 2mm aluminium adherends.

solutions to overcome this problem: an additional measurement can be made to identify the bondline thickness, or the joint can be scanned and a step change in bond condition will be revealed by a step change in mode 1 frequency. These options are discussed further in chapter 6.

3.3.3 Higher order modes

Higher order modes have been used by previous workers to determine the cohesive properties of a bonded joint (see chapter 2, section 2.2.2). As mentioned previously, these are not suitable for robust disbond detection, hence the use of higher order modes is not considered here. The encroachment of higher order modes into the mode 1 frequency range for bonded joint is, however, an area of concern. The second thickness mode has been predicted using the multilayer wave propagation model, in the same way as for mode 1. Figure 3·11 shows the mode 1 and the lower part of the mode 2 frequency ranges for a 2mm aluminium bonded joint. The shaded region indicates where the two frequency ranges overlap. As with the bonded and partially bonded frequency ranges, this overlap only occurs when the bondline thickness variation is large. Again, there are two frequency ranges of significance; a reading in the mode 1 frequency range below the overlap region indicates the joint is bonded; in the overlap region, modes 1 and 2 will be present. Although some ambiguity therefore exists this can be easily resolved and mode 1 identified by taking the frequency of the lower of the two peaks.

3.3.4 Comparison of steel and aluminium adherends

The adherend mass and stiffness significantly affect the mode 1 response. The mode 1 frequencies presented so far are only for aluminium adherends, which have been the focus of the work. For the technique to be generic to applications in the automotive

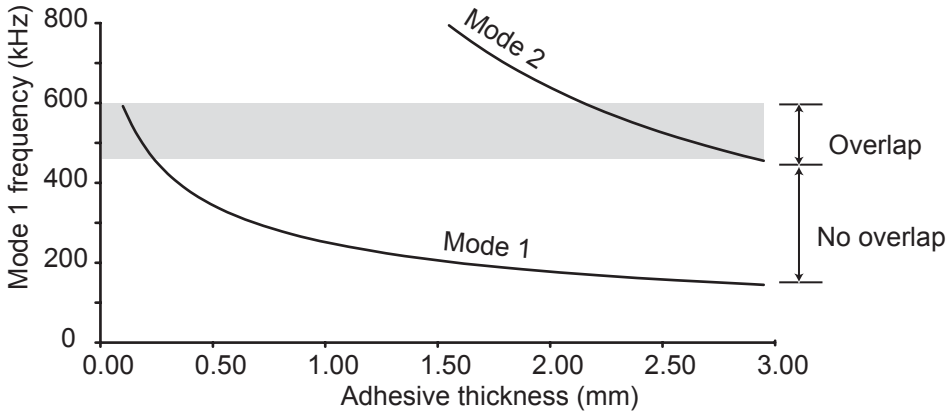

Figure 3·11 Mode 1 and mode 2 frequency variation with adhesive thickness for bonded joints with 2mm aluminium adherends.

industry, it must also be possible to test steel structures in the same way. A brief comparison of steel and aluminium frequency ranges is therefore provided in this section.

Aluminium adherends of 1-3mm are typical in automotive structures, whereas 0.7-1.5mm is more typical for steel structures. Since it is the mode 1 frequency ranges which provide the diagnostic information relevant to the test, not the adherend thickness, the mode 1 frequency variation with adhesive thickness has been shown in figure 3·12 using the typical thickness ranges for the particular adherend metal. In this way, the extremes of the mode 1 frequency ranges can be identified and used to assess the viability of the test. The results show that in fact the frequency ranges for steel and aluminium joints are similar. This is beneficial for testing because aluminium and steel can be tested using similar transducers.

3.4. Validation

3.4.1 Experimental set-up

The mode 1 frequency and amplitude predictions have been validated experimentally using prepared bonded and partially bonded joint samples. The joints comprised 2.0mm thick degreased aluminium adherends with a nominally constant thickness XD4600 adhesive layer, and have been cured at 180ºC for 35 minutes. Bondline thicknesses ranged from 0.1mm to 3.0mm, and were controlled by placing shims of the required thickness between the adherends at the edges. A compressive load was then applied to the joint to cause the viscous adhesive to spread out to the required thickness. Partially bonded joints were produced by coating one of the adherends in release agent (Freekote) prior to bonding; this adherend was then removed after curing.

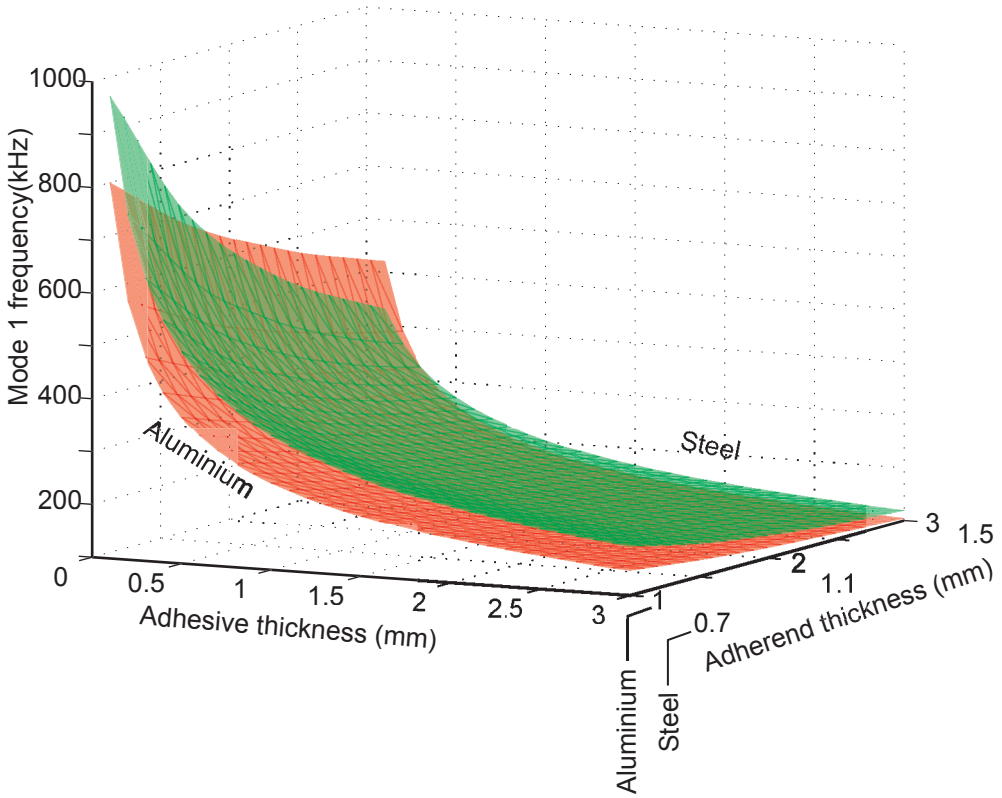

Figure 3·12 Comparison of mode 1 frequency variation with adhesive thickness for bonded joints with steel and aluminium adherends.

The adherends (75mm x 150mm) and adhesive layer were chosen to be much larger than the diameter of the transducers used, creating an approximation to a one-dimensional system.

Automotive testing precludes the use of liquid couplant, and it was envisaged early on in the project that a dry rubber coupling would be used. A rubber with a low acoustic attenuation (low-loss rubber) has been developed for dry coupling for wheel probes (see chapter 5). This rubber has an acoustic impedance very similar to water which means that the joints can be tested in an immersion tank, and will give similar results to those expected using dry rubber coupling. This allowed mode 1 validation to be carried out prior to the development of a device for dry coupling. In a real test environment the rear face of the joints is air backed. In the immersion tank this is achieved by positioning the joint on the surface of water so that the rear face was in air. Figure 3·13 shows the experimental set-up; the transducer (pointing upwards) was aligned normal to the surface with a 30mm stand-off from the joint to allow sufficient time for several cycles of the joint resonance to be captured before the second front face reflection. In order to cover the expected mode 1 frequency ranges for bonded joints with bondlines ranging from 0.1mm to 3.0mm, two transducers were used,

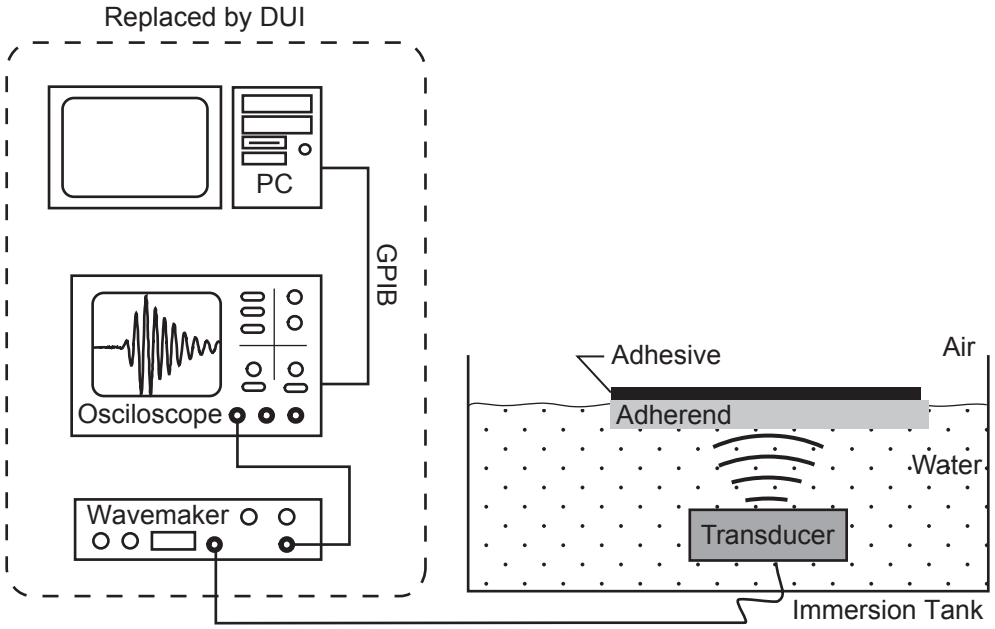

Figure 3·13 Experimental set-up in immersion tank for validation of mode 1 predictions.

operating in pulse-echo. These were 500kHz (V301 series – Panametrics) and 200kHz (Matec) centre frequency immersion transducers. In initial tests, excitation was provided by a waveform generator and amplifier (Wavemaker Duet – MacroDesign) capable of driving a toneburst or pulse with a centre frequency of between 50kHz and 5MHz. A pulse centred around 500kHz was used for the 500kHz transducer, but the low frequency device was found to have a much higher centre frequency than claimed and in fact had very little energy below 200kHz. A 5 cycle tone burst excitation was therefore used in this case, centred around 250kHz, in order to excite the resonances of the thicker joints. A lower frequency tone burst was not used because as the frequency was reduced, the recovery time of the amplifier increased and a longer stand-off would have been needed. Low frequency transduction issues are addressed in chapter 7.

The output of the amplifier was connected to a digital oscilloscope (Model 9400 – LeCroy) which was connected to a PC which downloaded the digitised time domain waveforms for subsequent processing. In later tests, the waveform generator, oscilloscope and PC were replaced by a general purpose instrument (Model DUI – NDT Solutions Ltd.) developed by one of the collaborators. This instrument was able to perform the data capture and signal processing on-board to give a bond/disbond indication to a factory operator if required.

3.4.2 Signal processing

Figure 3·14 shows a typical received time domain waveform. The front face (water-aluminium interface) reflection (F1) is seen followed by 'ringing' in the joint at the resonance frequency. Towards the end of the time trace, a second front face reflection (F2) is observed as a result of the water path (delay line) reverberation; the spacing of these front face reflections is governed by the transducer stand-off distance and the compression wave velocity of the delay line.

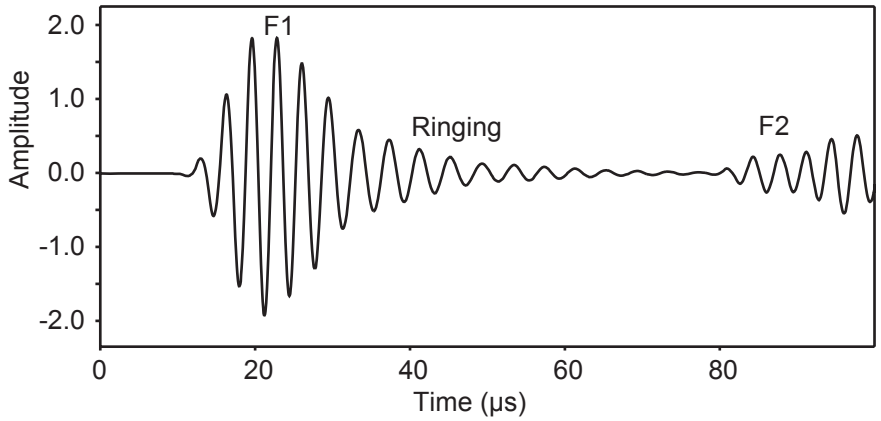

Figure 3·14 Example of time domain trace received when testing a bonded joint.

Several methods can be used to extract the mode 1 resonance frequency from the experimental data. The main requirements are that the signal processing technique must be robust and fast. Various techniques are discussed in the following sections.

3.4.2.1 Amplitude spectrum

The time domain signal can be gated to remove F2 and the subsequent signal, then transformed to the frequency domain using an FFT algorithm. Figure 3·15 shows the result of the FFT, an amplitude spectrum, in which the impulse response of the transducer in seen with a minimum at the resonance frequency. In this case, only mode 1 lies within the transducer's frequency range.

There are several problems in using this technique. Figure 3·16 shows a series of simulated frequency domain responses (produced using DGLOBAL software [96]) from a 2mm aluminium bonded joint with a 0.1mm bondline having a resonance frequency at 593kHz. These signals are representative of signals collected using the amplitude spectrum technique. The centre frequency of the transducers in each case has been increased in 50kHz increments from 550kHz to 750kHz; the bandwidth has

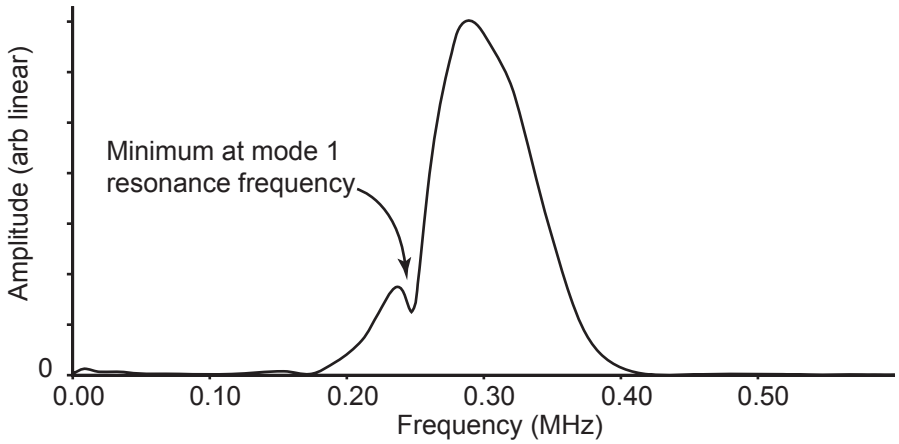

Figure 3·15 Example of amplitude spectrum after gating out F2.

been kept constant at 500kHz. The depth of the minimum is large where the resonance

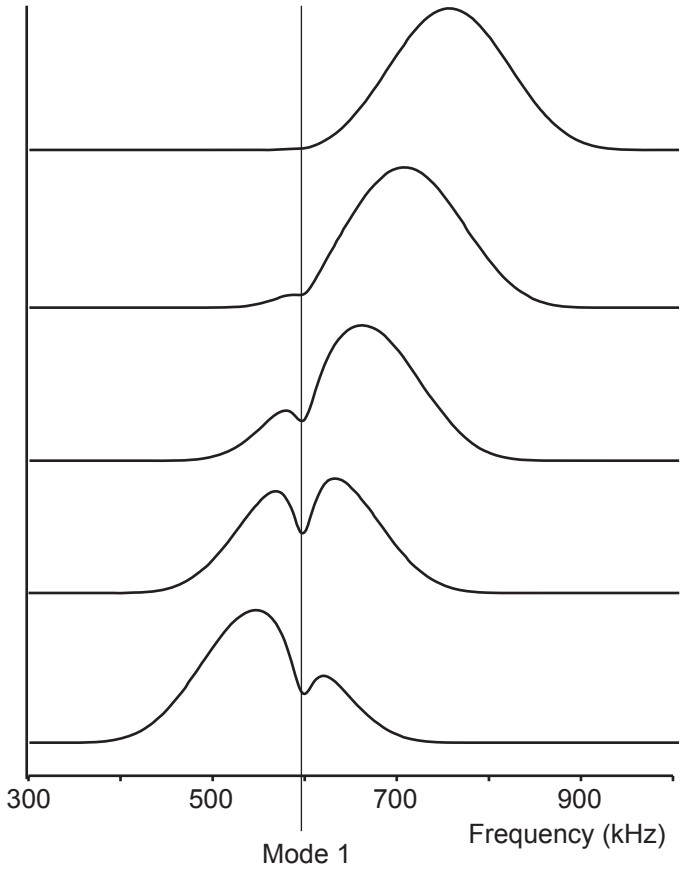

Figure 3·16 Simulated frequency domain responses of bonded joint being tested with transducers of varying centre frequency and constant bandwidth.

frequency is close to the centre frequency of the transducer and mode 1 is therefore most easily detectable. Towards the ends of the tails of the transducer's operating

frequency range, the minimum is barely visible since the resonance is weakly excited. Automatic detection is therefore unreliable. This technique was used by Weise [74], and unreliable detection of mode 1 was one of the main problem experienced.

Additional confusion for a minimum detection algorithm is introduced by resonances in the transducer or delay line reflections which result in additional minima in the response. Where the mode 1 resonance is small, these other minima could be confused for joint resonances.

3.4.2.2 Normalised amplitude spectrum

One alternative approach would be to deconvolve the frequency response of the transducer from the amplitude spectrum, thereby producing a normalised amplitude spectrum, or reflection coefficient spectrum. This is done by dividing the amplitude spectrum from a joint by the response of a front face reference reflection. The process is shown in figure 3·17. This front face reflection is taken from a thick block of adherend material so that no resonances are excited in the transducer's operating frequency range.

In the resulting spectrum, the minimum can be seen much more clearly. The effect of unwanted resonances in the transducer are also theoretically cancelled out (although none are present in this example). Although this method yields better results, there are several disadvantages. The reflection coefficient spectrum in figure 3·17 should have a reflection coefficient of unity away from resonance, but this is clearly not the case; the amplitude of the reference response towards the ends of the operating frequency range is smaller than the response from the joint, resulting in a reflection coefficient above unity in this region. These two measurements were made using the same transducer and excitation, and were set-up in the same manner but on different occasions. This serves to illustrate the differences in results between two independently made measurements. In this case, the absolute difference in measured amplitude is small, but at the ends of the operating frequency range, division of two small numbers results in a significant error in results. Another disadvantage is that the division of the two spectra is computationally expensive; since a read-out of the mode 1 frequency (i.e. bond condition) is required in real time, any additional computation would increase the update time.

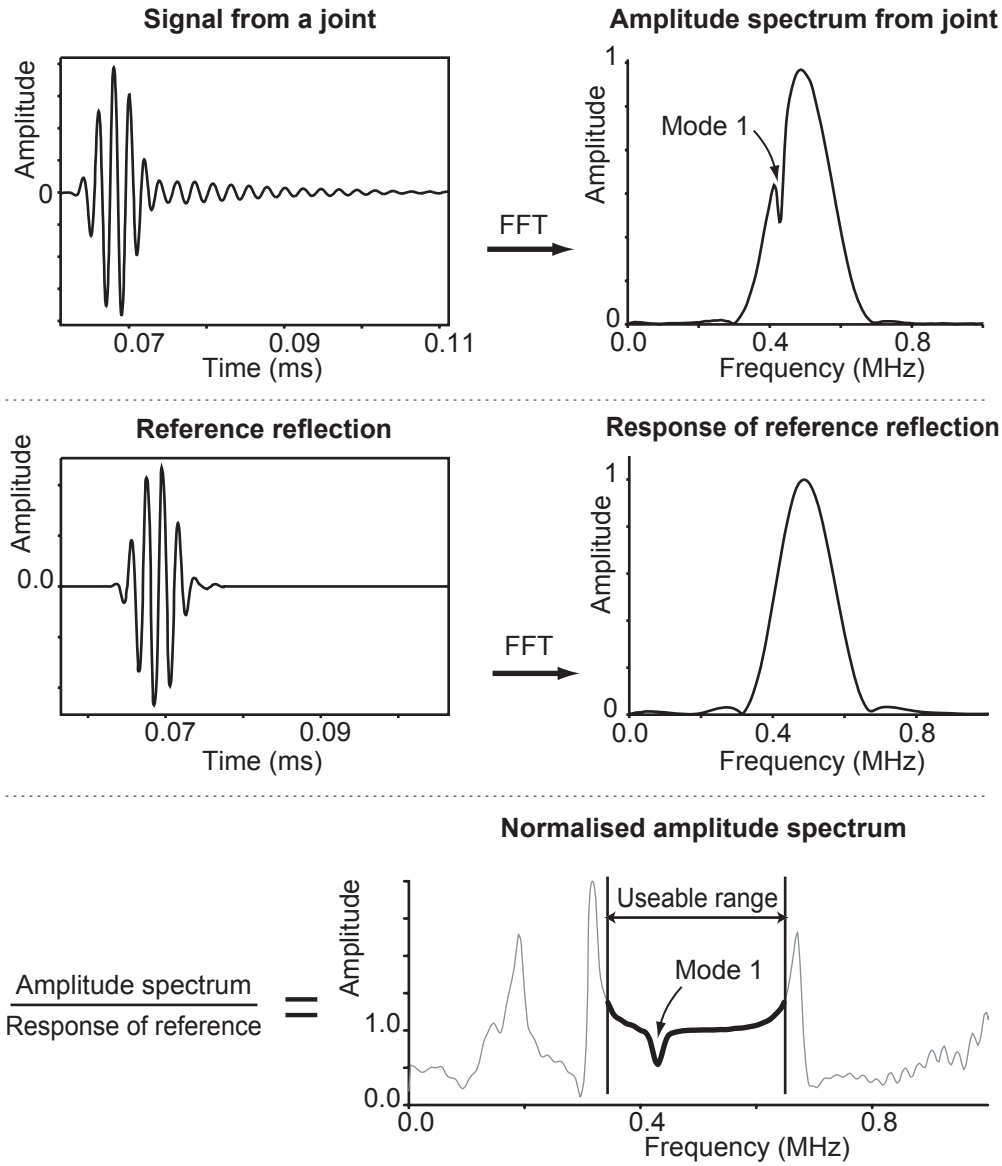

Figure 3·17 Obtaining a reflection coefficient spectrum from experimental data.

3.4.2.3 Wiener filtering

Using the method described in section 3.4.2.2, unwanted additive noise contributes to the distortion of the normalised amplitude spectrum away from resonance. One possible solution to reduce this is to use a Wiener filter [98, 99]. This is an adaptive filter which minimises the mean-square value of error between the filter output and the ideal normalised amplitude spectrum (where the reflection coefficient is unity away from resonance). The algorithm requires a conservative value for the noise level in the system. However, this has the effect of reducing the effective bandwidth of the output.

For this application, the increased frequency domain processing time and the decreased bandwidth would make such a filter unattractive for use, compared to the much simpler signal processing solution described in section 3.4.2.4.

3.4.2.4 Window ringing

An alternative approach, which requires less processing, is to gate out the front face reflection in the time domain, and transform the remaining ringing to the frequency domain. A peak in the response will then occur at the resonance frequency, as shown in figure 3·18. A similar procedure was used by Papadakis [56] who identified

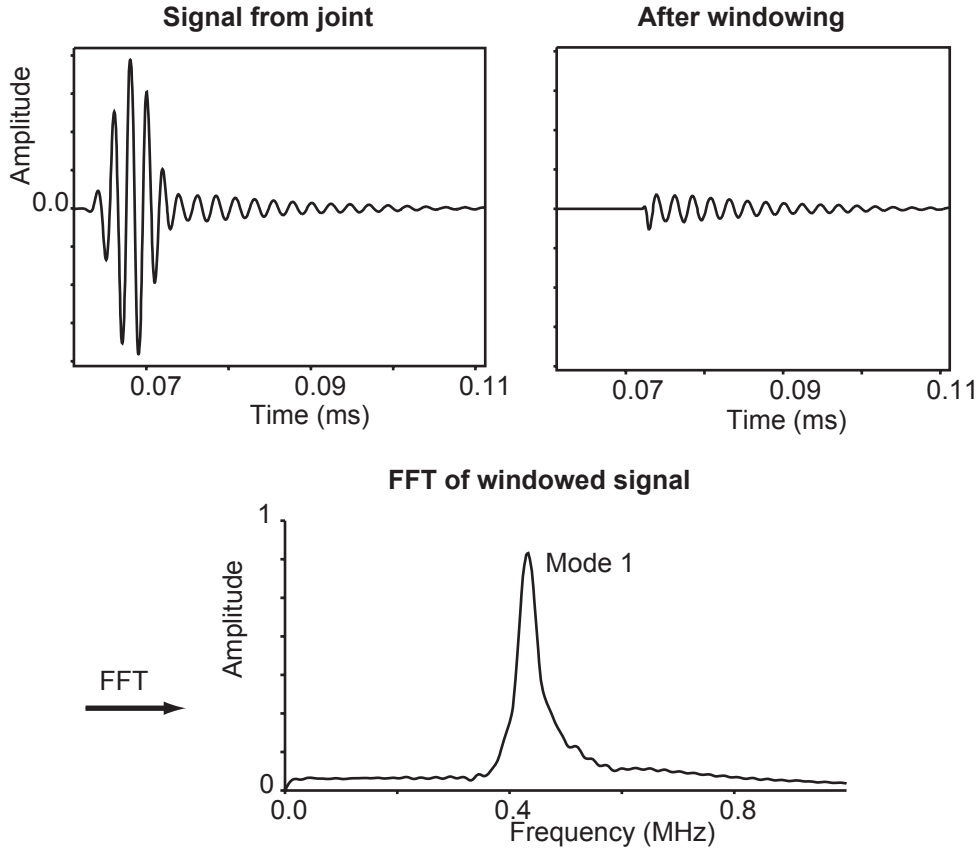

Figure 3·18 Obtaining a resonance peak from experimental data.

adhesive presence from the ringdown or decay rate of the signal from a joint when excited with a high frequency pulse; in this method, part of the 'ringing tail' was gated and the amplitude of the FFT of the signal used to test for adhesive presence.

This method has several practical advantages over the other techniques discussed: gating the time domain signal once the waveform is stored does not take up significant processing time, hence the update rate of the frequency domain display is faster. By eliminating the need for reference reflections, the signal processing becomes simpler and more robust.

In order for this signal processing technique to be successful, the amplitude of the resonance peak must be large enough to be detected. In practice, there will be a level of 'background' noise in the ringing window originating from unwanted resonances in the transducer, reflections in the delay line and incoherent noise. These have a certain amplitude in the frequency domain and must not be incorrectly identified as mode 1 resonance. A threshold amplitude in the frequency domain can be set to avoid this; a mode 1 resonance must have a peak above this level to be identified. The threshold amplitude is dependent mainly on the transducer and delay line, and the level will generally be low compared to the mode 1 resonance peak amplitude. However, this does impose a minimum amplitude for detectability. This is discussed further in chapter 6. The mode 1 resonance peak amplitude depends on several factors, namely amplitude of ringing, the time window used, and the strength of the excitation. These are discussed in the following sections.

3.4.2.4.1 Strength of excitation

The amplitude of the ringing is dependent on the amplitude of the excitation at the resonance frequency. In figure 3·16, it was shown that the minimum at resonance is very difficult to detect towards the end of the transducer's operating frequency range. If the 'ringing window' method is used, the amplitude of the resonance peak will be small at the tails of the transducer response, but a clearly defined resonance peak is still present. This can be much more easily identified than the inflexion which is seen when the whole time domain signal is transformed, as in figure 3·16.

3.4.2.4.2 Amplitude of ringing

The amplitude of the resonance peak depends on the damping of the resonance. Consider a system with low material damping, such as a metal plate. At resonance the damping of the response is determined by the impedance of the surrounding half-space

media; as the half-space impedance rises towards that of the plate, more energy is transferred to the surrounding media, the effective damping increases, and the amplitude of the ringing decreases.

In the adhesive joint case, the surrounding media, namely water (or rubber) and air, are of fixed impedance. There is, however, significant frequency dependent attenuation in the adhesive layer and the relationship between bondline thickness and ringing amplitude is not straightforward; at a particular frequency, the total attenuation increases with bondline thickness; this increase is offset because as the layer thickness increases, the resonance frequency decreases, which has the effect of reducing the attenuation. For this work, an in-depth understanding of the variation of attenuation with bondline thickness is not required; the main concern is simply that the resonance amplitude is high enough to be detected.

The variation in the decay of the amplitude of the ringing with changing bondline thickness has therefore been predicted using the multilayer simulation software (DGLOBAL) described earlier. In the modelling, reflection coefficient spectra were generated for joints with 2mm aluminium adherends and adhesive layers of different thicknesses up to 3mm. In order to obtain a realistic time domain signal, these spectra were convolved with a typical transducer response function to give an amplitude spectrum. The centre frequency of the transducer response was chosen to be coincident with the mode 1 frequency to ensure that the amplitude of excitation at the mode 1 frequency remained constant for each case. Throughout, the bandwidth was set equal to the centre frequency of excitation. The amplitude spectrum was then transformed to the time domain using an inverse FFT. The peak excitation amplitude in the time domain was constant for all the cases. Since the bandwidth remained a fixed proportion of the centre frequency across the range of bondlines tested, the number of cycles in the excitation remained constant. The portion of the time domain waveforms up to the end of the excitation were gated out, leaving just the joint resonance. This gating inevitably removed some of the joint response, as occurs in practice. The maximum amplitude of the remaining signal in the frequency domain was then recorded.

Figure 3·19 shows the modelled time domain signals before gating with attenuative bondlines of 0.15mm and 3.0mm. Interference can be seen between the front face reflection and the joint resonance signals which are out-of-phase. On the figure, the middle and end of the front face reflections are marked; the latter was taken as the start

time for the rectangular window used to extract the mode 1 resonance. Figure 3·20 shows the peak amplitude variation with adhesive thickness for bonded joints with and without attenuation in the adhesive layer.

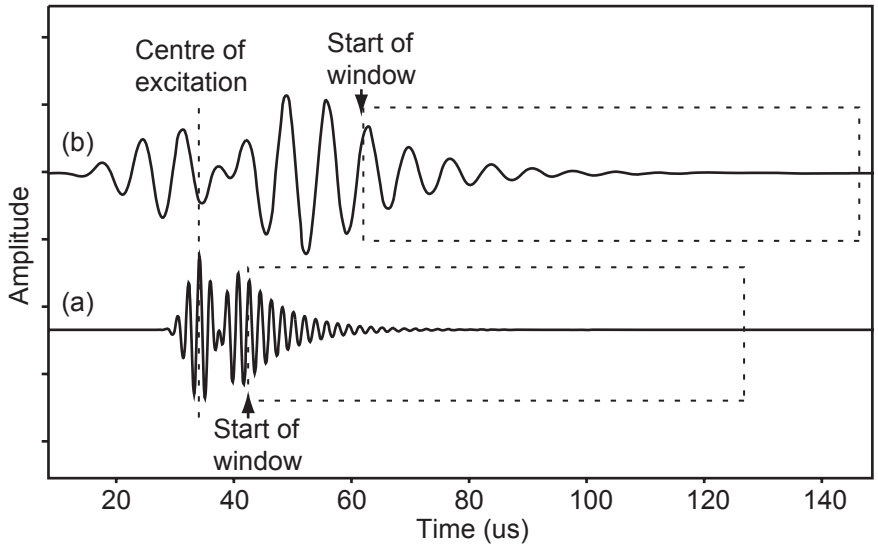

Figure 3·19 Predicted time domain waveforms for bonded joints with 2mm aluminium adherends and (a) 0.15mm and (b) 3.0mm attenuative adhesive layer.

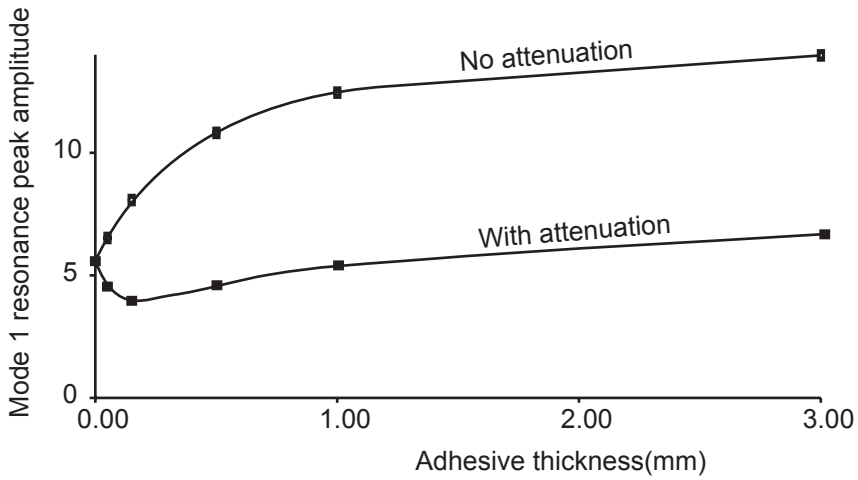

Figure 3·20 Variation of amplitude of mode 1 resonance with bondline thickness for bonded joints with 2mm aluminium adherends with and without attenuation in the adhesive layer.

In order to explain the characteristics of this graph, the bonded joint will be considered by approximating it as a 1D mass-spring-mass model. Considering firstly the adhesive without attenuation, as the adhesive thickness increases, the specific stiffness (see equation 2·3 for definition) of the adhesive layer decreases. The magnitude of response at resonance is inversely proportional to stiffness, hence the resonance peak amplitude

increases with adhesive thickness. Including attenuation in the adhesive now shows some interesting features. Attenuation per wavelength is frequency dependent, increasing with frequency, but the total attenuation is also a function of thickness. As the bondline thickness increases, the mode 1 frequency decreases and the attenuation per wavelength reduces correspondingly. However, this effect competes with the increase in thickness which also affects the total attenuation. Inspection of the curve with attenuation in figure 3·20 shows that where the adhesive is thin and the mode 1 frequency falls quickly with increasing thickness, the total attenuation increases up to about 0.14mm adhesive thickness, where the peak amplitude reaches a minimum. Maximum energy is dissipated in the adhesive at this point. At higher bondline thicknesses, the effect of attenuation decreases and the peak amplitude increases with bondline thickness. The changes in amplitude with adhesive thickness are relatively small, which means that a varying bondline thickness does not cause a problem with detectability.

3.4.2.4.3 Time window

The frequency domain response of the mode 1 resonance is affected by the shape and size of the window in the time domain. This has been broken down into its constituent parts which are discussed briefly in this section, namely start time, length and shape.

Window start time

An ideal time domain signal received during testing is made up of the impulse response of the transducer, which is seen as the front face reflection, and the ringing in the joint. As the amplitude of excitation increases, the amplitude of the resonance builds up and peaks close to the time of the maximum excitation amplitude. The resonance amplitude then decreases as the excitation amplitude falls and will die away exponentially after the excitation has finished. To maximise the amplitude of the resonance peak, the window must start as close as possible to the maximum resonance amplitude. However, the window must start after the front face reflection has died away, otherwise there will be interference between the two parts of the signal. This then defines the earliest possible start time. If a transducer is poorly damped, the front face reflection may continue for some time and reduce the total window length, hence causing a reduction in amplitude. This is one reason why a poorly damped transducer is unsuitable for this technique.

Window length

The window length will also affect the peak amplitude, since a short window will have fewer cycles of the mode 1 resonance and there will be less energy at that frequency. For a fixed window length, if the resonance amplitude is assumed constant, then the resonance peak will be smaller at low frequency. The maximum window length is determined by the stand off distance, or delay line length, between the joint and the transducer. This must be chosen to ensure that a sufficient number of cycles can be captured. In addition, the frequency resolution is $1/T_w$, where T_w is the window length [100]. Therefore, a long time window is desirable to give good frequency resolution.

Window function

The shape of the time domain window can also affect the frequency domain response. Where a signal contains discrete frequency components, such as the mode 1 resonance, windowing in the time domain results in a convolution of the spectrum of the original signal with that of the window function. In this work, a rectangular window has been used and it was considered that leakage might be an issue. This leakage results in the generation of side lobes in the spectrum, but for this technique, it is the frequency of the peak of the main lobe which produces the diagnostic information. A variety of other window functions, such Hanning or an exponential window, can be applied which reduce the amplitude and increase the fall off of the side lobes, but their use will not alter the frequency of the peak of the main lobe. Consequently, the use of a rectangular window was found to be satisfactory, providing a fast, robust method of extracting the mode 1 frequency.

3.5. Results

Joints were produced with 2mm aluminium adherends and various bondline thicknesses, and tested as described in section 3.4.1. The window ringing signal processing technique described in section 3.4.2.4 was used to process the time domain data collected. Figure 3·21 compares the mode 1 frequencies measured experimentally with predicted values based on bondline thickness measured with a micrometer. Excellent agreement between the predictions and experimental results can be seen. Slight variation in bondline thickness was found across the joints, which accounts for the slight scatter in mode 1 measured frequencies from the predictions; mode 1 measurements were made in the centre of the plate to approximate a 1D situation, but

due to the limited reach of the micrometer, it was not possible to make a measurement of the bondline thickness coincident with the transducer centre-line. Instead, several measurements were taken over the plate and the mean thickness used to plot the measured data. This accounts for the slight scatter between the measured and predicted data.

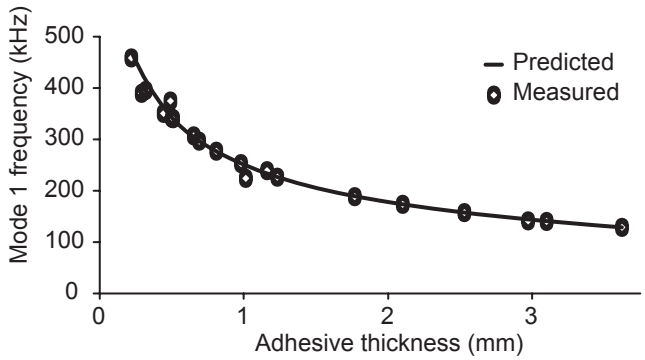

Figure 3·21 Comparison of experimental and predicted mode 1 frequency results for bonded joints with 2mm thick aluminium adherends.

3.6. Conclusions

The analysis presented here has shown that the mode 1 frequency of a joint can be used to identify the bond condition. Where the bondline thickness limits are such that the bonded and partially bonded frequency ranges are separated, a single measurement can be used. In practice, this has been found to be the situation in all structural joints, since a thick bondline has lower cohesive strength and is therefore undesirable. In non-structural applications, a wide bondline thickness variation is often found which can result in overlap between bonded and partially bonded frequency ranges. In this case a single measurement falling in the predicted bonded frequency range below the lowest overlap frequency confirms the joint is bonded; a measurement in the overlap region, however, cannot be used to determine the bond condition alone, and another measurement is required. Possible solutions are discussed in chapter 6.

Experimental validation has shown excellent agreement with frequency values predicted using a 1D model. This also shows that the mode 1 frequency data can be extracted reliably from the time domain signal by gating out the front face reflections and transforming the resulting joint resonance to the frequency domain. Provided the amplitude of the resulting peak is above a threshold, the peak frequency can be easily identified.

Identification of the adhesive thickness limits to avoid overlap, and the signal processing to give a bonded/disbonded indication are key areas of novel work in the development of the test.

The analysis carried out has assumed the joint can be represented by a one-dimensional system, but this may not be valid where the adhesive layer varies in width and thickness in the area under the transducer. Hence, some further work is required to quantify the two-dimensional effects, and this is presented in chapter 4.

In addition, this assessment of the viability of using mode 1 to confirm the fully bonded condition has highlighted several other areas which must be addressed before a system is suitable for use in the field. A dry coupled probe able to make spot measurements would be of great benefit for lab and field use. The development of such a device is discussed in chapter 5, and a discussion of laboratory testing and industrial test results using this device is given in chapter 6.

The predictions made also show that for a typical automotive joint the frequencies involved can cover a wide range and are at low frequency. Transduction issues, and the development of a low frequency transducer are discussed in chapter 7.

Chapter 4

Suitability of One-Dimensional Approximation

The mode 1 predictions made in chapter 3 assume the joint is one-dimensional. This is not necessarily the case in the automotive industry. The effect on the viability of the mode 1 technique when testing real joints which are not one-dimensional, is investigated in this chapter.

4.1. Introduction

A one dimensional system can be approximated experimentally where the transducer is aligned normal to the surface, the joint is larger than the transducer diameter, and the layers in the joint have constant thickness in the region under test. Unfortunately, real automotive joints are not like this; bondlines can vary significantly in width and placement, primarily due to incorrect application. This may result in the transducer contact region being over a step change in bond condition at the edge of the adhesive layer. Where the adhesive bead is narrow compared to the transducer diameter, there effectively becomes a narrow strip of adhesive under the contact region. These cases are illustrated in figure 4·1(a) and (b).

There can also be significant variation in bondline thickness under the contact region giving a tapered adhesive layer, as illustrated in figure 4·1(c). This arises mainly from variations in fit between the mating panels especially where they are pinched and riveted together. In order to investigate the effect these conditions have on the mode 1 response, the different cases have been modelled using Finite Element (FE) analysis.

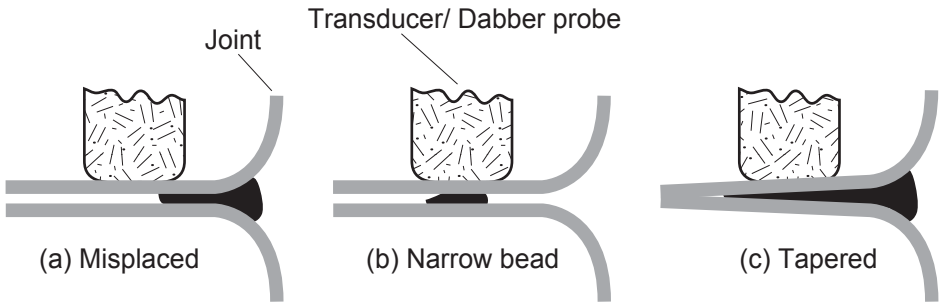

Figure 4·1 Cross-sections of automotive joints with (a & b) a step change in bond condition, and (C) a tapered adhesive layer under the transducer contact region.

4.2. Finite Element model set-up

FE software [101] has been used which was specifically developed for modelling wave propagation in solids using a time marching algorithm. General modelling points applicable to all the FE models described in this chapter are given in this section.

The cases outlined in section 4.1 have been modelled as a joint in cross-section. 2D plane strain quadrilateral 4 node elements are used. Basic rules for wave propagation models which have been developed by previous workers [88] dictate the mesh size and time step. The side length of an element must be between 8 and 20 times smaller than the wavelength of the highest frequency in the excitation signal. The bandwidth was limited by using a 5 cycle tone burst to keep the number of elements per wavelength for the highest frequency component within the above bounds. In this work, 15 elements were used per wavelength at the higher frequency where the amplitude was -40dB below the maximum amplitude. The time step was chosen so that the fastest wave would not propagate more than 80% of the way across an element in one time step.

The transducer was modelled by applying a sinusoidally varying force to a number of nodes on the surface, across a width of 30mm, which was the diameter of the transducer used experimentally. The amplitude of the force at each node was weighted spatially using a Hanning function to approximate the output pressure distribution of a transducer. Models were run for many time steps and the resulting displacements were monitored periodically at the same nodes as the excitation was applied. At each point, 50μs of time domain data was collected. The monitored displacements were then also weighted with a Hanning function and integrated to produce a waveform which is representative of the signal received by a transducer in pulse-echo. The material elastic properties used for the layers in the model are as indicated in table 3·1. However, it was not possible to include attenuation or the water half-space in the FE model.

4.3. Transducer over step change in bond condition

4.3.1 FE model

A step change in bond condition has been modelled by a 2mm aluminium plate with a 1.5mm adhesive layer attached to one half, as shown in figure 4·2. This represents a through-thickness model of a joint with a step change in bond condition from partially bonded to fully disbonded. This simple situation has been modelled to gain an understanding of the effects on the mode 1 frequency, from which the same concepts

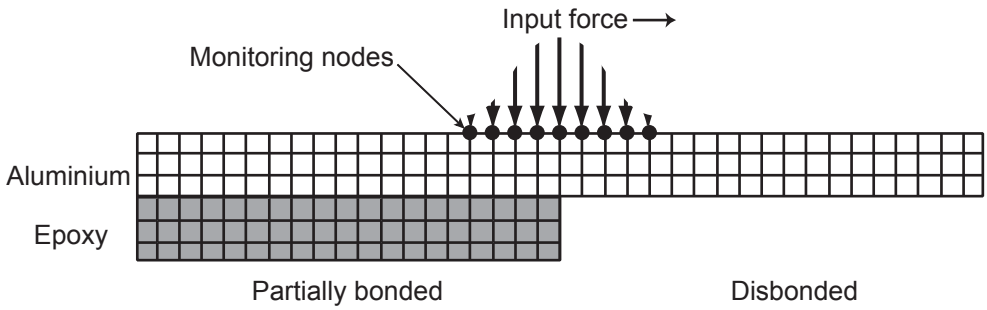

Figure 4·2 FE model used to investigate the effect of a step change in bond condition.

can be applied to a three layer joint. The model was made 150mm wide so that there would be no guided waves reflected from the ends of the joint during the monitoring period. A 5 cycle tone burst excitation was applied at a frequency centred around 500kHz, which corresponds approximately to the mode 1 frequency of the partially bonded part of the joint. In order to study the effect of the step change, several models were run; the transducer was positioned initially entirely over the fully disbonded plate, then moved progressively across the step change in bond condition.

4.3.2 Experimental validation

Experimental validation was carried out with a prepared sample of similar layer thicknesses to the FE model. Adhesive was bonded to half of the plate with the step change in bond condition extending approximately 60mm (twice the transducer diameter) in the z-direction (normal to the cross-section), as shown in figure 4·3. It was

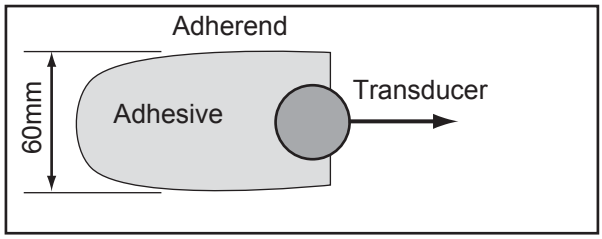

Figure 4·3 Top view of experimental set-up for validation of the effect of step change in bond condition.

tested air backed in an immersion tank as described in chapter 3, section 3.4.1. As with the FE model, a 5 cycle tone burst excitation centred around 500kHz was used with the transducer operating in pulse-echo. The transducer was placed 25mm from the front face of the joint and moved progressively across the step change in bond condition with the time domain signals being recorded at each position.

4.3.3 Results

The time domain waveforms from the FE model and experimental validation were processed by gating out the front face reflections, as described in chapter 3, section 3.4.2, and the resulting mode 1 frequency and peak amplitude recorded. This procedure was adopted to mimic real testing conditions.

Figures 4·4 and 4·5 give the FE and experimental results respectively, showing the variation of mode 1 frequency and peak amplitude with the percentage of the area of the transducer over the bonded region. The FE model is 2D assuming infinite extent in the z-direction (normal to the cross-section) for both the joint geometry and the transducer (i.e. excitation and monitoring nodes). Hence the area of the transducer over the step varies linearly with position. In the experimental case, the transducer is circular, and the actual area of the transducer over the step has been calculated at each position. The peak amplitudes have been normalised to the case where the transducer is entirely over the bonded region

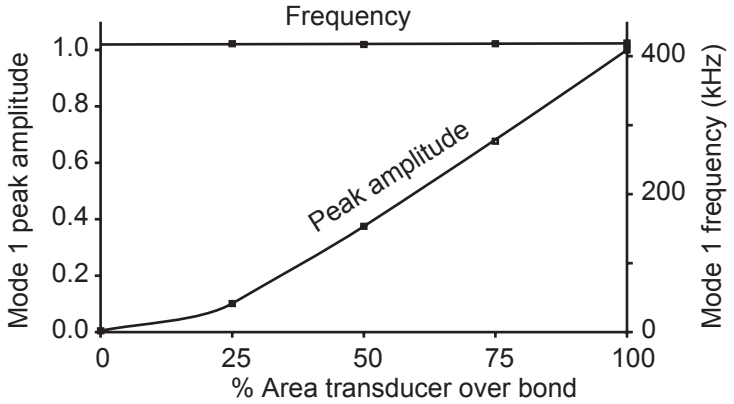

Figure 4·4 FE results showing variation of mode 1 frequency and peak amplitude with area of transducer over the bonded region.

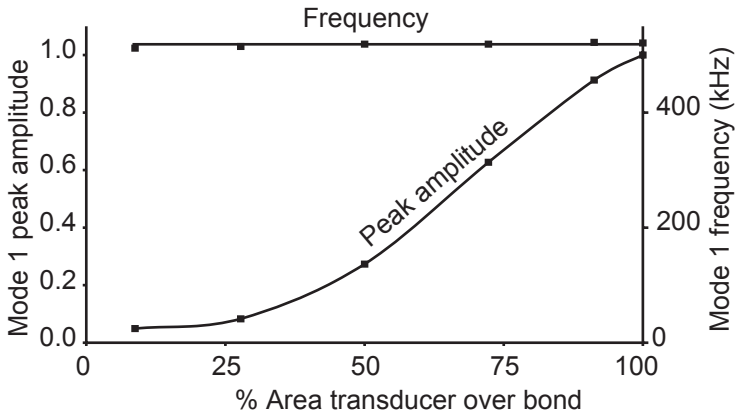

Figure 4·5 Experimental results showing variation of mode 1 frequency and peak amplitude with area of transducer over the bonded region.

It is clear from these graphs that the mode 1 frequency of the bonded region does not change where the transducer is partly over the step, for the range of joints tested. The peak amplitude decreases as the transducer moves away from the bonded region. A transducer which behaves as a piston source with uniform pressure over the face would be expected to show a linear decrease in resonance amplitude with area of the transducer over the resonant system of interest. In these tests, the pressure distribution across the transducer face is not constant which causes the non-linearity in the variation of amplitude with area. Further work would be required to establish whether these findings are applicable in the general case.

4.3.4 Analysis

From these results it appears that the resonance in the bonded region is unaffected by the presence of the adjacent unbonded region. This was also found to be the case when the model was extended to three layers. In order to confirm observation, another FE model has been constructed in which the resonance frequencies of the two parts are closer together in frequency and can be excited simultaneously. Figure 4·6 shows this FE model which comprises a steel plate with a step change in thickness from 4mm to 7mm. The two parts have fundamental through thickness resonance frequencies of 750kHz and 450kHz respectively. Each part of the plate was 150mm wide and excitation was applied to nodes spanning 30mm. A two cycle tone burst centred around 600kHz with a Hanning window was used to excite the resonances in both parts of the plate. As before, the transducer (i.e. the nodes being excited and monitored) was moved progressively across the plate and the displacements at the monitoring nodes recorded and processed.

Figure 4·7 shows the variation in amplitude of both resonance peaks with position across the step change. Again, this was validated experimentally using the same procedure as described earlier, but with a steel plate with a step change in thickness from 5mm to 6mm. Experimental results are shown in figure 4·8. In both cases, no change in the mode 1 frequencies of the two parts was found as the transducer was moved across the step change

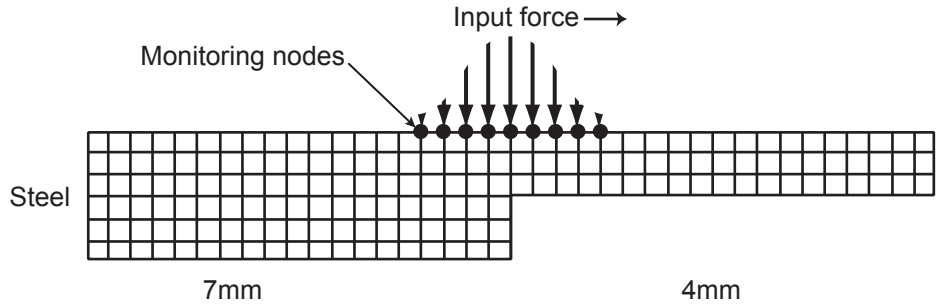

Figure 4·6 FE model of steel plate with step change in thickness from 4mm to 7mm.

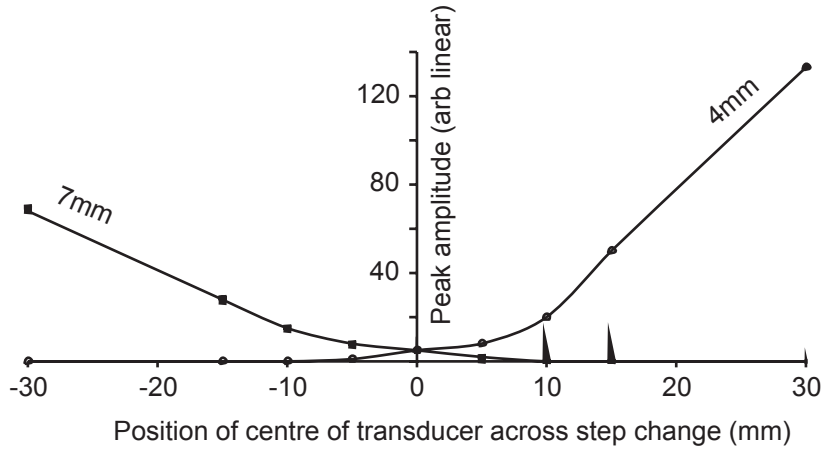

Figure 4·7 Variation of peak amplitude of the 4mm and 7mm mode 1 resonances with position across the step change; FE results.

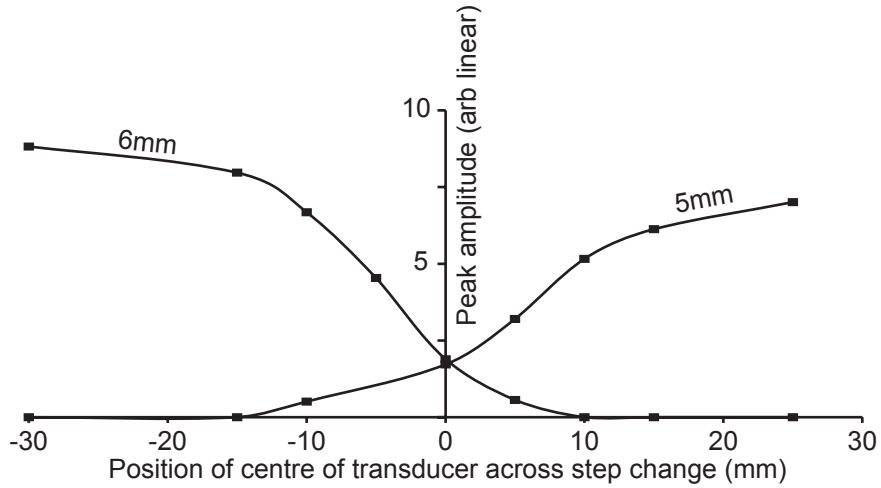

Figure 4·8 Variation of peak amplitude of the 5mm and 6mm mode 1 resonances with position across the step change; experimental results.

These results confirm that the mode 1 frequency is unaffected by the adjacent system and that the strength of the resonance is dependent only on the strength of the excitation; at the frequency where through thickness resonance occurs in the plate, there is no coupling between the two parts of the plate. In other words, the vibration in the two parts of the plate is independent.

4.3.5 Implications for disbond detection

The objective of this work was to investigate what happens to the mode 1 frequency where the bondline is varying in width in the region under test. Results have shown that a step change in bond condition under the contact patch does not affect the measured mode 1 frequency of the bonded region. This means that the frequency range predictions discussed in chapter 3 are still valid. The amplitude, however, decreases proportionally to the area of the bonded region under the contact patch. In practice, amplitude measurements cannot be used to identify the location of the edge of the adhesive relative to the transducer since they are sensitive to coupling conditions (see chapter 5) and the bondline thickness (see chapter 3). Where only a small portion of the bonded region is in the contact patch, the mode 1 peak amplitude will be small and it is likely that it will fall below the threshold level, giving a disbonded reading.

Since amplitude measurements are unreliable, to give greater spatial resolution and accurately assess the adhesive width, a small test region is desirable so that several measurements can be taken across the width of the joint. The optimum transducer diameter will therefore depend on the application. For rapid testing, where only complete absence or a small amount of adhesive need be identified as a disbond, a large diameter contact area can be used. To accurately map out the bond thickness and width for optimisation of the bonding process, a small diameter contact area is needed.

4.4. Taper

4.4.1 FE model and validation

A joint with a tapered adhesive layer has been modelled by a 2mm aluminium plate with an adhesive layer of increasing thickness attached to the plate, as shown in figure 4·9. Again, the two layer joint case was modelled in preference to a bonded joint to minimise the size of the model, giving faster computation time.

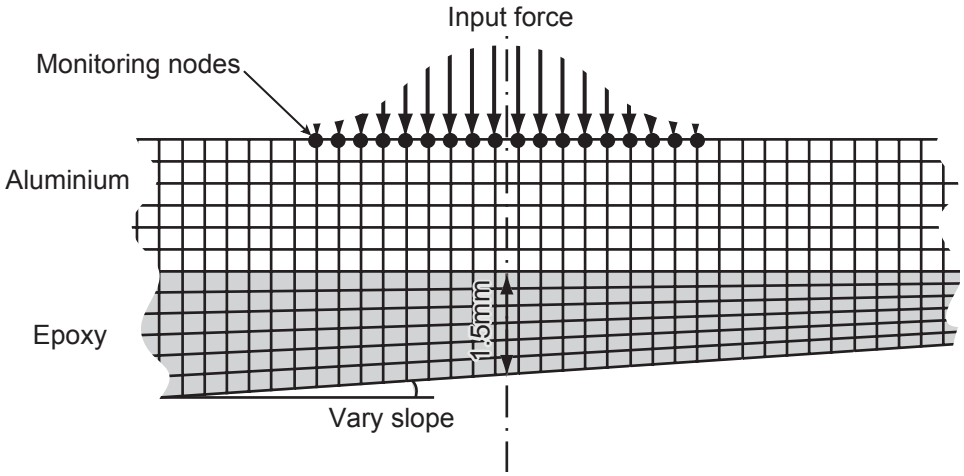

Figure 4·9 FE model used to investigate the effect of a tapered adhesive layer.

In this model, the position of the transducer remained fixed and the slope of the adhesive layer was varied for each run, but the mean thickness was held constant at 1.5mm. The centre of the transducer was coincident with the point where the adhesive was 1.5mm thick. The transducer diameter was set to 60mm to emphasise the effect of the taper. Excitation with a 5 cycle tone burst was centered around 500kHz, which corresponded approximately to the mode 1 frequency predicted by the 1D model with an adhesive layer of 1.5mm. Experimental validation was carried out in an immersion tank as described previously, using samples prepared with different degrees of adhesive taper.

4.4.2 Results

Mode 1 frequency and peak amplitude results have been plotted against adhesive slope. The adhesive thickness at the centre of the transducer could easily be controlled in the FE model. For the experimental results, readings were taken at several locations on each tapered joint sample; the slope of the adhesive in each sample remained roughly constant, but the adhesive thickness at the centre of the transducer varied. Hence a direct comparison of mode 1 frequencies cannot be made. Instead, the measured mode 1 frequency was normalised at each test point by dividing by the values predicted for a one-dimensional case. This was obtained using the multilayer model (DGLOBAL) with the bondline thickness at the centre of each test point measured using a micrometer. The FE and experimental results are shown in figures 4·10 and 4·11 respectively. The peak amplitudes have been normalised by the value at 0º taper.

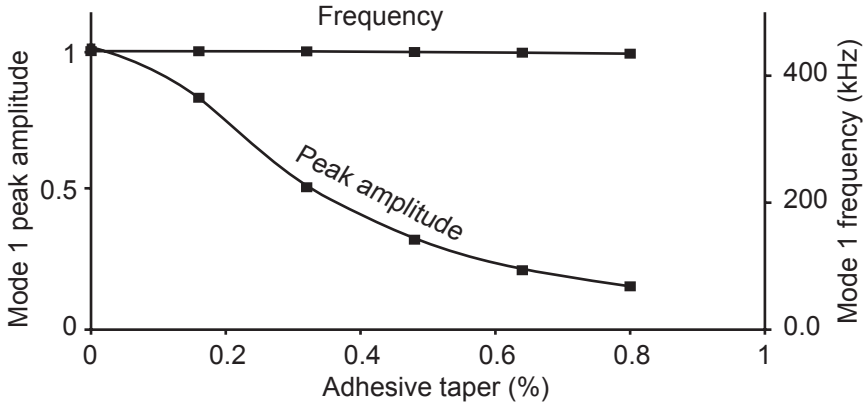

Figure 4·10 FE results showing variation of mode 1 frequency and peak amplitude with adhesive taper.

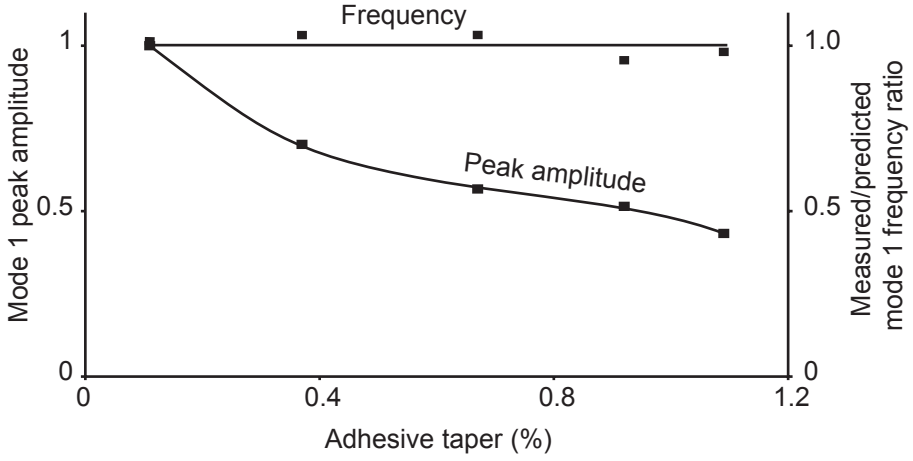

Figure 4·11 Experimental results showing variation of mode 1 frequency and peak amplitude with adhesive taper.

4.4.3 Analysis

An understanding of why the mode 1 frequency does not change but the resonance peak amplitude decreases can be obtained from the results of the FE modelling. The FE model output out-of-plane displacements at each monitoring node with time. The mode 1 frequency was extracted from these time domain signals and the bondline thicknesses at the position of each monitoring node were then calculated. Figure 4·12 shows the variation of mode 1 peak frequency with bondline thickness across the monitoring nodes of a joint with a 1º taper. Also shown on the figure is the variation of mode 1 frequency predicted using the 1D model across the same adhesive thickness range.

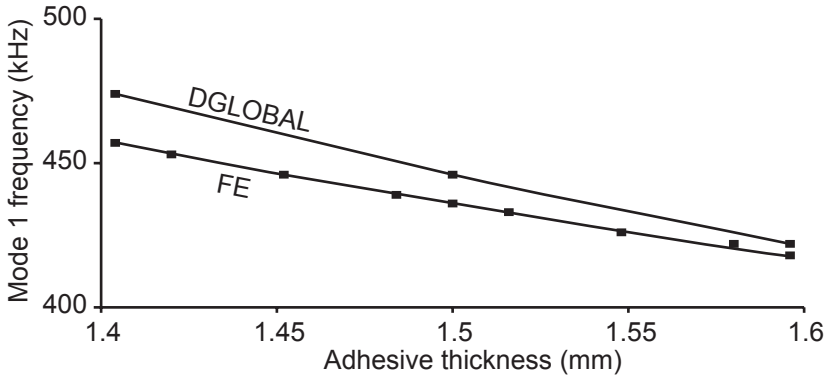

Figure 4·12 Frequency-nodal position contour plot for a partially bonded joint with a tapered adhesive layer.

This result shows that the mode 1 frequency extracted from the individual node time traces is determined by the bondline thickness at that node, and so decreases with increasing adhesive thickness. Comparison with the 1D predictions shows that a reasonable approximation to the mode 1 frequency obtained from the time trace at a given node is given by the 1D model with a corresponding adhesive thickness.

When the waveforms from all the nodes are integrated or summed, the effect is to 'smear' the individual resonances together. The effect on the overall response is twofold. The mode 1 frequency at the centre of the test area is dominant (assuming that the taper is linear). As the taper increases, the spread of the frequencies increases and the resonance peak becomes flatter than with no taper, and appears as though the damping has increased, or the Q (Quality) factor has decreased. This phenomenon can clearly be seen in the experimental results.

The Q factor has been measured for the responses at several degrees of taper using the half power points method; Q is given by:

$$Q = \frac{\omega_n}{\omega_2 - \omega_1} \qquad (4\cdot1)$$

where ω_n is the frequency at peak amplitude, $\hat{p}$, and ω_2 and ω_1 are the frequencies at $\hat{p}/\sqrt{2}$ on either side of the peak. Figure 4·13 shows the variation of measured Q obtained from experimental results taken from prepared bonded joints with varying degrees of taper.

The increase in Q with adhesive taper can be clearly seen. At low adhesive taper, there is not much change in Q since the damping is dominated by material damping and radiation into water.

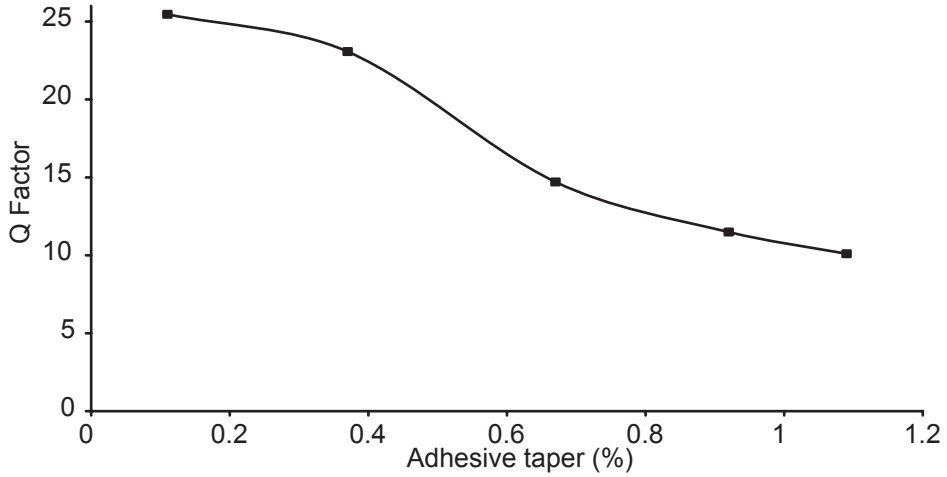

Figure 4·13 Apparent damping ratio variation with adhesive slope for experimental results from bonded joints with 2mm aluminium adherends and tapered adhesive layers.

4.4.4 Implications for disbond detection

The results have shown that the mode 1 frequency is in effect unchanged where the adhesive taper varies but where there is a constant mean adhesive thickness in the region under test. As taper increases however, the amplitude of the resonance peak decreases. In real joints, the slope has been found to be a maximum of 1% and at this level, the resulting peak amplitude decrease is over 50%.

The experimental results are for a 30mm diameter transducer and tests were done in an immersion tank. When a dry coupled probe of small diameter contact patch is used instead, the variation in thickness over the contact area is much reduced. The effective damping will therefore be less.

4.5. Transducer misalignment

The modelling in chapter 3 assumes the transducer is aligned normal to the joint. In practice, with measurements made in the field some misalignment is inevitable. Drinkwater [102] has used holders and collars to mount wheel and static dry coupled probes to minimise misalignment, but these devices were designed for high frequency work where misalignment is more critical. At the low frequencies used for this mode 1 test, misalignment is less critical but the effect on the mode 1 technique has been nevertheless briefly been investigated.

Where a transducer is aligned at an oblique incidence to a structure, some mode conversion will take place, and shear waves can be generated in the structure from the incident compression waves. These have through thickness resonances which occur at

lower frequency than the compression waves and can therefore potentially introduce unwanted resonances which are detrimental to the test. Fortunately, the shear attenuation in the adhesive is very high. The damping of any shear resonances will therefore be high. In use, the test is carried out with a dabber or wheel probe (see chapter 5) and the effect of alignment has been confirmed using a dabber probe aligned at 5º to a bonded joint with 2mm aluminium adherends and a 0.2mm bondline. To ensure coupling remained constant, a thin layer of coupling gel was applied to the contact tip. Figure 4·14 shows the received signals in the frequency domain after processing. No shear modes are present in the signal, and the peak remains at the same frequency.

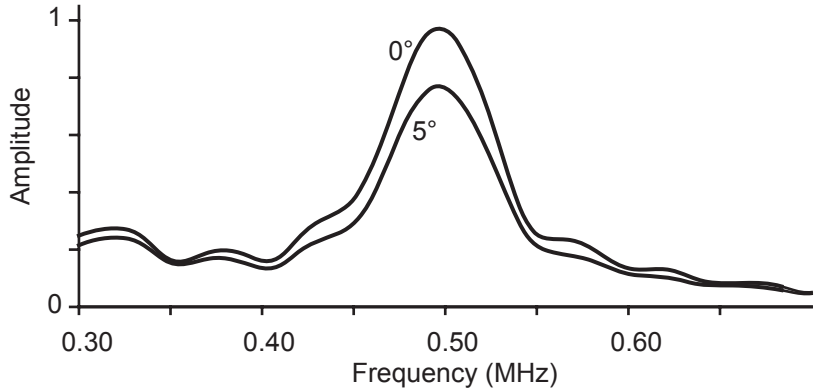

Figure 4·14 Response of processed signals from a bonded joint using a dabber probe inclined at 0º and 5º to the surface.

It is also important that the mode 1 resonance peak is detectable in the event of misalignment. The results in the figure show that even at 5º, the peak amplitude is relatively large due to the low test frequency. This means that a dabber probe can be applied by hand without having a detrimental effect on the results.

4.6. Conclusions

The effect on the mode 1 test discussed in chapter 3, where real joints are tested has been investigated through FE modelling and experiment. Real adhesive geometries can vary in width and thickness in the part of the joint being tested. The principal conclusion is that the mode 1 frequency results predicted using a 1D model are not adversely affected by real geometries.

Where there is a step change in bond condition under the transducer, the resonances in both parts are independent and if they fall within the transducer's operating frequency range will both be excited. Fully disbonded joints and, in many cases, partially bonded

joints have a mode 1 frequency well above the transducer's operating frequency range and will not be excited. For a constant sound pressure across the transducer or contact face, the mode 1 resonance amplitude is proportional to the bonded area under test. Therefore, unless the bonded area under test is very small, the mode 1 resonance can be detected.

Where the adhesive thickness varies, the mode 1 frequency is given by the mean adhesive thickness; the amplitude is a function of the degree of taper. In fact, the mode 1 frequency at any point is determined by the local adhesive thickness. Therefore, where a varying thickness is being tested, the resonances across that adhesive thickness range are smeared together, and it appears as though the damping is increasing, and Q factor decreasing.

Although there would be no change in the mode 1 frequency, both these test conditions are affected by the contact tip size. A small contact tip is better suited for accurate detection of adhesive width and placement since several measurements can be made across the joint width. For rapid testing of a large area, a larger tip diameter is more suitable, but is less sensitive to detecting adhesive width. Over a tapered adhesive layer, since the spread of the resonance peak is determined by the variation in bondline thickness, a small contact tip will have a relatively narrow resonance peak compared to a large diameter contact area.

It was also found that transducer misalignment was unlikely to pose a problem in practice due to the low test frequencies.

Chapter 5

Dabber probe

5.1. Dabber probe motivation

After the viability of the mode 1 technique for disbond detection was established, it became evident that a system comprising a transducer and delay line for making dry coupled spot measurements would be very convenient to evaluate the mode 1 technique on real structures (rather than using an immersion tank) and allow test results to be collected on real automotive structures without the use of couplant.

Analysis of the adherend and adhesive thickness specification provided by automotive manufacturers indicated that many of the automotive joints requiring testing had aluminium adherends around 2mm thick and a bondline thickness range of 0.1-0.4mm. This gives a predicted mode 1 frequency range in the region of 400-600kHz (more precisely, 377-592kHz). These joints could therefore be tested with a commercially available 500kHz transducer (V301 series – Panametrics) which has almost 100% bandwidth. With this adhesive thickness range, mode 1 frequency ranges for bonded and partially bonded joints are well separated in frequency, hence a single mode 1 measurement can be used to detect whether a joint is fully bonded. A dry coupled spot probe for making mode 1 measurements could therefore be of great benefit to industry.

Dry coupled probes can be obtained commercially. For example, Ultran [103] produce low frequency transducers with a rubber shoe attached and contact transducers to which a dry coupled delay line can be fitted. These devices can be obtained with a centre frequencies of 250kHz and 500kHz having bandwidths of up to 70% (at -6dB) and element diameters of between 19mm and 50mm. However, a test area of less than 10mm diameter is required to achieve good spatial resolution, and the required adhesive range (0.1-0.4mm) could not be tested with this bandwidth. Further, as described in section 5.2.4, conventional delay lines (unless of large diameter) cannot be used since they will pollute the diagnostic signal. Consequently, such commercial devices are not suitable for this application and work in this chapter describes the development of a dry coupled delay line with a novel approach to reducing unwanted reflections in the delay line. This device has been termed a ‘dabber’ probe.

5.2. Development

The design of the dabber probe has been divided into two sections, namely contact tip and delay line. These parts are defined in figure 5·1, and issues relating to their design are discussed in sections 5.2.3 and 5.2.4. Here, an exploded view is shown for clarity; in reality, the contact tip and delay line are formed in one part from the same material.

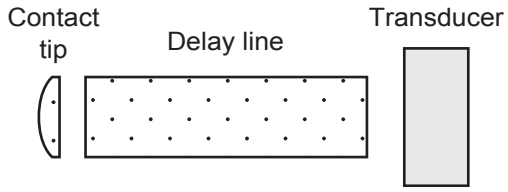

Figure 5·1 Exploded view showing contact tip and delay line of dabber probe.

5.2.1 Requirements

There are several requirements which must be satisfied for the successful development of a dabber probe, as listed below. Many of these parameters are interrelated and are addressed in the following sections.

- Dry coupling
- Low attenuation
- Must not introduce any unwanted reflections into the ringing window
- Provide delay between successive front face reflections
- Small contact tip
- Easily manufactured

5.2.2 Materials

Delay lines for ultrasonic transducers are widely available (typically made from a low loss plastic such as Perspex) but generally require the use of couplant. Elastomers are an obvious choice of material type for dry coupling since, under load, they can conform to the microscopic undulations on the surface to give good acoustic coupling, and have already been used successfully in commercially available transducer delay lines [103], and in the literature [102, 104, 105]. Readily available rubbers such as natural and Nitrile rubber exhibit high attenuation to ultrasound waves and are therefore generally unattractive. However, the advent of low-loss rubbers which exhibits attenuation an order of magnitude less than any of the readily available rubbers offers a significant improvement for dry coupling [104, 105]. Acoustic properties for the rubbers mentioned are given in table 5·1. Based on the previous successful application of the

low-loss rubber material for dry coupling with low attenuation, it has been selected for use as the delay line material. The composition of this material has been withheld for commercial reasons.

Material	Density (kg/m^3)	Compression wave velocity (m/s)	Compression wave attenuation (Np/λ)
Low loss rubber	925	1562	0.010
Natural Rubber	1002	1502	0.132
Nitrile rubber	1047	1800	0.391

Table 5·1 Material properties of rubber for dry coupling (after Drinkwater [102])

5.2.3 Contact tip

The design of the contact tip is essential for achieving good dry coupling. The factors which affect dry coupling are:

- Surface roughness
- Rubber material properties
- Applied load
- Contact tip profile

Contact pressure requirements

In order to achieve perfect coupling, the contact pressure between the rubber and the surface must be high enough for the rubber to conform to the peaks and troughs which are present on the surface at a microscopic level, the size of which is indicated by the surface roughness. Previous work [102] has shown that for p1000 grade abrasive paper, for example, a contact pressure of 0.3MPa is required to achieve perfect acoustic coupling. The testing carried out in the automotive industry will be on painted surfaces which have a significantly lower surface roughness. To provide a conservative estimate of the required contact pressure, 0.3MPa has been used for the development work described here.

Tip geometry

The pressure distribution across the face of a rod with a square cut flat end, when pressed against a flat surface, is very high at the edges and low elsewhere. A flat undeformed contact tip is therefore unsuitable. In contrast, a hemisphere has highest

contact pressure at the centre, decreasing with radius. An analytical solution for this case can be obtained from Hertzian theory [106]; the pressure distribution, *p(r)*, is given by:

$$p(r) = p_0 \sqrt{\left(1 - \left(\frac{r}{a}\right)^2\right)} \qquad (5{\cdot}1)$$

where p_0 is the maximum pressure, r is the radius, and a is the contact area. Unfortunately, this hemispherical geometry cannot be used. In order to explain this, consider a hemispherical delay line with diameter equal to that of the transducer, as shown in figure 5·2.

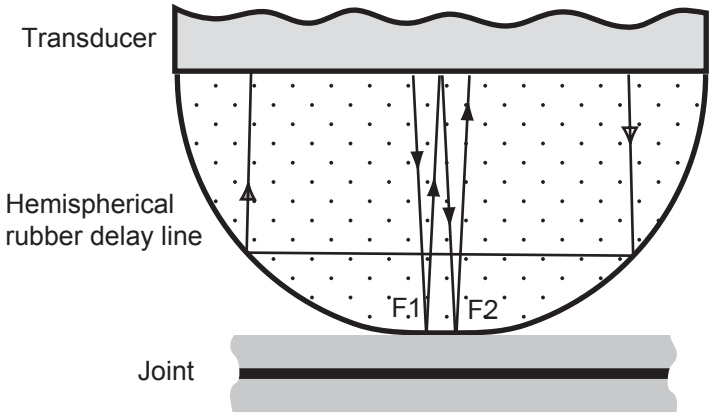

Figure 5·2 Ray paths in a hemispherical contact tip.

In the deformed state, when pressed against a joint, the contact area will be flat and parallel to the transducer face. The diameter of the contact patch in this example is 10mm, but will obviously depend on the applied load and the radius of the hemisphere. In the figure, ultrasound waves are shown as rays normal to the transducer face; only two ray paths are shown for clarity. The first is a ray towards the centre of the transducer, which is reflected directly from the flat contact region giving the front face reflection (F1). Successive reverberations in the delay line (F2 etc.) follow. It is during the period between F1 and F2 in which the ringing in the joint is captured and it is important that there are no other reflections of significant amplitude returning to the transducer during this time, otherwise they will interfere with the mode 1 resonance.

The second ray path in the figure shows a reflection from the curved part of the hemisphere, adjacent to the contact region, which is backed by air. At the point shown, the hemisphere is at 45º to the ray path. This ray returns to the transducer but has travelled approximately 15mm further, hence it will arrive 10µs later than F1 and will be received during the ringing window, which is undesirable.

This situation can be avoided by having no material backed by air adjacent to the contact tip. If this cannot be achieved, due to a delay line of different shaped cross section for example, any uncoupled material should be parallel to the transducer face. For purposes of contact tip design, a hemispherical tip cannot therefore be used. Instead, a domed contact tip was used which would deform to give a flat contact face. No analytical solution exists for the contact pressure distribution in this case and so Commercially available Finite Element (FE) software [107] was used to obtain an appropriate tip shape.

The dabber probe system was modelled in axisymmetry. It was found that including the delay line has some effect on the distribution of the pressure at the contact tip, and was therefore included in the model. The completed dabber probe has a lossy rubber layer bonded to the delay line (see section 5.2.4) which provides additional circumferential constraint around the outside of the delay line. This affects the contact tip deformation, hence this additional layer has been included in the model. The elastic properties of the low-loss rubber used in the model have been measured previously [102]; Poisson's ratio is 0.5 and Young's Modulus is 1.3MPa.

The tip diameter and radius of curvature define the profile of the tip. Several factors affect the choice of tip diameter. Firstly, the diameter of the contact patch needs to be smaller than 20mm, which is the width of a typical joint, so that several measurements can be made across the width. A maximum contact diameter of 10mm was therefore chosen. Secondly, as the contact region increases, the maximum contact pressure decreases for a given load. Where the device is applied by hand, this becomes a limiting factor. Thirdly, a small contact region will have a high contact pressure and excellent coupling, but since the area is small, the amplitude of the joint resonance will be small which is undesirable. For the 10mm diameter chosen, low amplitude was not found to be a problem in use. However, where a small contact tip is needed, the minimum required amplitude of the joint resonance limits the minimum diameter.

The dabber probe is intended for manual application and the load applied has therefore been limited to 25N. In the FE model, the load is applied via a stiff plate to represent the load being transferred into the delay line via the transducer. At the surface of the contact tip, contact elements were used to model the contacting surfaces.

Various contact tips shapes were modelled to find a profile which would give the required contact pressure across a suitable area with the chosen applied load (25N). The results shown in the remainder of this section are for a contact tip geometry which has a contact pressure greater than 0.3MPa over a suitably large area. The FE model used is shown in its undeformed and deformed states in figures 5·3(a) and (b).

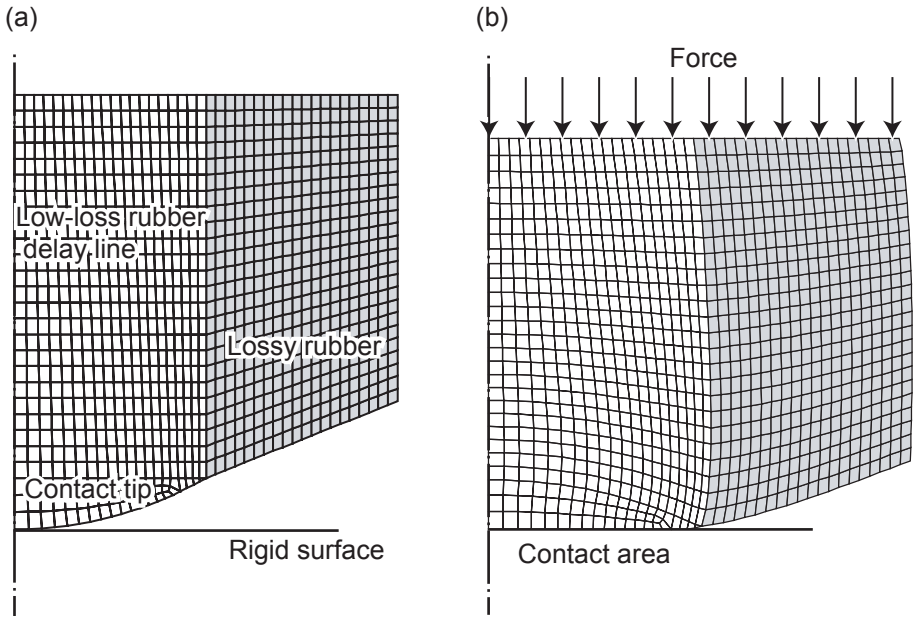

Figure 5·3 FE model of axisymmetric dabber probe shown in the (a) undeformed state and (b) deformed state with 25N applied.

Figure 5·4 shows contact pressure distribution produced by the model for a domed tip of 10mm diameter and radius of curvature of 10mm when a load of 25N is applied. This is sufficient to make the tip flat in its deformed state. The contact pressure is greater than 0.3MPa (minimum contact pressure) over a radius of 4.15mm. Since a conservative estimate of the minimum required contact pressure was used (i.e. 0.3MPa) this tip profile was deemed suitable.

5.2.4 Delay line body

It is important that stray reflections which are not directly from the contact face are minimised to avoid unwanted signals in the ringing window used to extract the diagnostic mode 1 data. It was shown in section 5.2.3 that reflections from the non-

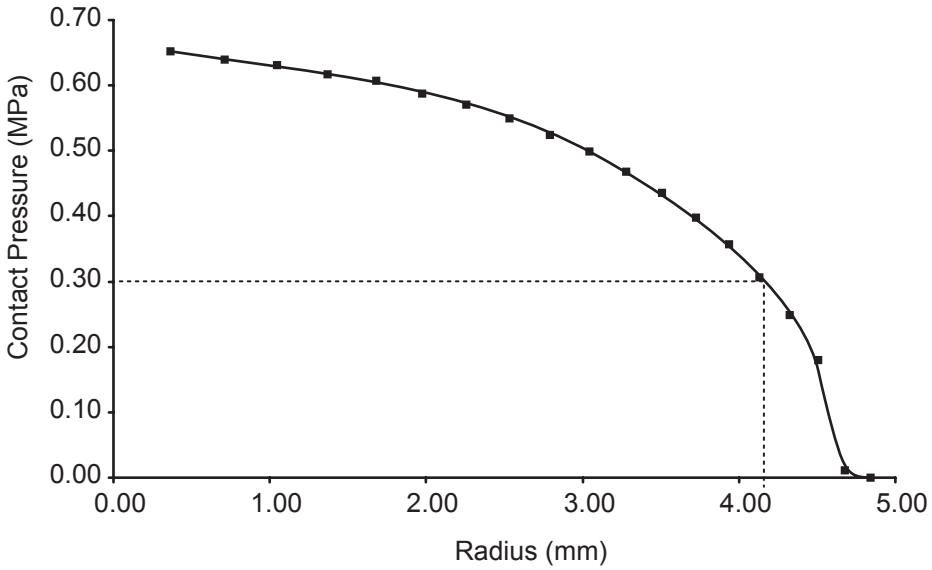

Figure 5·4 Contact pressure distribution for a 10mm diameter contact tip with 10mm radius of curvature and an applied load of 25N.

contacting area around the contact tip could be one source. Another significant source is from reflections from the side walls of the delay line. At the low frequencies required for the mode 1 test, beam spread is significant. A 10mm diameter delay line has been chosen to match the contact tip diameter, hence there will be some reflection from the side walls. This has been illustrated, as before, with a ray based approach. A divergent beam can be considered as a series of diverging rays produced from a point. Figure 5·5 shows a cross section of a transducer coupled to a cylindrical delay line with the tip in the deformed shape pressed against a joint. Only two rays are shown for clarity. Rays

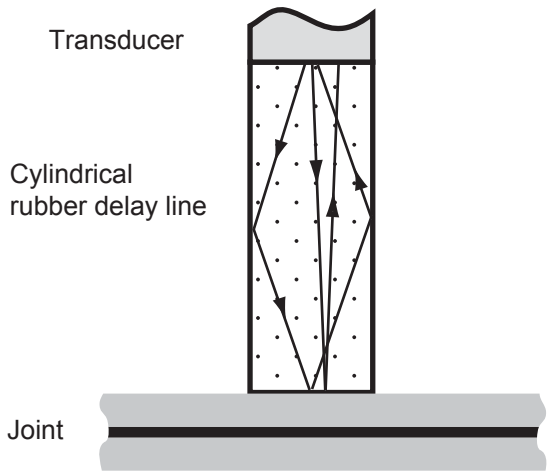

Figure 5·5 Ray paths in a cylindrical delay line of 10mm diameter with a flat deformed contact tip.

at a shallow angle of incidence are reflected from the flat contact tip and return directly to the transducer (i.e. F1, F2 etc.). At a larger angle of incidence, rays are first reflected from the side walls of the delay line. The path of the ray is dependent on the angle of incidence and geometry, and some can be reflected several times before returning to the transducer. Of greatest concern for the mode 1 technique are those which return to the transducer after one or two reflections. These will have travelled further than F1 and if they arrive before F2, they will interfere with the mode 1 resonance in the ringing window.

Attenuation of side wall reflections

Although a large diameter delay line would eliminate this problem, this is not practical for testing since the diameter would need to be larger than the joint width. An alternative solution has been found by arranging for the side wall reflections to be attenuated. This has been achieved by surrounding the side walls with a highly attenuative material, well matched in impedance to the low-loss rubber. At the side walls there will then be almost complete transmission into the attenuative layer. If the attenuation is high enough or the layer thick enough, there will be no reflection from the outer face. A suitable material is available commercially (Aptflex F28 – National Physical Laboratories) in 10mm thick tiles. This has a density and longitudinal velocity of 1082kg/m^3 and 1440m/s respectively, giving an impedance of 1.558MRayl which is only 7% higher than low-loss rubber. Reflections at the side walls of the delay line will therefore be very small. Attenuation of F28 has not been characterised by the manufacturers at low frequency, thus this has been measured using the normalised amplitude spectrum technique described in appendix A. Figure 5·6 shows the variation with frequency of the attenuation and transmission loss through 20mm of the material.

The dabber probe will operate centered around 500kHz which gives an attenuation of 40dB over the 20mm return path through the tile. In reality, the attenuation is much higher since waves will travel through the material at oblique incidence, therefore the path length in the F28 is increased. This fact may allow a reduction in tile thickness whilst still giving satisfactory results.

The F28 sheets are relatively stiff and cannot be wrapped around an axisymmetric delay line. A square bar of cross-section 10x10mm was used instead, with a domed contact tip as described earlier. F28 was then cut and bonded directly to the faces of

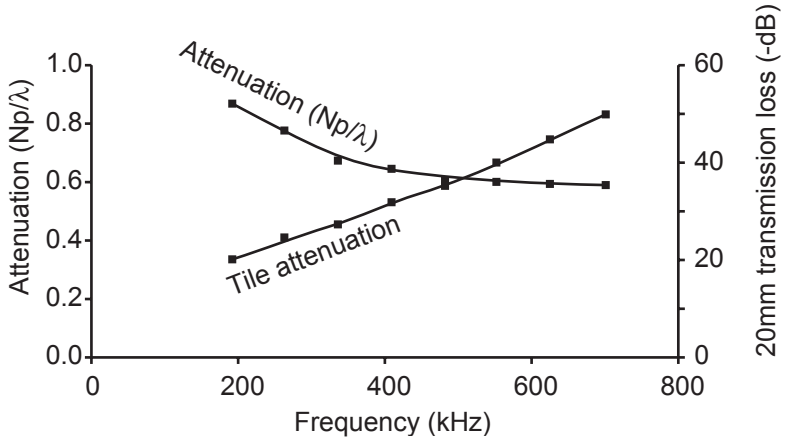

Figure 5·6 Variation of attenuation and transmission loss with frequency in F28 attenuative rubber.

the delay line; cynoacrylate adhesive (Loctite 404) was found to be suitable for this purpose. The delay line assembly was then aligned concentrically with the transducer and bonded directly to the face. The dabber probe construction is shown in figure 5·7.

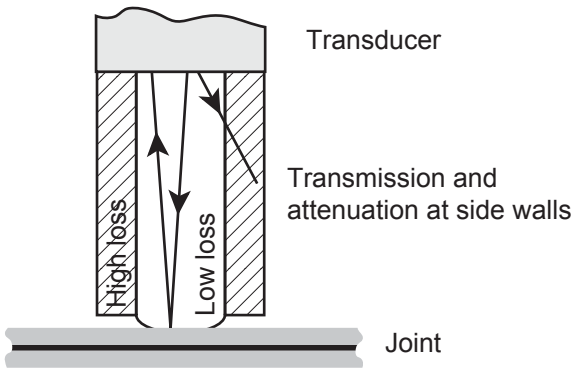

Figure 5·7 Schematic diagram showing construction of the dabber probe.

The effectiveness of surrounding the delay line with attenuative rubber is illustrated in figure 5·8. This shows the received time domain signals for a 500kHz transducer coupled to the delay line described above, with the side walls surrounded by air, and then with 10mm of F28 bonded to each face. The extent of the contribution from side wall reflections without F28 is clear. With F28 on the faces, the amplitude of the side wall reflections is very small.

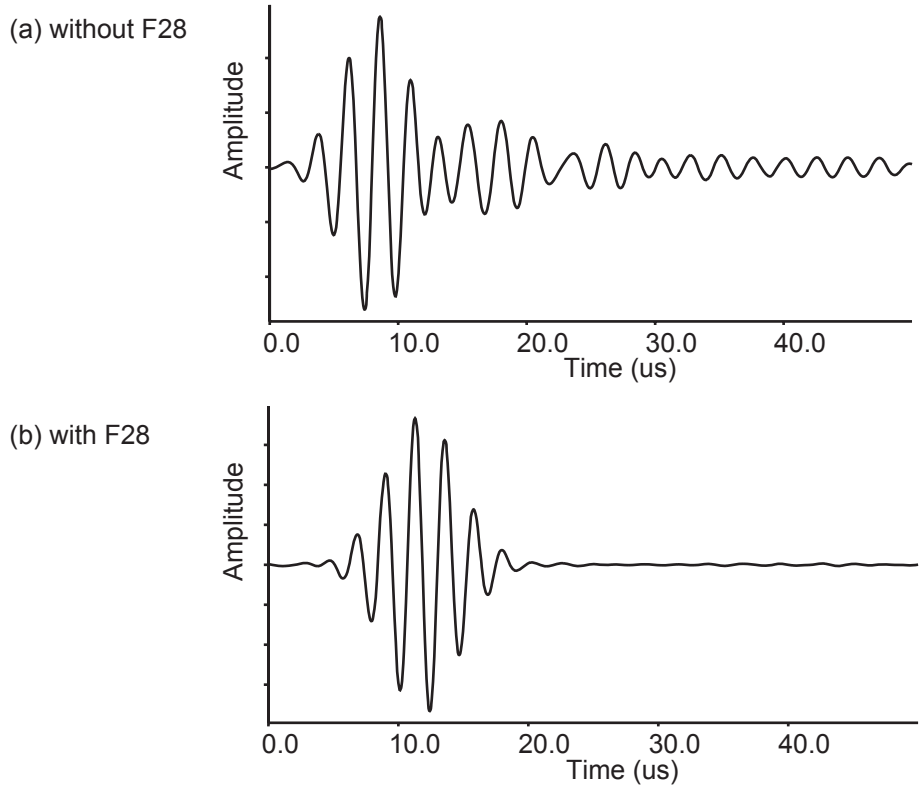

Figure 5·8 Received waveforms from the tip of a dabber probe surrounded by (a) air and (b) F28 attenuative rubber.

Delay line length

The final parameter to be defined is the length of the delay line. This determines the time between successive front face reflections (F1,F2), T_f. This is related to the maximum length of the ringing window, T_w, by:

$$T_f = T_w + T_e \qquad (5{\cdot}2)$$

where T_e is the time taken for the response of the transducer to the input excitation to die away (i.e. the duration of the front face reflection), which is specific to the transducer and excitation. The 500kHz transducer used with the dabber probe is used here as an example. The impulse response of the transducer corresponds to about 6 cycles at 500kHz in the time domain, lasting 12μs. A window length of 20μs has been chosen to give a clear frequency domain results, which corresponds to 10 cycles at 500kHz. A return time of 32μs is therefore required which is given by 25mm of low-loss rubber. At low frequency, T_e will be longer, so for the same length delay line T_w will be shorter. It is desirable to have the window as long as possible so as to capture as many cycles as realistically possible in order to give a large resonance amplitude and good frequency resolution; this will ensure the mode 1 resonance peak for a bonded

joint is well above the threshold amplitude and the peak frequency can be identified accurately. Hence it is desirable to increase the delay line length for low frequency use. The maximum length has however been found to be limited my the manufacturing process. The low-loss rubber is compression moulded and problems with surface tearing on square sections have been encountered on delay lines greater than 40mm long.

Delay line attenuation

The total attenuation, *A*, in the rubber delay line at a frequency ω, is given by:

$$A(\mathrm{dB}) = \frac{8.69 t \omega A(\mathrm{Np}/\lambda)}{c} \qquad (5{\cdot}3)$$

where *t* is the length. At 40mm long, this gives a total attenuation of 1.11dB at 500kHz. This is not a significant reduction in the mode 1 resonance signal, hence attenuation in the delay line is not significant.

5.3. Comparison with immersion test results

Figure 5·8 has shown that side wall reflections have been almost entirely eliminated by adding F28 to the side faces. In this section a direct comparison is made of the response from joints using the dabber probe and immersion testing. The dabber is intended initially to test the 0.1-0.4mm bondline thickness range with 2mm aluminium adherends (mode 1 between 377 and 592kHz) and so joints around this range have been used for the comparison. Two similar 500kHz transducers (V301 series – Panametrics) have been used, one being bonded to the dabber probe, and the other set-up in the immersion tank, as described in chapter 3, section 3.4.1. Excitation was provided with a pulse centred around 500kHz and the results processed by gating out the front face reflections and transforming the remaining mode 1 resonance to the frequency domain (see chapter 3, section 3.4.2.4).

A dabber probe with a 25mm long delay line was used for the comparison and applied dry to prepared joints by hand. The compression wave velocity of the rubber is slightly higher than for water and to enable the signals to be gated at the same times, the standoff distance in the immersion tank was set to 23mm. Figure 5·8 compares the time domain waveforms for three cases: no joint, 0.29mm and 0.44mm bondlines. Also shown in the figure is a comparison of the frequency domain responses of the processed waveforms; a window length of 20μs was used, starting at 16μs as indicated in the figures. The waveforms obtained from a disbonded joint (figure 5·8(a)) show

negligible amplitude in the window, as expected. For the bonded cases (figure 5·8(b) and (c)) the mode 1 resonance is clearly visible. It occurs at the same frequency for dabber and immersion testing, as expected; any slight difference in mode 1 frequency is due to small variations in bondline thickness across the sample and the testing points not being necessarily coincident. The peak amplitude for the dabber results are in fact much lower than the immersion results since the contact area is 10mm diameter on the dabber probe, compared with the 30mm diameter immersion transducer. In the plots, the receiver amplifier gain was set to 42dB for the dabber probe results, and 20dB for immersion.

5.4. Conclusions

A dabber probe has been developed to dry couple a transducer to bonded joints via a low attenuation rubber delay line. Surrounding this by attenuative, well matched rubber avoids problems arising from side wall reflections. A 10mm diameter contact tip of 10mm radius of curvature has been found to give adequate dry coupling to smooth metal and painted surfaces with a predicted load of 25N applied by hand. Stray reflections from the contact tip are avoided by having any uncoupled material adjacent to the contact tip parallel to the transducer face.

Comparison of results from joints tested with a dabber probe and in an immersion tank have shown good agreement, and that the mode 1 resonance can be clearly identified using the dabber. This dabber probe therefore provides a means of dry coupled testing, allowing spot measurements to be made on real structures.

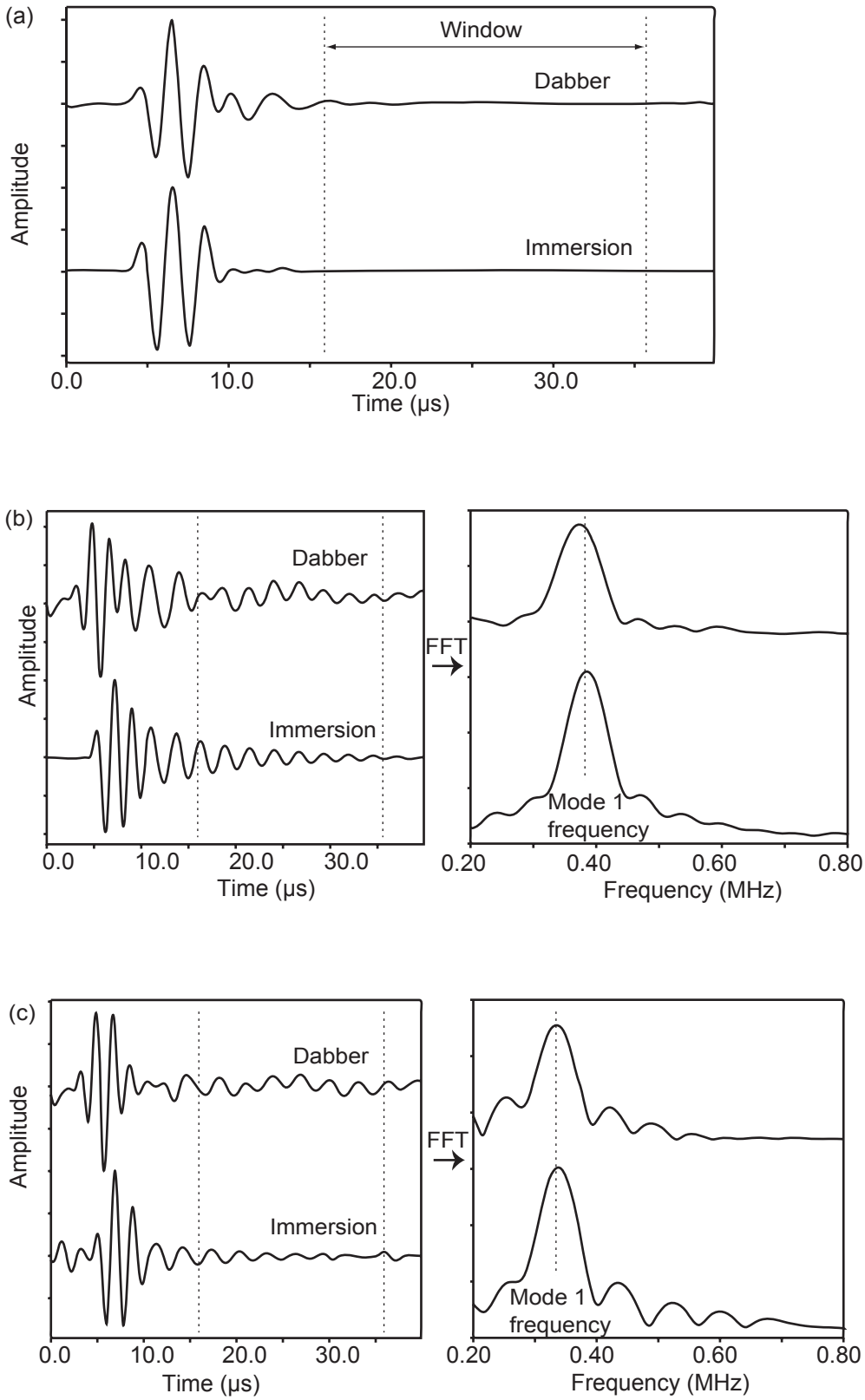

Figure 5·9 Comparison of time and frequency domain responses from measurements made in an immersion tank and with a dabber probe for (a) no joint, and bonded joints with (b) 0.29mm and (c) 0.44mm bondlines.

Chapter 6

Industrial testing

6.1. Introduction

In chapter 3, a test technique for disbonds was established based on the mode 1 frequency of a joint and this was validated experimentally on prepared samples in an immersion tank. In order to transfer this to the industrial setting, a dabber probe was developed in chapter 5 to enable dry coupled spot measurements to be taken. The principal industrial requirement, namely testing automotive structural joints, can be met with a commercially available 500kHz transducer. This chapter discusses the details of the testing protocol and presents the results obtained from automotive type structures with bondline thicknesses in the 0.1-0.4mm range.

6.2. Testing

6.2.1 Strategy and procedure

The basic principle of the test is that if the measured mode 1 frequency of a joint falls into the predicted frequency range, then it is confirmed bonded. For the joints tested in this chapter, there is no overlap between bonded and partially bonded mode 1 frequency ranges. Possible solutions where this overlap exists are discussed in section 6.5. The testing procedure is summarised in a flow chart, figure 6·1, and details relating to the particular stages are discussed in the following sections.

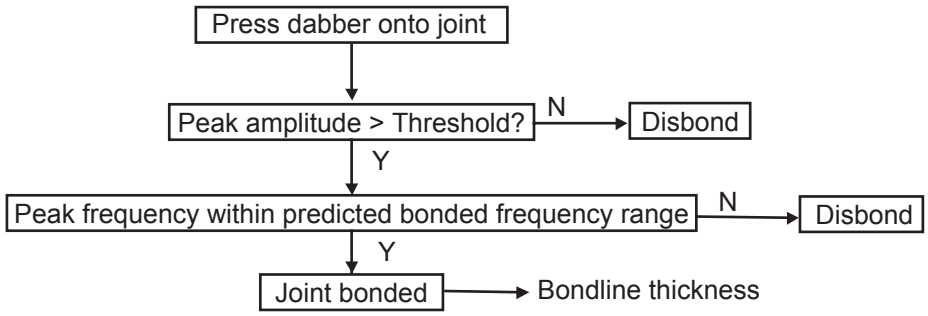

Figure 6·1 Flow chart showing mode 1 test procedure.

6.2.2 Frequency ranges

Prior to testing, the adherend thickness and the limits of the adhesive thickness will be known. This enables the mode 1 frequency ranges to be defined. Frequency ranges for each set of adherend and adhesive thickness ranges which are found on the vehicle structure can be stored in a lookup table. If the adhesive thickness is also to be

determined for each test point, an array of values can be stored for each adherend thickness combination and interpolation performed to give the bondline thickness from the measured mode 1 frequency. This procedure has been adopted for the results presented in this chapter.

6.2.3 Threshold amplitude set-up

In the absence of bonded joint resonance, either because the dabber is not coupled, or the joint under test is disbonded, there will still be some 'background' signal present in the ringing window, as mentioned in chapter 3, section 3.4.2.4. Contributions are made up from side wall and contact tip reflections in the dabber probe which have not been fully attenuated, resonances in the transducer, and incoherent noise. The transducer resonances can be reduced by adjusting the start time and duration of the window, but some artefacts may still remain, especially when low frequency transducers are used. Where the amplitude of response of such a signal is significant and lies in the mode 1 frequency range, the portion of the impulse response in the ringing window may be deconvolved (in the frequency domain) from the signal from a joint, thereby removing the unwanted resonances. However, this would require a reference reflection and would increase signal processing time making it unattractive for fast, robust testing.

This background signal must not be incorrectly identified as a joint resonance, and an amplitude threshold is set in the frequency domain to overcome this. The background level will be greatest where the probe is uncoupled since almost perfect reflection will occur at the contact tip. Hence the effect of transducer resonances or insufficient side wall attenuation will be greatest. The maximum amplitude of the uncoupled frequency domain signal in the ringing window is taken as the threshold. By using this amplitude threshold, 'false positive' readings as a result of poor coupling would be avoided. For example, if the probe was not applied with sufficient force, or the tip became covered in dust, the may be a resonance peak but it would be below the threshold level.

6.2.4 Coupling

To achieve good dry coupling a load of about 26N has been shown to give adequate contact pressure with the dabber described in chapter 5. Clearly good coupling is needed to maximise the joint resonance in the ringing window, and there are several approaches which can be taken to achieve this.

A pragmatic approach is simply to press the dabber hard onto the joint. This has been the approach taken for collection of results presented here and has proved to give excellent results. During testing, if a maximum is detected above the threshold, the joint is confirmed bonded and the bondline thickness deduced. If a maximum is not detected, the load should be increased; if there is still no peak above the threshold, then the joint is disbonded.

Drinkwater [102] developed a dry coupled static probe for use at high frequency and added an adjustable collar around the contact tip area which acted as a depth stop. When the collar touched the surface, the tip displacement hence load and contact pressure were known. In that application, alignment was critical which the collar also provided. For automotive testing, a collar arrangement is not well suited for curved surfaces and increases the overall diameter, reducing the access to joints.

6.3. Structures

6.3.1 Industrially prepared top-hat sections

Top-hat sections were prepared by an automotive manufacturer using the same materials and production processes (i.e. bonding, riveting, curing) as the automotive structures. They comprised 2mm aluminium adherends front and back, and were bonded and riveted every 40mm to give an intended bondline thickness variation of 0.1-0.4mm. None of the joints were made partially bonded, hence this condition was created in places by machining away the rear adherend. The bond condition at the test points could then be identified from visual inspection. Figure 6·2 shows a diagram of the structure.

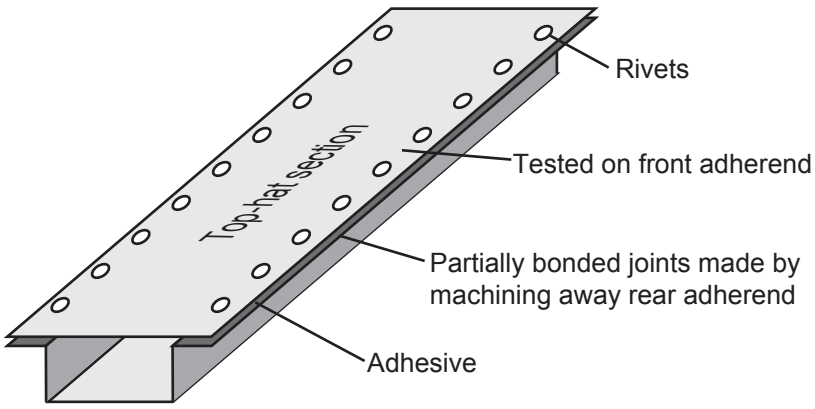

Figure 6·2 Top-hat structure used for testing.

Joints were tested using the mode 1 technique. To assess the accuracy of the measurements, frequency values in a 'mode 1 frequency–bondline thickness' table were interpolated to give corresponding bondline thicknesses (termed 'mode 1 thickness'). These were compared with measurements made with a ball tipped micrometer (termed 'micrometer thickness'). For the results to be valid, the micrometer measurements had to be coincident with the centre of the mode 1 test point. Ultrasonic testing was done at random points on the joints by hand, rather than using a scanning frame which would record positional information. The mode 1 test point location was identified by coating the joint surface with a very thin film of WD40 lubricant; after the dabber was pressed onto the surface the contact area was just visible in the thin oil film. A slight depression at the centre of the contact tip (which occurred as a result of shrinkage during moulding) was also visible on the surface and aided location of the micrometer measurements. Note that the WD40 was not needed for coupling. Many measurements were taken, recording the mode 1 frequency and amplitude of the processed signal, micrometer measured thickness and visual inspection of bond condition.

6.3.2 Pre-production body shell

A pre-production aluminium vehicle was made available for testing. Unfortunately, the vehicle was fully painted which meant that many joints suitable for testing were covered by seam sealer to prevent water ingress and could not be tested. Several joints on the vehicle were, however, identified for testing, but only two could be accessed from both sides for micrometer measurements. An example of a joint tested is shown in figure 6·3.

Figure 6·3 Example of bonded joint tested on automotive structure.

The adherend thicknesses were known before testing and were confirmed by micrometer measurements on an unpainted body shell where possible. Measurements were then made on the painted vehicle in the same location to gauge the paint film

thickness. Destructive testing on the joints was not possible, hence it was desirable to compare mode 1 thickness results with micrometer thickness measurements. Application of an oily film to mark the test position was not successful owing to the underlying white gloss paint. Instead, test points were marked on a grid with a chinagraph pencil and the dabber positioned by eye.

6.4. Results

Samples of 139 and 19 test results have been obtained from the top hat sections and vehicle body shell respectively. These are too numerous to list and have been collated statistically. At each point the bond condition, micrometer thickness, mode 1 frequency and amplitude data were recorded. The threshold for the amplitude data was set using the procedure described earlier at 20% of the maximum peak amplitude encountered. A peak above this level was recorded as bonded, and readings below this were assumed disbonded. During testing, only one mode 1 and micrometer measurement were made at each point. The difference between mode 1 and micrometer thicknesses was calculated and the mean and standard deviation determined for this data.

The top-hat section was unpainted, but the body shell was painted with a significant thickness of top-coat paint. The manufacturers claim that paint thicknesses are typically thin (10μm), on body panels to avoid chipping. However, inside and underneath the body shell, paint thicknesses are not carefully controlled which may lead to significant error in ascertaining the bondline thickness. This is because it is the total joint thickness which is measured; the paint and adherend thicknesses are then subtracted. A few measurements made on single painted sheets inside the vehicle have shown that the paint film varies between 10μm and 50μm. A value of 30μm per layer has therefore been used throughout the analysis.

The bonded joint results are presented in table 6·1 and disbonded joint results (for which bondline thicknesses are not applicable) are presented in table 6·2.

	Top-hat	**Vehicle**
Number of test points	102	13
Bond detection success	100%	100%
Mean mode 1-micrometer thickness difference	14%	7%
Standard Deviation of mode 1-micrometer thickness difference	17%	17%

Table 6·1 Test results indicating bonded joints: peak amplitude>threshold.

	Top-hat	Vehicle
Number of test points	37	6
Disbond detection success	100%	Unknown

Table 6·2 Test results indicating bonded joints: peak amplitude<threshold.

Top-hat results

In the top-hat sections tested, all the test points which were visually identified as bonded were detected as bonded using the mode 1 technique. All of the disbonded joints, including those partially disbonded, were correctly identified as disbonded through the absence of a resonance peak above the threshold in the frequency range of interest. None of the disbonded regions were incorrectly identified as bonded, and vice versa. A large number of measurements were taken and this shows the reliability of the technique under real testing conditions.

Bondline thicknesses were found to range from 0.1mm to 0.56mm (based on micrometer measurements) with a mean of 0.29mm and standard deviation of 0.05mm. This range is clearly wider than the 0.1-0.4mm range specified. At 0.56mm the bonded and partially bonded frequency ranges are well separated in frequency and therefore spot measurements are still valid. In the table, all bonded joints, including those with bondlines exceeding 0.4mm, have been included in the bonded joint results. In the industrial setting, since the mode 1 technique can determine the bondline thickness, joints with adhesive in excess of 0.4mm thick could be rejected if required.

The difference between the bonded joint mode 1 and micrometer measured thickness results shows that the technique is relatively accurate. The 40μm mean difference represents a 13% difference at 0.29mm (the mean thickness), and the 50μm standard deviation represents a 17% difference at 0.29mm. There are several sources of random and systematic error which account for the bondline thickness differences. Firstly, mode 1 frequencies were measured ‘on-screen’ and were only accurate to within 10kHz; this alone is equivalent to a 20μm difference at around 0.29mm. Secondly, although efforts were made to align the centres of the mode 1 and micrometer measurements, errors in positioning would result in bondline thickness errors due to adhesive layer taper. The micrometer measurements can also only be considered accurate to within a few microns. Thirdly, small differences in material properties may

result from different batches of adhesive with different cure cycles. It was found that the majority of mode 1 readings were larger than micrometer measurements, and this is therefore a likely explanation for the mean difference.

Vehicle results

The tests carried out on the vehicle also indicate that the mode 1 technique can be used reliably on automotive structures. Whilst the bond condition of automotive joints was not obvious from visual inspection, measurements made on aluminium sheet away from the joint (i.e. fully disbonded) all had a mode 1 response less than the threshold, confirming that disbonds could be detected on real vehicles. The bondline thickness on the vehicle was measured with the micrometer to vary between 0.09mm and 0.58mm, assuming a total paint film of 60µm. However, this paint film was found to be very variable and is a likely cause for errors between the mode 1 and micrometer measured thicknesses.

6.5. Overlapping frequency ranges

The analysis in chapter 3 showed that where a wide bondline variation exists there can be an overlap between the bonded and partially bonded frequency ranges, in which case the bond condition cannot always be determined from a single measurement. Where a measurement falls into this overlap region, there are two approaches which can be taken to overcome this problem. These are outlined in this section, but since the principal focus of the project was to develop a disbond detection system for joints where this overlap does not exist, these suggestions have not been tested experimentally.

When a bonded joint with a wide bondline thickness variation is scanned along its length, the variation of the frequency will be smooth. The mode 1 frequency with a thick bondline occurs below the overlap region and the bond condition can be identified definitively. A step change in bond condition, at the boundary of a disbond for example, will cause a step change in mode 1 frequency; this can be used to indicate the presence of a disbond. This is indicated schematically in figure 6·4.

Alternatively, where scanning is not possible, or spot measurements are required, the bond condition in the overlap region can still be determined by making an additional measurement with the high frequency technique using adaptive filtering described in chapter 2, section 2.2.1.4. The limited bondline thickness range which can be

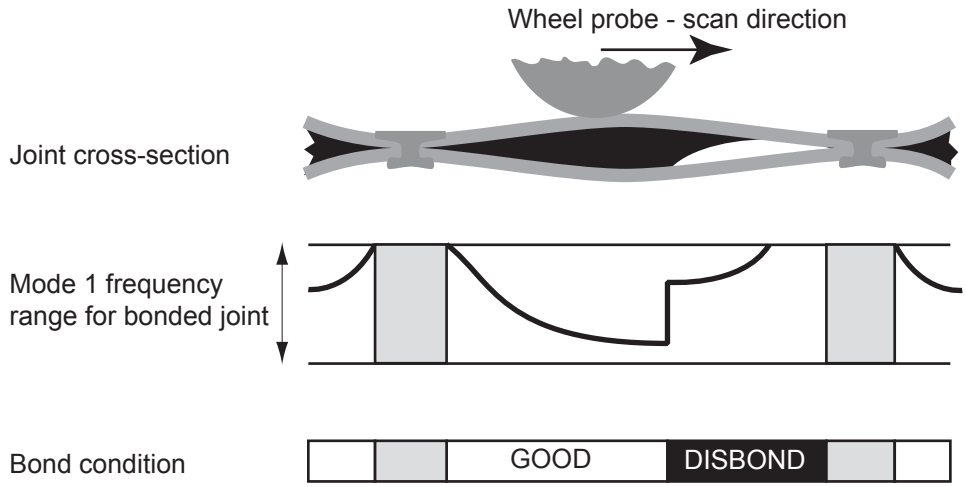

Figure 6·4 Schematic diagram showing possible technique for disbond detection where bonded and partially bonded frequency ranges overlap.

successfully tested, which is the main drawback of this time domain technique, does not cause a problem when used in conjunction with the mode 1 method. A mode 1 frequency in the overlap region indicates either a bonded joint with a thin bondline, or partially bonded joint with a thick bondline; the mode 1 frequency can be used to give two possible bondline thicknesses. A high frequency measurement is then well suited to testing for the bonded case, and can be set up accordingly.

6.6. Conclusions

Testing has been carried out on industrially prepared joints with a dry coupled dabber probe and using the window ringing signal processing method to extract the mode 1 data. Many measurements have been made, all with 100% of bonds and disbonds successfully detected. The mode 1 frequencies have been used to determine an equivalent bondline thickness which has been compared to independently measured values. Good agreement has been found, with differences within the bounds of measurement error. The mode 1 technique and dabber probe therefore provide a robust test suitable for automotive use.

The joints considered for this work have an adhesive thickness of less than 0.5mm and the bond condition can be confirmed with a single measurement taken with commercially available transducer fixed to the dabber probe. As a more general purpose tool capable of much wider adhesive thickness variations, there are two complications. First, there may be some overlap between the bonded and partially bonded frequency ranges, which either requires the joint to be scanned or an additional

measurement to be made. Secondly, a wider bondline thickness range means a wide mode 1 frequency range at lower frequencies. Transduction issues are discussed in the next chapter.

Chapter 7

Low frequency non-resonant transducer development

7.1. Motivation and requirements

The relatively narrow adhesive bondline thickness range specified for the automotive manufacturer's structural requirement (0.1-0.4mm) can be tested using the mode 1 technique with a 500kHz commercially available transducer in conjunction with a dry coupled dabber probe.

It was shown in chapter 3 that a wide variation in bondline thickness requires testing at lower frequency. A specific wide bondline thickness range has not been given by the automotive manufacturers, but it was generally felt that a thickness range of 0.2-3.0mm would cover most adhesive bonding applications. The equivalent mode 1 frequency ranges for joints with 2mm aluminium adherends, or 1mm steel adherends is approximately 150-450kHz. This range is equivalent to a 300kHz centre frequency with 100% bandwidth. Over such a range at low frequency, commercially available devices were found to be unsuitable. In chapter 3, section 3.4.2 it was shown that in order to minimise signal processing and ensure the mode 1 technique is robust, there should be little ringing from the transducer in the ringing window used to process the received signal. In commercially available transducers this has been found to be a significant problem, either because the bandwidth is relatively narrow and the transducer rings for a long time at the centre frequency, or other modes are present. This is generally due to poor damping of low frequency transducers, and is made worse by the small physical size requirements; to allow the probe to be used where there is restricted access, the overall dimensions must be no more than 15mm diameter and 15mm long; the device must also be suitable for immersion in order to make measurements in an immersion tank.

In summary, the main requirements for the transducer are:

- Low frequency (300kHz centre frequency), wide bandwidth (100%)
- No ringing within operating frequency range
- 15mm diameter maximum.
- Waterproof

In this chapter, the factors affecting the performance of the different types of transducer available are discussed, and the implications for use at low frequency. This is followed by the development and results from a non-resonant transducer which aims to meet the above specification.

7.2. Evaluation of transducers for low frequency work

7.2.1 Piezo-ceramic damped resonant transducers

Piezo-ceramic materials, such as PZT, have been traditionally used in the manufacture of ultrasonic transducers and are still used in the majority of commercially available devices. These transducers comprise a piezo-ceramic disc with electrodes on the flat faces and an attenuative backing material bonded to the rear face. They operate across the first through-thickness resonance mode, which is damped by the lossy backing to increase bandwidth, and have hence been termed piezo-ceramic damped resonant transducers. The thickness of the piezo-ceramic disc is chosen so that this thickness mode occurs at the required centre frequency. Unimodal behaviour is desirable and this can be achieved where the diameter to thickness (D/T) ratio of the disc is greater than 20, or much less than unity [108-111]. However, the transient response of a piezoelectric disc becomes more complex at other D/T ratios [112] giving a mixed-mode response. Piezo-ceramics used for transducers typically have a frequency constant of 2000Hz.m [113]; a 300kHz centre frequency device would therefore require an element approximately 6mm thick, and the optimum diameter for such a disc would be greater than 120mm to provide a unimodal response. Clearly this is impractical, and the disc diameter is compromised, leading to a less desirable frequency response.

The diameter also governs the shape of the soundfield, or 'beam profile' generated by the transducer [114]. This determines the extent of the interference field, and the degree of collimation of the beam in the far field; for good spatial resolution, a narrow beam is required. For an unfocused transducer [110] the extent of the near field, *N*, is given by equation 7·1, and the half width of the beam, *w*, is given by equation 7·2:

$$N = \frac{D^2 - \lambda^2}{4\lambda} \qquad (7\cdot1)$$

$$w = 1.2\lambda(R/D) \qquad (7\cdot2)$$

where *D* is the transducer diameter, and *R* is the range. Hence, at low frequency, a large diameter is needed. In practice, again this dimension must be compromised to produce a device of useable size, in this case leading to a more undesirable beam profile.

In use, piezoelectric transducers are often coupled to test structures via Perspex or water delay lines, which have much lower acoustic impedance than the piezo-ceramic disc. Hence the transfer of energy at the interface is relatively poor, and an unbacked piezo-electric disc alone will resonate, or 'ring' for a considerable period of time. Although undamped resonant devices may find specialist applications, the highly resonant nature of the response is of little use within NDT since the useable frequency range is very narrow, and it does not provide the short pulse needed for good axial resolution.

Piezo-ceramics used for NDT have a mechanical quality factor (typically 80 [113]) which is low within the range of piezo-ceramics available, but too high for use in a transducer without additional damping. The standard technique to increase the damping is to back the element with an attenuative backing, which absorbs much of the energy. Efficient energy transfer between the two materials is required and this means that the acoustic impedances should be well matched. Since lossy materials are usually polymeric and have relatively low acoustic impedance, tungsten-epoxy composites have been developed to have high impedance and high attenuation [115]. Their use as a backing material allows increased bandwidth to be obtained.

Although there are manufacturing issues [110] which can cause some variation in the performance of similar transducers, production of these devices is well established and there are numerous transducers on the market which have a wide bandwidth and short pulse shape operating above 1MHz. Below that frequency, however, the performance of devices is more variable, and below 500kHz centre frequency, only large diameter transducers can offer satisfactory performance without ringing. This is because the attenuation of bulk waves in backing materials is generally proportional to wavelength. Consequently, at low frequencies a considerable thickness of backing material is required to avoid reverberations in the backing. Limiting the size of the transducer (hence backing thickness) to a manageable size compromises the performance, with the 'ringing' in the backing increasing the pulse length. Whilst a thick backing is

required for good low frequency performance, a wider diameter is also needed since where the length/diameter ratio is large, undesirable flexural modes may occur in the backing.

The poor impedance matching of piezo-ceramics to the coupling media (such as water) not only requires the elements to be backed, but also means that the coupling efficiency is poor. This can be improved through the addition of matching layers, although practical difficulties and a cost penalty are reported [110]. These polymeric layers can, however, introduce transmission loss, but this is not a significant problem at low frequency.

7.2.2 Piezo-polymers

Piezo-polymers [116-118], notably PVDF film, have an apparent advantage over piezo-ceramics in that their acoustic impedance is much lower and better matched to lossy polymeric materials which can be used as a backing. These materials are only available in thin film form which makes them unsuitable for low frequency operation in thickness mode [119]. In comparison to piezo-ceramics, as transmitters their efficiency is an order of magnitude lower, and although they have a higher receiver efficiency parameter [110] (due to their small thickness) which improves their pulse echo efficiency, they are still less efficient overall. For high frequency use, this reduced efficiency can be a worth while trade-off for the decreased impedance, and good transducers are readily available. Their low impedance makes them particularly attractive for air coupled low frequency applications, such as range finding.

7.2.3 Piezo-composites

A significant improvement in the performance of piezo-ceramic materials has been gained by combination with a polymer phase to form a piezo-ceramic composite [120-122]. Small elements of piezo-ceramic material are embedded in the polymer to provide a certain pattern of connectivity of both materials between the opposite faces of the composite. For example, the commonly used 1-3 composite has piezo-ceramic rods connecting 1 pair of opposite faces (on which the electrodes are deposited) whilst the polymer directly connects all 3 pairs of opposite faces, as shown in figure 7·1.

Combination of materials in this way reduces the acoustic impedance and increases the damping. This increases the energy transmitted into the coupling material and conventional backing methods can be used more easily to increase the bandwidth. A considerable amount of work has been directed towards the development of such

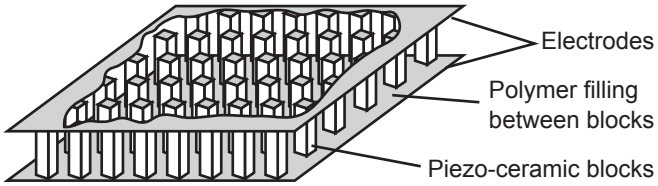

Figure 7·1 Schematic diagram of 1-3 composite structure.

devices since the dimensional and material parameters can have a large effect on their operation [110, 121-125]. Whilst this technology holds much promise for the future, small, highly damped devices operating at low frequency are not commercially available, and an alternative approach was sought which would not require the specialised manufacturing techniques required to make piezo-composite transducers.

7.2.4 Broadband Transducers

A variety of broadband transducers are available which claim operating frequency ranges of below 100kHz up to 1MHz. Such devices are typically designed for acoustic emission work and may indeed have wide band responses. However, typical responses have been found to be far from flat, as often claimed, and exhibit considerable amounts of ringing. Figure 7·2 shows an example of the received time domain waveform from a reflector using a broadband commercially available broadband transducer (B1025 – Digital Wave Corporation). The transducer was tested in an immersion tank pointing upwards, with the water-air interface providing the reflector; excitation was with a pulse centred around 250kHz. The ringing within the device is clearly visible, and it is therefore not suitable for this application.

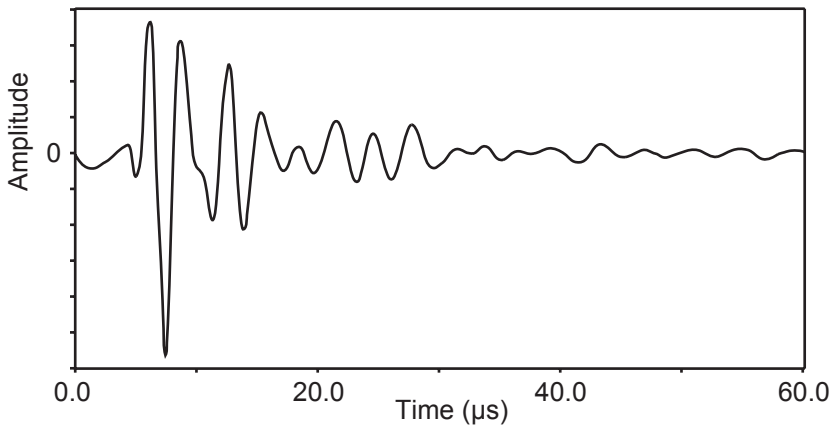

Figure 7·2 Pulse-echo reference reflection from a broad band transducer.

7.2.5 Capacitive transducers

An electrostatic, or capacitive transducer is basically two parallel metal plates with a small air gap which behaves as a capacitor. The rear plate is fixed, but the front plate is displaced by pressure variations. A DC bias, or polarisation voltage is required. The device is very sensitive as a receiver, but less efficient as a transmitter [110]. These devices are generally used as air coupled devices [126]. Use in water may be possible, but they would require sealing which adds to the complexity of construction [127]. Again, an alternative approach was sought with simpler construction.

7.2.6 Conical piezo-electric element transducers

Acoustic emission applications require transducers with a small contact area and wide bandwidth. One such device, first developed by the National Bureau of Standards (NBS), employed a conical piezo-electric element backed with a large brass block The conical element has been shown to have an increased bandwidth compared to a standard disc element [128]. The absence of parallel sides in the conical element means that there is no true thickness mode of vibration (around which conventional transducers operate), and although the conical element has more mechanical resonances than a disc, the modes are less dominant than the thickness mode in a disc. Since the device is not designed to operate at a particular resonance frequency, it can therefore be considered to be non-resonant. However, the presence of the additional modes would appear as ‘ringing’ in the time domain, making them unsuitable for the intended application.

7.3. Non-resonant transducer design and construction

The insufficiently wide bandwidth and ringing found in commercially available low frequency transducers has led to an alternative approach for the development of a transducer to meet the requirements mentioned in section 7.1. This design uses piezoelectric ceramic elements, but operates below the first excitable resonance mode, and is therefore termed ‘non-resonant’.

Numerous prototypes were tried before arriving at the current design. In section 7.3.1, the details of the final design of a non-resonant transducer using a single element is presented. In section 7.3.2, the implications of the excitation on the design, and subsequent modification to use an array of elements is discussed.

7.3.1 Final design: single element device

The final design of non-resonant transducer with a single piezo-electric element is shown in figure 7·3. The different elements of the design are discussed below.

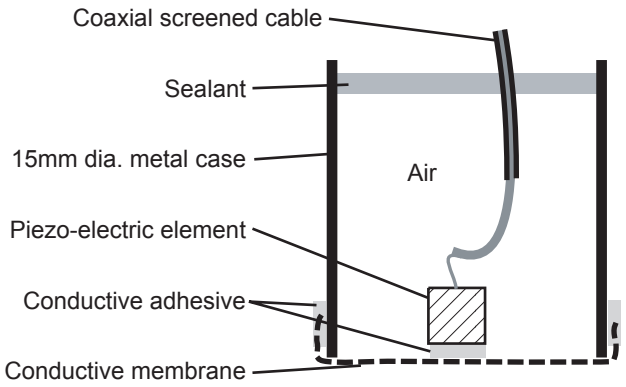

Figure 7·3 Schematic diagram showing construction of a single element non-resonant transducer.

Piezoelectric Elements

The active element of the transducer is a piezo-ceramic element. For a successful non-resonant design, there must be no modes excited in the transducer below the first mode of the piezoelectric element. The transient response of a thin piezoelectric disc has been shown to be relatively complex, and would have modes below the first predicted though thickness mode. However, if the disc is chosen to have a D/T ratio of 1, then such unwanted modes are avoided.

A PZT cube is suitable, and the first 4 modes of vibration have been predicted using finite element modal analysis [101]. The aim of the analysis was to determine the approximate frequency of the first mode likely to be excited. In the model, several simplifications were made. Firstly, the electrodes and piezo-electric effects were not included. However, since the electric field is approximately uniform between the electrodes, only symmetric modes will be excited and any asymmetric modes in the FE model can be ignored. Secondly, the PZT was modelled as an isotropic material without damping. Whilst PZT exhibits material damping and anisotropic properties, the simplifications in the model were deemed appropriate to give an approximate value for the first thickness resonance. From this, approximate dimensions for the PZT cube could be established as a basis for a more accurate determination of the response experimentally.

Figure 7·4 plots the deformed and undeformed shape of these modes. The first three modes are not symmetric and so it is only mode 4 which will be excited. This mode is predicted to occur at 645kHz for a 2mm side length cube, and at 500kHz for a 3mm cube. The 2mm element was chosen in the final design to allow operation up to 500kHz whilst still being below the highly resonant first mode. In practice, the first mode was found to occur at around 600kHz

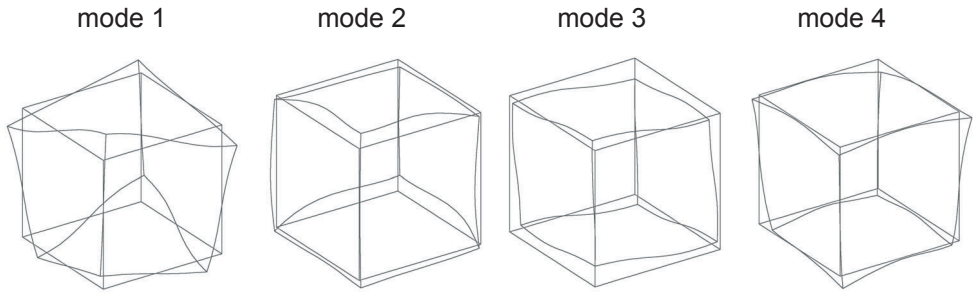

Figure 7·4 First four modes for a 2mm side length cube.

Driving the piezo-electric element off resonance gives transmitted and received amplitudes which are small compared to conventional damped resonant devices, and this is the main disadvantage of the design. In order to maximise the response in the operating frequency range, elements are backed only by air so that maximum energy is transmitted into the test structure. In addition, this avoids any reverberations which would be present if a small amount of backing material were used. In contrast to conventional resonant transducers, the resonance of the first thickness mode therefore has a large Q factor, but this is of little consequence since the device operates below resonance.

Enclosure

The piezoelectric elements are coupled to water for immersion testing via a waterproof membrane. Whilst thin metal sheet would provide a relatively robust face to the transducer, and bond easily to the PZT and casing, waves could propagate easily along the sheet and the subsequent reverberations would add unwanted features to the signal. Instead, a thin rubber membrane has been used. The lossy nature of the rubber, and the small impedance difference between the rubber and water means that any waves propagating along the membrane are quickly attenuated. However, with the membrane being thin, the attenuation of the compression waves from the face of the element can be neglected.

The electrical connection to the rear face of the piezoelectric element is made with fine wire soldered to the electrode. The solder must be small and located centrally to avoid any asymmetry which could excite some of the unwanted lower frequency modes. On the front face of the PZT element where solder connections are less favourable, the element is bonded to the membrane. An electrically conductive silicone membrane is used (Shieldseal 106 – James Walker & Co Ltd.), and the PZT elements are bonded with specially manufactured electrically conductive adhesive (Bondshield BS100 – RFI Shielding Ltd.). Although readily available cyanoacrylate adhesive, when combined with a poleofin primer, will successfully bond to silicone rubber and silver electrodes, its non-conducting nature inserts a large dielectric loss, even with very thin bondlines, resulting in significantly reduced voltage across the piezoelectric elements, and so is not recommended for use. The membrane used was 0.5mm thick and has a measured resistance of 2Ω between two points 10mm apart. This greatly eases manufacture and ensures that the elements are electrically screened. The membrane is bonded, also with electrically conductive adhesive, to the metal tube, so completing the electrical screen; the top of the can is sealed to prevent water ingress.

7.3.2 Excitation and implications for transducer design

Transducers produced at the start of the development phase used 3mm side length elements which had a first thickness resonance measured experimentally at approximately 410kHz. They were at first driven with a waveform generator (Wavemaker Duet – Macro Design) which could deliver 100V peak into 50Ω, but the amplifier had a long recovery time between transmission and reception in pulse-echo mode at low frequency. A device operating in pulse-echo would have required an unacceptably long stand-off for the signal to be received. Early devices were therefore designed to operate in pitch-catch mode; the case was separated into two compartments by a brass plate fixed across the diameter to provide electrical screening. A single PZT element was bonded to the membrane, in the same way as described earlier, in both compartments, one acting as transmitter and the other as receiver. These devices worked well at low frequency when excited with a 5 cycle tone burst between 150kHz and 250kHz.

Later, an instrument (DUI – NDT Solutions Ltd.) which had improved low frequency performance and could generate arbitrary waveforms was used instead. This had almost negligible amplifier recovery time in pulse-echo, and would allow a single element to be used in pulse-echo, thus simplifying construction. Unfortunately, the

maximum output voltage was half that of the Wavemaker. At the same time, 2mm elements were used to extend the operating frequency range up to around 500kHz. The area of the 2mm elements being less than half that of the 3mm element, coupled with the lower output excitation voltage meant that the amplitude at low frequency, 200kHz for example, with a single element was extremely small. To lessen this problem, all later devices were constructed with an array of several elements bonded to the membrane, connected electrically in parallel to increase the surface area and signal to noise ratio. The elements were typically spaced 2mm or more apart. Using an array of elements also improves the beam profile; this is discussed in section 7.5.

7.4. Frequency response

7.4.1 Excitation with narrow band tone burst

The frequency response of a transducer can be determined either by exciting at a particular frequency and sweeping across the frequency range of interest, or by driving the transducer with a broad band signal. The transducer is highly resonant at about 600kHz and excitation at this frequency would cause a large resonance amplitude which would use up the available quantisation in the 8 bit digitisers and mask the smaller response below resonance. In this section, the pulse-echo frequency response of a non-resonant device was determined by exciting with a narrow band signal (10 cycle tone burst) with constant input amplitude, and increasing the frequency in steps over the range 150-450kHz.

The transducer used had 9 elements of 2mm side length and was set-up in an immersion tank pointing upwards with a 50mm standoff from the water-air interface. The received signal was transformed to the frequency domain and the peak amplitude and frequency recorded. The response over the range 150-450kHz is shown in figure 7·5.

These results show the pulse-echo response increasing with frequency. This is due to the capacitive nature of the piezoelectric element, whose impedance is inversely proportional to frequency. In order to confirm this effect, comparison has been drawn with a 1D model [129]. The system modelled comprised air-PZT-water; the PZT thickness was set to also have a first resonance frequency at 600kHz. The predicted pulse-echo response is also shown in figure 7·5 and confirms the reason for the frequency dependence.

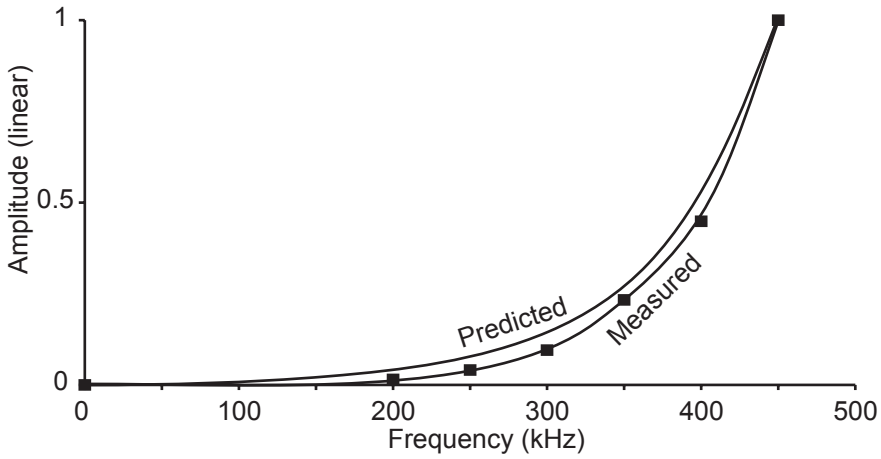

Figure 7·5 Measured and predicted frequency response curves with flat input response

7.4.2 Excitation with 5 cycle toneburst

With the frequency response of figure 7·5, to avoid exciting the resonance, the input signal must have very little energy around the resonance frequency and a relatively large amplitude at lower frequencies (150-300kHz for example). This can be achieved simply by using a 5 cycle tone burst. Figure 7·6(a) shows the pulse-echo response of the transducer when excited by a tone burst centred around 230kHz. The convolution of the pulse-echo response and excitation is clearly evident from the shift in the frequency of the maximum amplitude; the maximum response in the received signal occurs at 310kHz corresponding to the input centred at 230kHz. In order to remove the first resonance (600kHz) from the received signal, it has been filtered out in the frequency domain using signal processing software (Spectrum – Imperial College) by applying a low pass filter starting at 450kHz and having a response decreasing to zero at 550kHz with a cosine taper function. The time domain signal after filtering is shown in figure 7·6(b).

Although the response is clearly not flat, the device now has a useable frequency range of 200-500kHz. However, a 230kHz tone burst is not suitable to strongly excite mode 1 resonances in the range 150-450kHz. For this work, 5 cycle tone bursts of different centre frequencies were used. Results from bonded joints using this excitation are given in section 7.6. Where this excitation is not convenient, when scanning is required for example, a broader band excitation, but which avoided exciting the first thickness resonance, would be required.

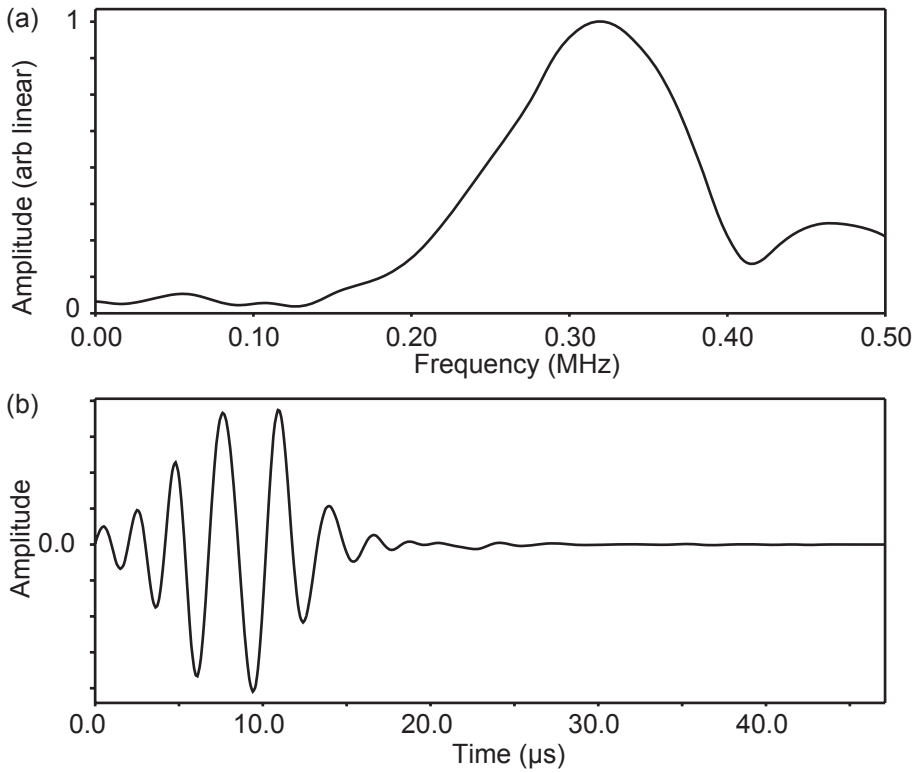

Figure 7·6 *(a) Pulse-echo response of non-resonant transducer when excited by a 5 cycle tone burst centred around 230kHz, and (b) time domain signal.*

7.5. Beam profile

7.5.1 Single element

Early transducers were produced with a single PZT element. These had two main short comings compared to conventional resonant transducers. Firstly, the received signal was low due to the small area of PZT bonded to the membrane, as mentioned in section 7.3.2. Secondly, since the side length of the elements was much smaller than the wavelength in water, it behaved as a point source, producing an undesirable beam profile.

The beam profile was measured with the transducer driven at 300kHz in an immersion tank by scanning with a hyrophone, in the plane normal to the transducer face, across the diameter of the face. The pressure variation is plotted as a C-scan in figure 7·7(a), and along the central axis in figure 7·7(b). The point source behaviour is clearly visible in the beam profile plot, and the pressure variation along the central axis falls as a function of the inverse of the distance from the transducer, as expected for a point source.

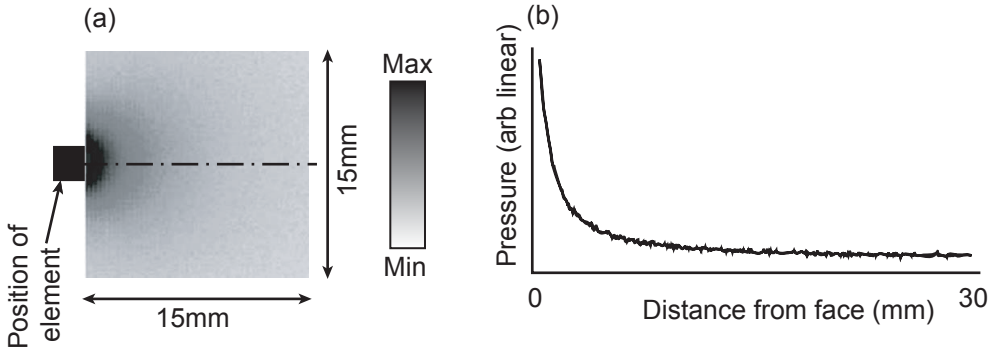

Figure 7·7 *(a) Beam profile of single element transducer at 300kHz and (b) pressure variation along the central axis.*

A wider diameter element cannot be used to improve the beam profile, since it would alter the D/T ratio and other unwanted modes would be introduced. However, a significant improvement is gained by employing an array of elements, each acting as a point source, electrically connected in parallel.

7.5.2 Multi-Element Device

Any waveform can be constructed from a large number of point sources of the same frequency (Huygens' principle). Increasing the effective total diameter of these point sources results in a more collimated beam making it better suited for testing.

Experimentally, an array of 9 elements have been laid out in a chequer-board pattern giving a total side length of 10mm. The spatial variation in pressure has been plotted normal to the face, and along the central axis using the same setup as for the single element device. In addition, C-scans have been obtained in the plane of the face of the transducer at 0mm and 5mm standoff from the face. These results are shown in figures 7·8 and 7·9 respectively.

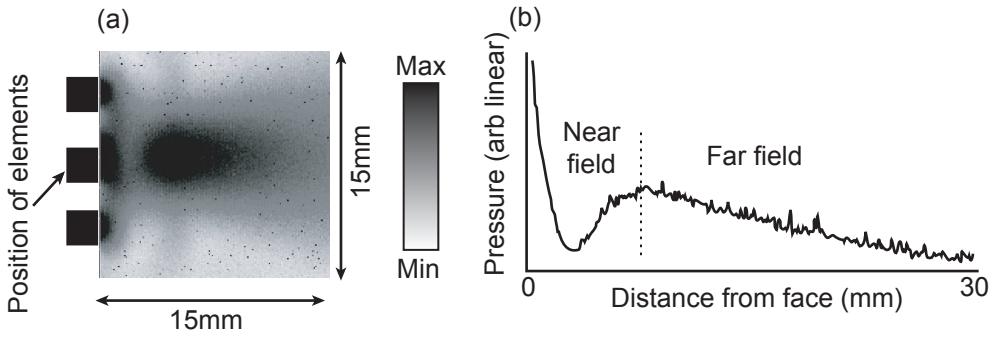

Figure 7·8 *(a) Beam profile and (b) pressure variation along the central axis for a nine element device.*

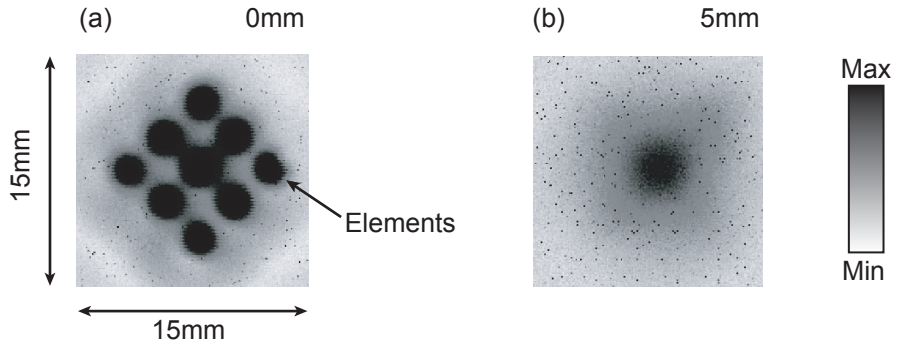

Figure 7·9 C-Scans showing pressure variation in the plane of the face of the transducer at standoff of (a) 0mm and (b) 5mm.

The beam profile shows that the addition of elements to increase the overall diameter from 2mm to 10mm produces a significantly more collimated beam. Pressure variation along the central axis exhibits the classical far field amplitude variation, with maximum pressure at the start of the far field, 7mm away from the transducer face. This agrees closely with the theoretical value of 6mm, given by equation 7·1. This value is small for the mode 1 testing application where standoff distances of greater than 30mm are needed. However, it is a significant improvement over the point source, but remains a limitation of using a small diameter transducer at low frequency.

In the scan in the plane of the transducer face (figure 7·9(a)), the elements can be clearly seen and there is negligible displacement of the membrane away from the elements. Figure 7·9(b) confirms that the maximum amplitude away from the transducer face is on the central axis. Further beam profile improvements can be obtained using more elements over a larger area.

7.6. Bonded joint results

The extended bondline thickness specification of 0.2-3.0mm has a mode 1 frequency range of 150-450kHz for 2mm aluminium adherends. The motivation for the development of the device described in this chapter was to develop a low frequency transducer with a wide operating frequency range, small enough to fit inside a wheel probe. Before supplying the transducer to Bristol for wheel probe development, it was first used to test bonded joints in an immersion tank.

The 9 element device described in the previous section was used to obtain the results presented in this section. The transducer was set-up in an immersion tank as described in chapter 3, section 3.4.1, with a 30mm standoff, which is similar to the delay line length in the wheel probe. No industrial samples were available at the time with this

specification, so prepared samples were used instead. As before, bonded joints with 2mm aluminium adherends and XD4600 adhesive were used, with bondlines varying nominally between 3mm and 0.2mm. An example of a received signal is shown in figure 7·10(a). The first resonance at 600kHz has been filtered out by applying a low pass filter starting at 450kHz and reducing, with a cosine function, to zero at 550kHz. The filtered time domain signal is shown in figure 7·10(b). The front face reflection (F1) and ringing are clearly visible.

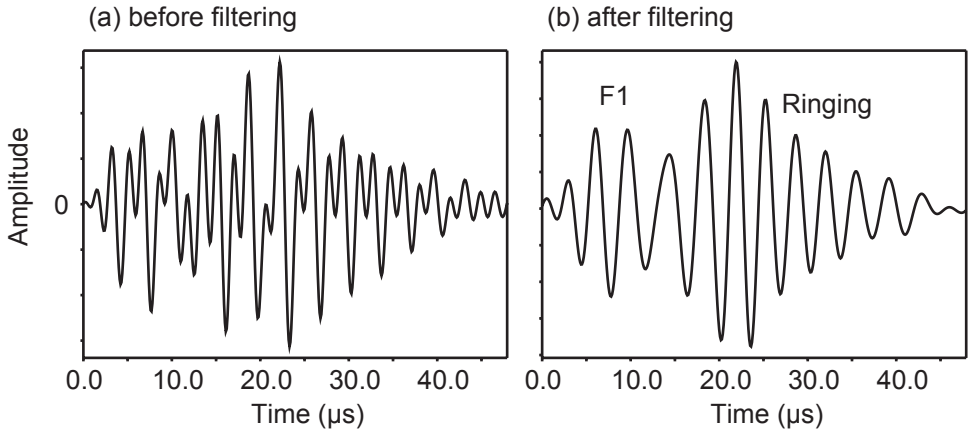

Figure 7·10 Example of received signal (a) unfiltered, and (b) filtered from a bonded joint using a non-resonant transducer.

The time domain waveforms were windowed and transformed to the frequency domain in the usual manner. Owing to the increased duration of excitation compared to the 500kHz transducer used in previous tests, a relatively short window length of 17μs was used, starting after the end of the front face reflection. In the tests, the centre frequency of the tone burst excitation was increased in steps over the range 150-350kHz, and the processed signal with the largest resonance peak in the range 100-500kHz was used. Frequency domain plots for several joints are shown in figure 7·11. The predicted mode 1 frequency based on the mean measured thickness (given in the figure) is shown with a vertical line. The results show good agreement between measured and predicted mode 1 resonance frequencies. Constant amplitude excitation was used, the centre frequency of which (ω_e) is also indicated on the plots. At lower frequency, the amplitude of the response is therefore much smaller, although this could be avoided by decreasing the amplitude of excitation as the frequency increases.

Whilst satisfactory results were obtained over the range approximately 0.2-1.8mm, problems outside this range were experienced. Although the thin bondline requirement has been met in this case, it was not possible to test joints with bondlines of less than

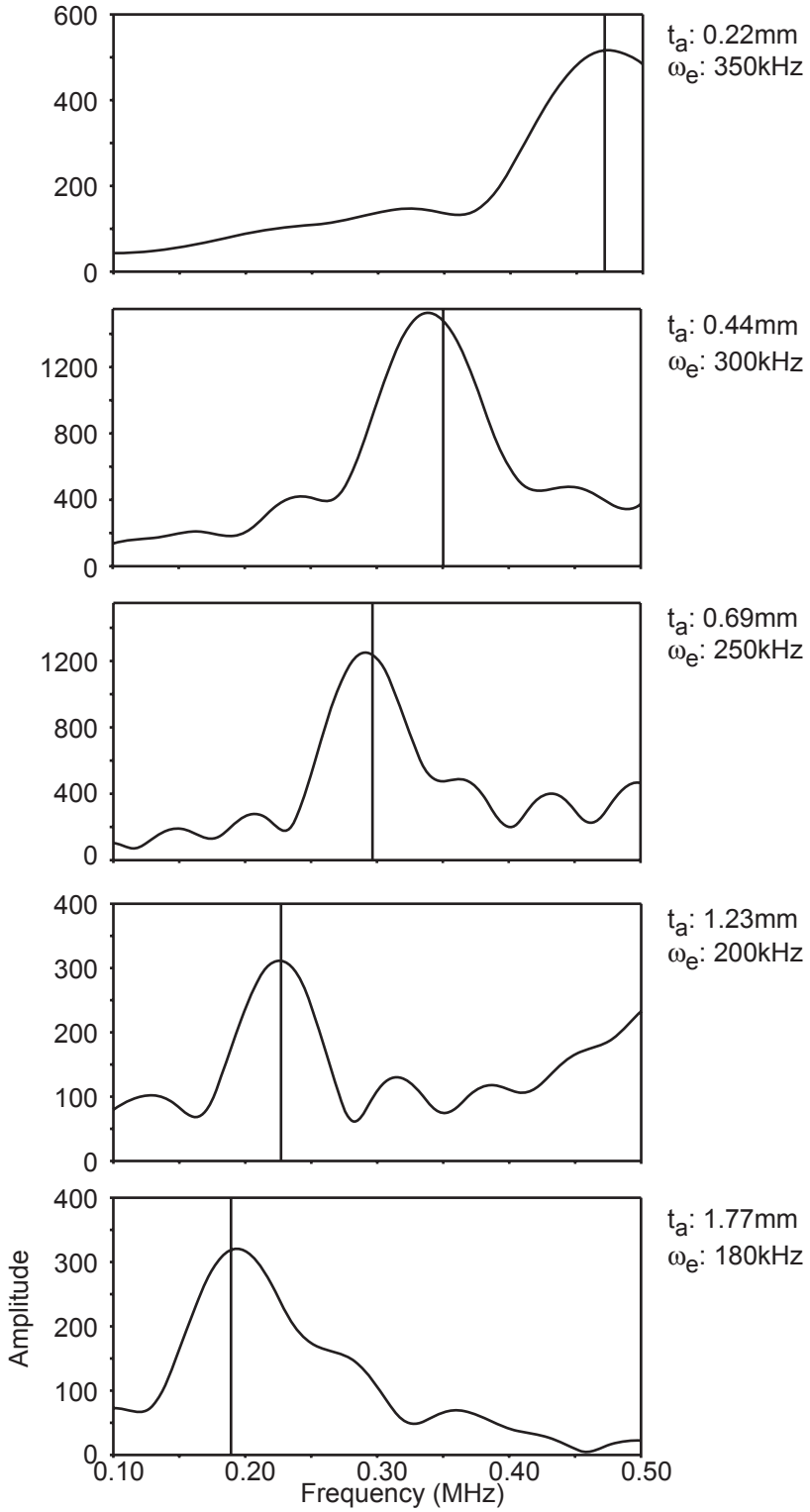

Figure 7·11 Frequency domain plots from bonded joints of varying adhesive thickness tested with a non-resonant transducer with 2mm elements.

0.2mm due to interference between the joint resonance and the transducer resonance. Poor response at low frequency proved problematic when testing joints much below 200kHz (i.e. joints with bondlines thicker than 1.8mm). The low amplitude excitation when a 150kHz tone burst was used, for example, meant that the joint resonance could not be distinguished reliably from the background noise. This problem was not encountered with the earlier devices with 3mm PZT cubes since their operating frequency range was lower. As an example, figure 7·12 shows the frequency domain response from a joint with a 3.1mm bondline where a device with a single 3mm cube was used, excited with a 150kHz tone burst.

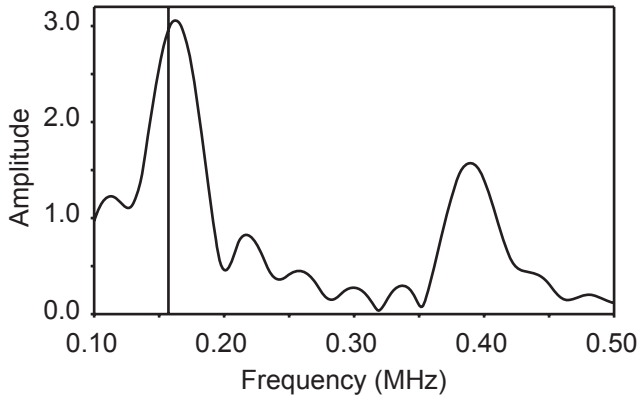

Figure 7·12 Frequency domain plot from a bonded joint tested with a non-resonant transducer with a 3mm element.

The mode 1 resonance peak can be clearly identified along with the first resonance around 400kHz. Using a transducer with 2mm cubes, not even the front face reflection could be reliably identified from the time domain signal. Using an instrument with a much higher output, especially at low frequency, and a more suitable excitation signal should however eliminate this problem.

7.7. Conclusions

A novel low frequency transducer has been developed which employs piezo-electric elements operating below their first thickness resonance mode. Unbacked PZT cubes of 2mm side length have been found to give an operating frequency range of about 200-500kHz. With the excitation available, a useable frequency response below 200kHz was not obtained. This was because the pulse-echo response of the transducer is very low at frequencies less than 200kHz and increases significantly with frequency up to resonance at about 600kHz. It is anticipated that low frequency operation with a 2mm

cube could be improved simply with a higher excitation voltage and a more suitable input signal. Alternatively, lower frequency operation can be achieved using larger PZT elements, but at the expense of reducing the upper operating frequency limit.

Bonded joints comprising 2mm aluminium adherends and adhesive thickness in the range 0.2-1.8mm were successfully tested in an immersion tank using a device with 2mm side length elements. It was also demonstrated that bondlines of 3mm could be tested with a device employing 3mm side length elements. The addition of an array of elements, increasing the effective diameter, was found to give a larger output, and a much improved beam profile with a more collimated beam.

Despite the shortcoming of low response below 200kHz, the non-resonant transducer does offer the equivalent of a frequency range of almost 100% of centre frequency in a small case of 15mm diameter, without any significant resonances in that frequency range. This cannot be currently achieved with commercially available devices.

Chapter 8

Conclusions

The development of a novel NDT system to detect disbonds in automotive adhesive joints has been presented in this thesis. In this concluding chapter, a review of the thesis is presented which highlights the main findings of each chapter. The success of the disbond detection technique is then considered, along with its limitations, and some suggestions for future work. Lastly, the main contributions of the thesis are summarised.

8.1. Review of thesis

Chapter 1 described the motivation and set out the objectives for this work. The motivation was provided by a major UK automotive manufacturer who required an NDT system for disbond detection to replace current destructive testing, and to provide feedback to enable the adhesive bonding process to be optimised. The area of primary concern was bonded structural joints with aluminium adherends and an adhesive layer thickness in the range 0.1-0.4mm. The main objective of this work has therefore been to develop a technique which can tests joints to this specification, to the point where it is ready for implementation on the production line. In addition, a more generic joint specification for bonded joints in other applications which can have bondline thickness in the range 0.2-3.0mm was also considered to ensure the technique developed was suitable for a wide range of automotive applications. Automotive testing considerations, principally couplant free testing and joints having attenuative adhesive layers which can vary significantly in width and thickness, precluded the use of existing disbond detection techniques. Other important considerations were that the system developed must be robust, simple-to-use, fast, low-cost, and be easily integrated into existing production processes.

The suitability of existing disbond detection techniques was reviewed in chapter 2. It was found that although none were suitable in their current form, ultrasonic techniques were most promising. Time domain techniques to identify bondline echoes were limited by high attenuation in the adhesive, and by reverberations in the front adherend which mask diagnostic echoes from the rear bondline. Spectroscopy has been used successfully in some bond testers (requiring couplant), and previous work has suggested that studying the first thickness mode (mode 1) would be promising for

automotive applications. However, the technique was not developed beyond an initial investigation, partly due to low frequency transduction problems and an unreliable signal processing method. The viability of using mode 1 was therefore investigated thoroughly in chapter 3.

Predictions of the mode 1 frequency for the specified bondline thickness ranges were made using a one-dimensional multilayer wave propagation model. It was found that for the 0.1-0.4mm bondline specification, the frequency ranges for fully disbonded and partially disbonded joints were much higher in frequency than the range for bonded joints. This meant that a single measurement of joint resonance frequency could be used to identify the bond condition. The permissible adhesive thickness range to determine the bond condition from a single measurement was also identified for the first time Further, the frequency range for this thickness specification is 375-590kHz (for 2mm aluminium adherends), which falls into the operating frequency range of commercially available, well damped transducers.

For the wider specification of 0.2-3.0mm, some overlap between the bonded and partially bonded frequency ranges was found. A diagnosis of bond condition from a spot measurement where the mode 1 frequency is in the overlapping region would therefore be impossible. Possible solutions would be to make an additional time domain measurement, or to monitor the change in frequency where a joint is scanned, with a wheel probe for example.

In chapter 3, signal processing to extract the mode 1 frequency data was also considered. Gating out the front face reflections to leave just the joint resonance, which was then transformed to the frequency domain, was found to offer a simple, fast and robust means of detecting the mode 1 resonance. Experimental validation confirmed the viability of using mode 1 for disbond detection.

The effect on the mode 1 resonance predicted by the 1D model when the adhesive layer varies in width or thickness, was examined in chapter 4. These situations were modelled using finite element methods, and the results validated experimentally. Where there exists a step change in bond condition in the region under test, as may occur where the adhesive bead is narrow or misplaced, the mode 1 frequencies of both parts were found to be independent and occur at the same frequency as the 1D case (for the cases modelled). This means that the 1D frequency predictions are still valid for joints with varying width adhesive layers. The amplitude of the resonance in both parts

is governed by the strength of the excitation at the resonance frequency. If the resonance frequency of one part is within the transducer operating frequency range then the resonance amplitude will increase with the area of the transducer over that part.

In the case of a tapered adhesive layer, the mode 1 frequency could be approximated by the frequency predicted by the 1D model using the mean thickness of the region under test. As the adhesive taper increases, the peak amplitude is found to decrease. This is because the resonance peak is made up from the range of mode 1 frequencies given by the range of adhesive thickness in the test region. In practice, it has been found that the reduction in peak amplitude is not sufficient to render the resonance undetectable.

Chapter 5 described the development of a dabber probe, which comprised a delay line permanently coupled to a transducer for making low frequency dry coupled, spot measurements. The delay line was formed from a low attenuation rubber which gave good acoustic coupling when pressed dry onto a joint. It was identified in chapter 3 that the time window from which the mode 1 resonance is processed should be as free from unwanted reflections and transducer resonances as possible. Since beam spread is significant at the low frequencies required for the test (less than 600kHz), side wall reflections from a 10mm diameter delay line (surrounded by air) were found to be large, and returned to the transducer during this time window. These side wall reflections were successfully reduced to a low level by bonding highly attenuative rubber to the side walls of the low attenuation rubber which formed the delay line. Contact tip design was found to be important both to achieve sufficient contact pressure for good acoustic coupling, and to avoid reflections from any uncoupled part around the contact tip; it was found that any uncoupled regions should be made parallel to the transducer face. The signals received from a joint using a dabber probe were found to be comparable to those made in an immersion tank and it was therefore concluded that the dabber could be used successfully to test real automotive structures.

The dabber probe was used, in chapter 6, in conjunction with the mode 1 technique to make a large number of measurements on industrially prepared joints and real automotive structures. Partial disbonds were introduced into the industrially prepared joints, and a 100% success rate was achieved in detecting these and full disbonds. The joint was determined to be disbonded where there was no resonance peak above a pre-

set amplitude threshold. The bondline thicknesses, which could be determined from mode 1 frequency measurements, were compared with thickness measurements made using a micrometer. The mean difference and standard deviation between the measurements was found to be within 0.05mm, or 17% of the mean adhesive thickness, which was considered to be within the bounds of experimental error. This demonstrates the success of the technique for testing automotive joints with bondlines of 0.1-0.4mm. This therefore meets the primary objective for testing the structural joints specified by the automotive manufacturer.

The wider bondline thickness specification (0.2-3.0mm) has mode 1 frequencies extending well below the frequency range of the 500kHz transducer used for the tests in chapter 6. The typically poor performance of low frequency transducers, coupled with a requirement for a small physical size (to maximise accessability), precluded the use of any commercially available devices. Chapter 7 described the development of a non-resonant transducer which was shown to be able to meet the requirements over a large part of the required frequency range. The device comprised unbacked cubic 2mm PZT elements bonded to a thin attenuative rubber membrane. The first mode of the elements which is excited occurs at about 600kHz, and the device, being non-resonant, operates below this frequency. The device has a very low response at low frequency, which increases quickly with frequency approaching resonance. Excitation with a 5 cycle tone burst with centre frequencies in the range 180-350kHz was found effective in providing sufficient signal to excite resonances in joints with bondlines in the range 0.2-1.8mm, corresponding to 190-490kHz. This significantly extends the range of joints which could be tested with the transducer used in chapter 6. Operation down to 150kHz, required for bondlines up to 3.0mm, was not possible with the 2mm cubes and existing hardware, although it was achieved with 3mm cubes at the expense of reducing the upper limit of the frequency range.

8.2. Evaluation

The work in this thesis has focused on three main areas of novel work, and resolved many issues which have precluded the use of existing disbond detection techniques in the automotive industry:

- an ultrasonic technique for disbond detection on automotive joints.

- a dry coupled transduction system for low frequency spot measurements, using a conventional transducer, for the 0.1-0.4mm bondline specified for structural aluminium joints.
- low frequency transduction to allow mode 1 testing on joints with a bondline extending to 3.0mm.

The main focus has been on developing a general purpose, robust technique to the point where it is ready for implementation on the automotive production line.

Adherend Thickness

There is a large number of combinations of adherend thicknesses which can be found on a body shell, and each will lead to a different range of mode 1 frequencies for a specified bondline thickness range. The 2.0mm aluminium adherend used throughout the bulk of this work is a thickness commonly found, but even for other likely adherend thicknesses the mode 1 frequency ranges for bonded and partially bonded joints are still separate in frequency, and can be detected with the 500kHz transducer. For example, 1.5mm adherends have a mode 1 frequency range of 446-743kHz, and for 3mm adherends it is 294-430kHz. Hence, although in some cases a transducer with a different centre frequency may be required, the dabber probe can be used on a wide range of joints.

Adhesive Thickness

The mode 1 technique developed in this thesis is only suitable where the bounds of adhesive thickness are known. In critical applications, this will be relatively well controlled, since a thick adhesive layer has a lower strength; the use of rivets in structural joints helps to control the maximum thickness. Since the adhesive is viscous when applied, it is extremely unlikely that the bondline thickness will fall below 0.1mm away from the rivets. However, the maximum adhesive thicknesses encountered when testing the industrially prepared joints was 0.52mm. This serves to illustrate that if the specified bondline thickness range cannot be maintained, a conservative estimate of bondline thickness range should be used, if acceptable, to define the frequency ranges to ensure maximum reliability of the technique. A bondline above a certain thickness can then be rejected.

In order to enable spot measurements to me made, there must be no overlap in mode 1 frequency ranges for bonded and partially bonded joints. For 2mm adherends, with a minimum bondline of 0.1mm, a maximum bondline thickness of 1.0mm can be used before any overlap is encountered. Where the bondline thickness range is wide so that this overlap exists, a spot measurement cannot be made reliably to determine the bond condition. This is one of the main limitations of the technique. Since this has not been the case for the main focus of the work, the suggestions made to overcome this limitation, namely making an additional measurement and scanning the joint, have not been validated experimentally. This is one area which would require further work before the technique could be used on joints of wide ranging bondline thickness.

Dabber Probe

The successful development of a dry coupled probe for making low frequency measurements is clear from the results in chapter 5. This could be extended further to incorporate a non-resonant transducer, for making low frequency measurements, and represents another possible area for further work.

Non Resonant Transducer

A low frequency, wide band transducer (150-450kHz) with a small physical size was required to test a wider range of bondline thicknesses. The non-resonant design developed in chapter 7 did meet a large part of the design requirements. Excitation with low frequency tone bursts enabled the mode 1 resonance of a wide range of joints to be detected. Insufficient excitation voltage severely limited the performance below 200kHz. With further work, it should be possible to drive the device down to 150kHz. An investigation into the response of the device using a chirp, possibly of varying amplitude, to give a flat output frequency response would be another avenue for further work.

8.3. Further work

Several area for further work were identified to compliment the work presented in this thesis. These are discussed in this section.

In order to allow the technique to be extended to allow fast scanning of joints, it could be used in conjuction with a dry coupled wheel probe [105, 130]. The probe could then be rolled along the joints, being driven either by hand or robotically. Integration of the signal processing algorithm into a general purpose instrument (for example, a Desktop

Universal Instrument - NDT Solutions Ltd.) could be carried out to provide turn-key instrumentation providing the factory operator with a simple pass-fail output. Fitting the wheel probe with a position encoder would enable the bond condition of individual vehicles to be mapped out, providing important quality control data for the automotive manufacturers. The envisaged industrial set-up is shown schematically in figure 8·1.

With the scanning capability, it would also allow testing of the proposed scheme to identify the bond condition of joints where there is such a range of adhesive thickness that an overlap between the bonded and partially bonded frequency ranges occurs; a change in bond condition could be identified by a step change in mode 1 frequency.

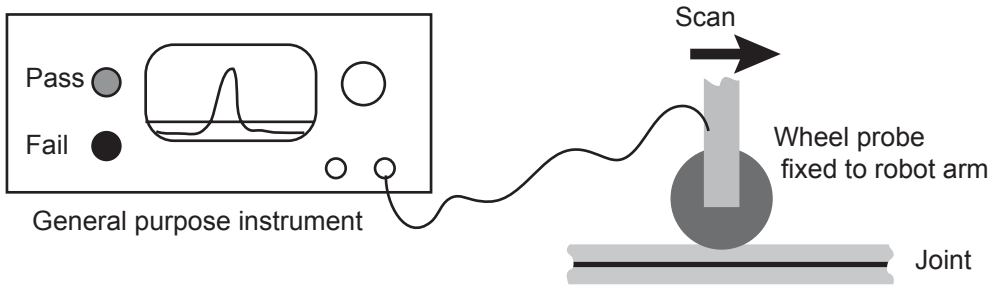

Figure 8·1 Schematic diagram of envisaged testing set-up.

For a wide range of bondlines to be tested, the wheel probe could be modified to accommodate the novel wideband transducer developed in chapter 7. Further work to maximise the output frequency range of the non-resonant transducer could also be carried out; the excitation signal could be tailored, by using a chirp or varying amplitude, for example, to compensate for the low amplitude response at low frequency

8.4. Summary of main contributions

This work has made contributions both in the field of NDT and to industry. It has been demonstrated in this thesis that, for the first time, mode 1 can be used to reliably identify the bond condition of joints where the adhesive thickness is unknown, using a transducer which is dry coupled to the joint.

In the development of this technique, a thorough assessment of mode 1 suitability was carried out which led to a novel testing protocol based on the frequency and amplitude of the mode 1 resonance of a joint. Investigation into the effects on the mode 1 resonance where bondlines varied in width and thickness have established that where there is a step change in mode 1 frequency, the resonance of both parts is independent

(within the limits of the range of systems investigated); where the adhesive layer thickness varies, the mode 1 frequency is given by the mean thickness of the region under test. Of significant importance to industry, this technique has been shown to work reliably on real automotive joints with bondlines of 0.1-0.4mm. It is now ready for implementation and evaluation on the production line.

The development of a dry coupled probe for use at low frequency was made possible by the novel addition of attenuative material to the side walls of a low loss material to reduce side wall reflections. This novel approach has potential applications in dry coupled testing, particularly low frequency, requiring a delay line where the time or frequency domain analysis is hampered by reflections in the delay line. For industrial testing, the dabber probe enabled the mode 1 measurements to be successfully made in the factory, demonstrating the viability of the technique.

Finally, a novel non-resonant immersion transducer has been produced which is able to operate at low frequency, over a wide frequency range and can be packaged in a small casing. This low frequency, wide band transducer may find numerous applications in NDT and is particularly attractive where a small physical size, or the absence of ringing in the operating frequency range is important. This device has enabled joints with bondlines up to 3mm to be tested successfully.

Appendix A

Material property measurements

A.1. Attenuation

The normalised amplitude spectrum method [131] used to determine the compression wave attenuation of the XD4600 epoxy adhesive (Ciba-Geigy Ltd.), is described briefly in this section. Several sheets of adhesive were produced to various thicknesses. They were tested in an immersion tank with the transducer accurately aligned normal to the surface to avoid generation of shear waves by mode conversion, and excited by a pulse. In order to obtain attenuation data over a wide range of frequencies, transducers with different centre frequencies from 1MHz to 5MHz were used. A complete set of decaying reflections from the adhesive sample was captured and transformed to the frequency domain producing an amplitude spectrum [132]. The resulting response contained minima which occurred as a result of interaction between the front and back face reflections in the joint which are out-of-phase. In order to obtain the normalised amplitude spectrum [131], the amplitude spectrum response was divided by the frequency domain response of the front face reflection from the joint. Where the frequency was not high enough to resolve front and back face reflections, a front face reflection was taken from a bulk sample of the material instead. This process is illustrated in figure A·1.

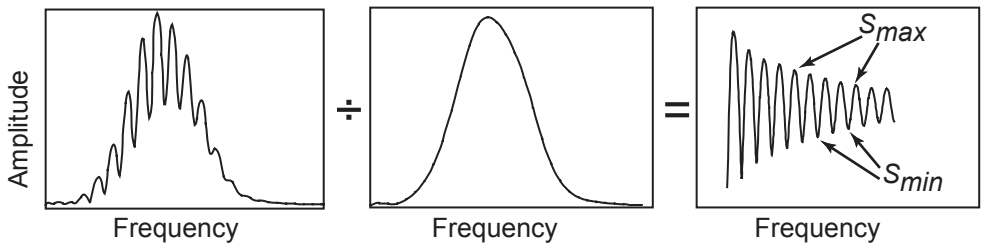

Figure A·1 Obtaining the normalised amplitude spectrum

The attenuation at a particular frequency, α (Np/m), can be determined from the normalised amplitude spectrum by the expression [131]:

$$\alpha = \frac{1}{2t}\ln\left(\frac{S_{max}-1}{1-R_{ca}{}^{2}S_{max}}\right) \qquad (A\cdot1)$$

where S_{max} is the amplitude of maxima in the normalised amplitude spectrum, and t is the sample thickness. The reflection coefficient of the adhesive, R_{ca} is given by:

$$R_{ca} = -\frac{F}{F_0} \qquad (A{\cdot}2)$$

where F is the front face reflection amplitude from the adhesive, and F_0 is the amplitude of a reflection from a perfect reflector (e.g. water-air interface). Attenuation was calculated at the frequencies of the maxima in the responses provided by the different transducers. Using this method to determine the attenuation, several attenuation measurements could be made across the frequency range of each transducer. Figure A·2 shows the variation of attenuation of the XD4600 adhesive with frequency.

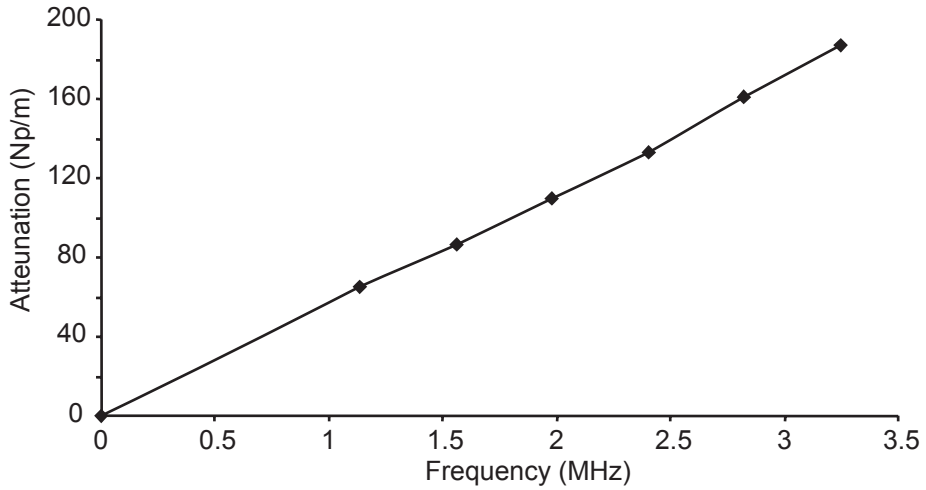

Figure A·2 Variation of attenuation with frequency in XD4600 adhesive.

The results show a linear variation with frequency. Consequently, a constant value of 0.145Nepers per wavelength has been used. This is equivalent to 0.51dB/mm/MHz.

A.2. Longitudinal velocity

The longitudinal phase velocity can also be determined either using the amplitude spectrum method or the normalised amplitude spectrum used to calculate the attenuation values. Using this method [132], the frequency difference between the minima in the amplitude spectrum (S_{min} in figure A·1), Δf, is related to the phase velocity, V_{ph} by:

$$V_{ph} = 2t\Delta f \qquad (A{\cdot}3)$$

The phase velocity was calculated over a frequency range of 1-3.5MHz. The results show a constant velocity of 2460m/s across this band, and it is therefore assumed to be constant at low frequency.

References

1. **H.J. Cornille (1993)** *A high volume aluminium auto body structure: the benefits and challenges,* International body engineering conference IBEC, Detroit, MI, pp. 5-21.

2. **T.A. Barnes and I.R. Pashby (2000)** *Joining techniques for aluminium spaceframes used in automobiles. Part I - solid and liquid phase welding,* Journal of Materials Processing Technology, vol. 99, no. 11, pp. 62-71.

3. **Y. Komatsu (1991)** *Application of all aluminium body for Honda NSX,* SAE technical reports, no. 910548910548, pp. 1-11.

4. **C. Emmelmann (1997)** *Robotic laser welding in the automotive industry,* Welding and Metal Fabrication, vol. 65, no. 33, pp. 7-8.

5. **I.N. Moody, P.A. Fay and G.D. Suthurst (1986)** *Can adhesives meet the challenge of vehicle bodyshell construction,* in Adhesion 11, edited by K.W. Allen, Elsevier Applied Science.

6. **E. Lawley (1990)** *The automotive challenge of the 1990s,* International Journal of Adhesion and Adhesives, July, pp. 221-224.

7. **P.A. Fay (1988)** *Adhesives for automotive construction - the increasing structural role of adhesives in mass produced steel bodyshells,* The Plastics and Rubber Institute Adhesives and Automotive Groups, Coventry.

8. **K.J. Schroeder (1996)** *Structural adhesives for aluminium vehicles,* Society of Automotive Engineers Technical Reports, no. 960166960166, pp. 55-62.

9. **A.J. Kinloch (1983)** *Durability of Structural Adhesives,* Applied Science Publishers.

10. **R.J. Davies and A.J. Kinloch (1989)** *The surface characterisation and adhesive bonding of aluminium,* in Adhesion 13, edited by K.W. Allen, Elsevier, London, vol. 13.

11. **M.J. Wheeler (1987)** *Aluminium structured vehicle technology - a comprehensive approach to vehicle design and manufacturing in aluminium,* SAE technical reports, no. 870146870146, pp. 1-11.

12. **B. Davies, S. Harris *et al.* (1996)** *Application experience of a robotic cell for automated adhesive dispensing,* Mathematics and Computers in Simulation, vol. 41, pp. 419-427.

13. **T.A. Barnes and I.R. Pashby (2000)** *Joining techniques for aluminium spaceframes used in automobiles. Part II - adhesive bonding and mechanical fasteners,* Journal of Materials Processing Technology, vol. 99, no. 11, pp. 72-79.

14. **J.R. Coleman (1988)** *Adhesives in automaking,* Assembly Engineering, vol. 3, pp. 22-28.

15. **R.D. Adams and P. Cawley (1988)** *A review of defect types and nondestructive testing techniques for composites and bonded joints,* NDT International, vol. 21, no. 44, pp. 208-221.

16. **P.B. Nagy (1991)** *Ultrasonic detection of kissing bonds at adhesive interfaces,* Journal of Adhesion Science Technology, vol. 5, no. 88, pp. 619-630.

17. **C.J. Brotherhood, B.W. Drinkwater and F.J. Guild (2000)** *The effect of compressive loading on the ultrasonic detectability of kissing bonds in adhesive joints,* Review of progress in quantitative NDE, edited by D.O. Thompson and D.E. Chimenti, American Institute of Physics, New York, vol. 20B, pp. 1111-1118.

18. **A. Higgins (2000)** *Adhesive bonding of aircraft structures,* International Journal of Adhesion & Adhesives, vol. 20, pp. 367-376.

19. **R.J. Lord (1985)** *In-Service Non-Destructive Inspection of Fighter and Attack Aircraft,* Materials Evaluation, vol. 43, pp. 733-739.

20. **D. Hagemaier and R. Fassberder (1978)** *Non-destructive testing of adhesive bonded structure,* Sampe Quarterly, July, pp. 36-58.

21. **T. Vogt, M.J.S. Lowe and P. Cawley (2001)** *Cure monitoring using ultrasonic guided waves in wires,* Review of Progress in Quantitative NDE, edited by D.O. Thompson and D.E. Chimenti, Plenum Press, New York, vol. 20, pp. 1642-1649.

22. **G. Light and H. Kwun (1989)** *Non-destructive evaluation of adhesive bond quality,* Report from Southwest Research Institute, San Antonio.

23. **C.C.H. Guyott, P. Cawley and R.D. Adams (1986)** *The non-destructive testing of adhesively bonded structures : a review,* Journal of Adhesion, vol. 20, pp. 129-159.

24. **I.J. Munns and G.A. Georgiou (1995)** *Non-destructive testing methods for adhesively bonded joint inspection - a review,* INSIGHT, vol. 37, no. 1212, pp. 941-952.

25. **R.D. Adams and B.W. Drinkwater (1999)** *Non-destructive testing of adhesively-bonded joints,* NDT & E International, vol. 30, no. 22, pp. 93-98.

26. **C.C.H. Guyott (1986)** *The non-destructive testing of adhesively bonded structures,* PhD Thesis, Department of Mechanical Engineering, Imperial College, London.

27. **Y. Bar-Cohen, A.K. Mal and C.C. Yin (1989)** *Ultrasonic evaluation of adhesive bonding,* Journal of Adhesion, vol. 29, pp. 237-274.

28. **E. Segal and J.L. Rose (1980)** *Non-destructive testing techniques for adhesive bonded joints,* in Research Techniques in NDT, edited by R.J. Sharpe, Academic Press, London, vol. 4, pp. 275-316.

29. **D.E.W. Stone (1986)** *Non-destructive methods of characterising the strength of adhesive-bonded joints - a review,* Report from Royal Aircraft Establishment, Farnborough, no. 86058.

30. **A.O.K. Nieminen and J.L. Koenig (1991)** *Macroscopic and modern microscopic NDE methods for adhesive-bonded structures,* International Journal of Adhesion and Adhesives, vol. 11, no. 11, pp. 5-10.

31. **G.J. Curtis (1982)** *Non-destructive testing of adhesively bonded structures with acoustic methods,* in Ultrasonic Testing, edited by J. Szilard, John Wiley & Sons Ltd., pp. 495-554.

32. **P. Cawley (1990)** *Low frequency NDT techniques for the detection of disbonds and delaminations,* British Journal of Nondestructive Testing, vol. 32, no. 99, pp. 454-461.

33. **P. Cawley and R. Adams (1988)** *The mechanics of the coin-tap method of non-destructive testing,* Journal of Sound and Vibration, vol. 122, no. 22, pp. 299-316.

34. **P. Cawley (1987)** *The sensitivity of the mechanical impedance method of non-destructive testing,* NDT International, vol. 20, no. 44, pp. 209-215.

35. **P. Cawley (1990)** *The detection of delaminations using flexural waves,* NDT International, vol. 23, pp. 207-213.

36. **A.P.M. Hurden (1982)** *An instrument for vibration mode analysis using electronic speckle pattern interferometry,* NDT International, June, pp. 143-148.

37. **P. Cawley (1994)** *The rapid non-destructive inspection of large composite structures,* Composites, vol. 25, pp. 351-357.

38. **J.W. Newman (1991)** *Shearographic inspection of aircraft structure,* Materials Evaluation, vol. 49, pp. 1106-1109.

39. **D. Rosenthal and J. Trolinger (1995)** *Holographic nondestructive testing,* Materials Evaluation, December, pp. 1353-1355.

40. **S.M. Shepard (1997)** *Introduction to active thermography for non-destructive evaluation,* Anti-corrosion Methods and Materials, vol. 44, no. 44, pp. 236-239.

41. **X. Han, L.D. Favro and R.L. Thomas (1998)** *Thermal wave NDI of disbonds and corrosion in aircraft,* 2nd Joint NASA/FAA/DoD Conference on Aging Aircraft, Virginia.

42. **D. Hopkins, D. Turler *et al.* (2000)** *On-line nondestructive inspection techniques for lightwieght automotive structures,* Society of Automotive Engineers Technical Reports, no. 2000-01-15602000-01-1560.

43. **J. Temple (1992)** *Inspection of adhesive joints : a review,* Report from Theoretical Studies Department Harwell Laboratory, Harwell, UK.

44. **L.F. Gladden and P. Alexander (1996)** *Applications of nuclear magnetic resonance imaging in process engineering,* Measurement Science Technology, vol. 7, pp. 423-435.

45. **B. Kenyon, R. Kleinberg *et al.* (1995)** *Nuclear magnetic resonance imaging - technology for the 21st century,* Oilfield Review, Autumn, pp. 19-33.

46. **W.M. Banks, D. Hayward *et al.* (1995)** *High frequency dielectric investigations of adhesive bonded structures,* Insight, vol. 37, no. 1212, pp. 964-968.

47. **D. Hayward, S. Affrossman and R.A. Pethrick (1991)** *The application of dielectric relaxation measurements to the non-destructive examination of adhesively bonded joint structures,* Non-destructive Testing Evaluation, vol. 6, pp. 45-63.

48. **S.B. Joshi, D. Hayward and P. Wilford (1992)** *A method for the non-destructive investigation of adhesively bonded structures,* European Journal of NDT, vol. 1, no. 44, pp. 190-199.

49. **F.I. Mopsik, S.S. Chang and D.L. Hunston (1989)** *Dielectric measurements for cure monitoring,* Materials Evaluation, vol. 47, pp. 448-453.

50. **J. Krautkramer and H. Krautkramer (1983)** *Ultrasonic Testing of Materials,* Springer-Verlag, Berlin.

51. **R. Halmshaw (1987)** *Non-Destructive Testing,* ed. P. Hancock, Edward Arnold, London.

52. **L.M. Brekhovskikh (1980)** *Waves in layered media,* Academic Press, New York.

53. **R.E. Challis, R.J. Freemantle *et al.* (1995)** *Ultrasonic compression wave NDT of adhered metal lap joints of uncertain dimensions,* Insight, vol. 37, no. 1212, pp. 954-963.

54. **R.J. Freemantle (1995)** *Ultrasonic compression wave evaluation of adhered metal sheets and thin sheet materials,* PhD Thesis, Department of Physics, Keele University, Keele.

55. **L. Goglio and M. Rossetto (1999)** *Ultrasonic testing of adhesive bonds of thin metal sheets,* NDT & E International, vol. 32, pp. 323-331.

56. **E.P. Papadakis (1978)** *Ultrasonic impulse induced resonance utilizing damping for adhesive disbond detection,* Materials Evaluation, February, pp. 37-40.

57. **R.J. Freemantle and R.E. Challis (1997)** *Ultrasonic compression wave NDT of adhesively bonded automotive structures,* UTonline Application Workshop, vol. 2, no. 55, www.ndt.net/article/wsho0597/freem/freem.htm.

58. **P.B. Nagy (1992)** *Ultrasonic classification of imperfect interfaces,* Journal of Non-destructive Evaluation, vol. 11, pp. 127-139.

59. **K. Vine, P. Cawley and A.J. Kinloch (1999)** *Degradation mechanisms in adhesive joints and the implications for NDE*, Review of Progress in Quantitative NDE, edited by D.O. Thompson and D.E. Chmenti, Plenum Press, New York, pp. 1301-1308.

60. **S.I. Rokhlin and D. Marom (1986)** *Study of adhesive bonds using low-frequency obliquely incident ultrasonic waves*, Journal of the Acoustical Society of America, vol. 80, no. 22, pp. 585-590.

61. **W. Wang and S.I. Rokhlin (1991)** *Evaluation of interfacial properties in adhesive joints of aluminium using angle-beam ultrasonic spectroscopy*, Journal of Adhesion Science Technology, vol. 5, no. 88, pp. 647-666.

62. **S.I. Rokhlin, W. Wang and Y.J. Wang (1990)** *Ultrasonic evaluation of interphasial properties in adhesive joints*, Review of Progress in Quantitative NDE, edited by D.O. Thompson and D.E. Chimenti, Plenum Press, New York, pp. 1231-1238.

63. **A. Pilarski, Rose, J.L. (1988)** *Ultrasonic oblique incidence for improved sensitivity in interface weakness determination*, NDT International, vol. 21, pp. 241-246.

64. **J.L. Rose, J. Dale and T.D.K. Ngoc (1990)** *Ultrasonic oblique incidence experiments for interface weakness*, British Journal of Nondestructive Testing, vol. 32, no. 99, pp. 449-452.

65. **P. Cawley (1992)** *Ultrasonic measurements of the quantitative NDE of adhesive joints - potential and challenges*, IEEE Ultrasonics Symposium, pp. 767-772.

66. **T.P. Pialucha (1992)** *The reflection coefficient from interface layers in NDT of adhesive joints*, PhD Thesis, Department of Mechanical Engineering, Imperial College, London.

67. **R.J. Schliekelmann (1972)** *Non destructive testing of bonded metal-to-metal joints 2*, Non-destructive Testing, vol. 5, June, pp. 144-153.

68. **D. Smith and C.V. Cagle (1966)** *Ultrasonic testing of adhesive bonds using the Fokker Bond Tester*, Materials Evaluation, vol. 24, pp. 362-370.

69. **R.J. Schliekelmann (1979)** *Non-Destructive Testing of Adhesive Bonded Joints*, Bonded Joints and Preparation For Bonding, AGARD Lecture Series, vol. 102.

70. **C.C.H. Guyott, P. Cawley and R.D. Adams (1987)** *Use of the Fokker Bond tester on joints with varying adhesive thickness,* Proceedings of the Institute of Mechanical Engineers, vol. 201, no. B1B1, pp. 41-49.

71. **C. Guyott, P. Cawley and R. Adams (1986)** *Vibration characteristics of the MK 2 Fokker Bond tester probe,* Ultrasonics, vol. 24, pp. 318-324.

72. **C.C.H. Guyott and P. Cawley (1988)** *The ultrasonic vibration characteristics of adhesive joints,* Journal of the Acoustical Society of America, vol. 83, pp. 632-640.

73. **D.A. Hutchins, L.F. Bresse and D.F. Billson (1992)** *Resonance studies of bonded aluminium joints,* Non-destructive Testing and Evaluation, vol. 10, pp. 149-165.

74. **V.L. Weise (1998)** *Ultrasonic techniques for adhesive bond examination on production automotive structures,* PhD Thesis, Department of Physics, Keele University, Keele.

75. **G.A. Alers, P.L. Flynn and M.J. Buckley (1977)** *Ultrasonic techniques for measuring the strength of adhesive bonds,* Materials Evaluation, vol. 35, no. 44, pp. 77-84.

76. **P.L. Flynn (1979)** *Cohesive bond strength prediction for adhesive joints,* Journal of Testing and Evaluation, vol. 7, no. 33, pp. 168-171.

77. **P. Cawley and M.J. Hodson (1988)** *The NDT of adhesive joints using ultrasonic spectroscopy,* Review of Scientific Instruments, La Jolla, California, edited by D.O. Thompson and D.E. Chimenti, Plenum Press, New York, pp. 1377-1384.

78. **C.C.H. Guyott and P. Cawley (1988)** *Evaluation of the cohesive properties of adhesive joints using ultrasonic spectroscopy,* NDT International, vol. 21, pp. 233-240.

79. **P.N. Dewen and P. Cawley (1992)** *The practical application of ultrasonic spectroscopy for the measurement of the cohesive properties of adhesive joints,* NDT & E International, vol. 25, pp. 65-75.

80. **A.I. Lavrentyev and S.I. Rokhlin (1997)** *Determination of elastic moduli, density, attenuation, and thickness of a layer using ultrasonic spectroscopy at*

two angles, Journal of the Acoustical Society of America, vol. 102, no. 66, pp. 3467-3477.

81. **V.K. Kinra and V.R. Iyer (1995)** *Ultrasonic measurement of the thickness, phase velocity, density or attenuation of a thin viscoelastic plate Part 1 The forward problem,* Ultrasonics, vol. 33, no. 22, pp. 95-109.

82. **V.K. Kinra and V.R. Iyer (1995)** *Ultrasonic measurement of the thickness, phase velocity, density or attenuation of a thin - viscoelastic plate Part 2 The inverse problem,* Ultrasonics, vol. 33, no. 22, pp. 111-122.

83. **R. Thompson and D. Thompson (1991)** *Past experiences in the development of tests for adhesive bond strength,* Journal of Adhesion Science Technology, vol. 5, no. 88, pp. 583-599.

84. **A.I. Lavrentyev and S.I. Rokhlin (1994)** *Ultrasonic evaluation of environmental degradation of adhesive joints,* Review of Progress in Quantitative NDE, edited by D.O. Thompson and D.E. Chimenti, Plenum Press, New York, pp. 1539-1546.

85. **A.I. Lavrentyev and S.I. Rokhlin (1994)** *Models for ultrasonic characterisation of environmental interfacial degradation in adhesive joints,* Review of Progress in Quantitative NDE, edited by D.O. Thompson and D.E. Chimenti, Plenum Press, New York, pp. 1531-1538.

86. **A.I. Lavrentyev and S.I. Rokhlin (1998)** *Ultrasonic Spectroscopy Of Imperfect Contact Interfaces Between A Layer And Two Solids,* Acoustical Society of America, vol. 103, no. 22, pp. 657-664.

87. **M.J.S. Lowe, R.E. Challis and C.W. Chan (2000)** *The transmission of Lamb waves across adhesively bonded lap joints,* Journal of the Acoustical Society of America, vol. 107, no. 33, pp. 1333-1345.

88. **R. Dalton (2000)** *The propagation of Lamb waves through metallic aircraft fuselage structure,* PhD Thesis, Department of Mechanical Engineering, Imperial College, London.

89. **P.N. Dewen (1992)** *The non-destructive evaluation of the cohesive properties of adhesively bonded joints,* PhD Thesis, Department of Mechanical Engineering, Imperial College, London.

90. **R.E. Challis, U. Bork and P.C.D. Todd (1996)** *Ultrasonic NDE of adhered T-joints using Lamb waves and intelligent signal processing,* Ultrasonics, vol. 34, pp. 455-459.

91. **G.W.C. Kaye and T.H. Laby (1995)** *Tables of physical and chemical constants*. 16th ed, Longman, Harlow.

92. **H. Kolsky (1963)** *Stress waves in solids*, Dover Publications, New York.

93. **E.A. Lloyd (1974)** *Non-destructive testing of bonded joints: a case for testing laminated structures by wide-band ultrasound,* Non-destructive testing, December, pp. 331-334.

94. **B. Pavlakovic and M. Lowe (1999)** *Disperse software*, v.2.01.

95. **R.E.D. Bishop and D.C. Johnson (1960)** *The mechanics of vibration*, University Press, Cambridge.

96. **T. Pialucha and M. Lowe (1992)** *DGLOBAL software*, v.2.0.

97. **W.T. Thomson (1950)** *Transmission of elastic waves through a stratified solid medium,* Journal of Applied Physics, vol. 21, pp. 89-93.

98. **Y. Murakami, B.T. Khuri-Yakub *et al.* (1978)** *An application of Wiener filtering to nondestructive evaluation,* Applied Physics Letters, vol. 33, no. 88, pp. 685-687.

99. **G.S. Kino (1987)** *Acoustic waves : devices, imaging and analogue signal processing*, Prentice-Hall Inc., New Jersey.

100. **R.B. Randall (1987)** *Frequency Analysis*, Bruel and Kjaer.

101. **D. Hitchings (2000)** *FINEL software*, v.4.

102. **B.W. Drinkwater (1995)** *The use of dry coupling in ultrasonic nondestructive testing,* PhD Thesis, Department of Mechanical Engineering, Imperial College, London.

103. **Ultran (1999)** *Modern ultrasonic transducers product catalogue,* Report from Second Wave Systems Corporation, Boalsburg, PA, USA.

104. **D.R. Billson and D.A. Hutchins (1993)** *Development of novel piezoelectric ultrasonic transducers for couplant-free ultrasonic testing*, British Journal of Nondestructive Testing, vol. 35, pp. 705-708.

105. **B. Drinkwater and P. Cawley (1997)** *Practical application of solid coupled ultrasonic transducers,* Materials Evaluation, vol. 55, no. 33, pp. 401-406.

106. **K.L. Johnson (1985)** *Contact Mechanics,* Cambridge University Press, Cambridge.

107. **Swanson (2001)** *Ansys software,* v.6.

108. **M. Redwood (1961)** *Transient performance of a piezoelectric transducer,* Journal of the Acoustical Society of America, vol. 33, pp. 527-563.

109. **G. Hayward, C.J. Macleod and T.S. Durrani (1984)** *A systems model of the thickness mode piezoelectric transducer,* Journal of the Acoustical Society of America, vol. 76, no. 22, pp. 369-382.

110. **M.G. Silk (1984)** *Ultrasonic Transducers for Nondestructive Testing,* Adam Hilger Ltd., Bristol.

111. **N.Q. Guo and P. Cawley (1991)** *Transient response of piezoelectric discs to applied voltage pulses,* Ultrasonics, vol. 29, pp. 208-217.

112. **N.Q. Guo and P. Cawley (1992)** *Measurement and predication of the frequency spectrum of piezoelectric discs by modal analysis,* Journal of the Acoustical Society of America, vol. 92, pp. 3379-3388.

113. **Ferroperm (2001)** *Piezo-electric product literature,* Report from Ferroperm Piezoceramics, Hejreskovvej, Denmark.

114. **D.A. Hutchins and G. Hayward (1990)** *Radiated fields of ultrasonic transducers,* Physical Acoustics, vol. XIX, pp. 1-80.

115. **B.A. Bainton and M. Silk (1980)** *Some factors which affect the performance of ultrasonic transducers,* British Journal of NDT, January, pp. 15-20.

116. **K.F. Bainton, M.J. Hillier and M.G. Silk (1986)** *An easily constructed, broad bandwidth ultrasonic probe for research purposes,* Report from United Kingdom Atomic Energy Authority, Harwell, no. AERE-R-9769.

117. **Q.X. Chen and P. Payne (1995)** *Industrial applications of piezoelectric polymer transducers,* Measurement Science Technology, vol. 6, pp. 249-267.

118. **R. Brown (1990)** *Piezo Film: form and function,* Sensors and Actuators, vol. A21-A23, pp. 729-733.

119. **R.S.C. Monkhouse, P.D. Wilcox and P. Cawley (1997)** *Flexible interdigital PVDF transducers for the generation of Lamb waves in structures,* Ultrasonics, vol. 35, pp. 489-498.

120. **W.A. Smith (1989)** *The role of piezocomposites in ultrasonic transducers,* IEEE Ultrasonics Symposium, pp. 755-766.

121. **G. Hayward, A. Gachagan *et al.* (1992)** *Ceramic-epoxy composite transducers for non-contacting ultrasonic applications,* SPIE, vol. 1733, pp. 49-56.

122. **C. Dias, D.K. Das-Gupta *et al.* (1993)** *Polymer/ceramic composites for piezoelectric sensors,* Sensors and Actuators, vol. A37, no. 3838, pp. 343-347.

123. **G. Hayward and J. Hossack (1990)** *Unidimensional modelling of 1-3 composite transducers,* Journal of the Acoustical Society of America, vol. 88, no. 22, pp. 599-608.

124. **P. Reynolds, J. Hyslop and G. Hayward (1996)** *The influence of constructional parameters on the practical performance of 1-3 piezocomposite transducers,* IEEE Ultrasonics Symposium, pp. 967-970.

125. **A. Gachagan, J.T. Bennett and G. Hayward (1994)** *A Finite Element modelling approach into the influence of mechanical matching and damping in 1-3 piezocomposites,* IEEE Ultrasonics symposium, pp. 995-998.

126. **D.W. Schindel (1999)** *Air-coupled ultrasonic measurements of adhesively bonded multi-layer structures,* Ultrasonics, vol. 37, pp. 185-200.

127. **W. Manthey, N. Kroemer and V. Magori (1992)** *Ultrasonic transducers and transducer arrays for applications in air,* Measurement Science Technology, vol. 3, pp. 249-261.

128. **M. Greenspan (1987)** *The NBS conical transducer: analysis,* Journal of the Acoustical Society of America, vol. 81, no. 11, pp. 173-183.

129. **P.D. Wilcox, R.S.C. Monkhouse *et al.* (1998)** *Development of a computer model for an ultrasonic polymer film transducer system,* NDT & E International, vol. 31, no. 11, pp. 51-64.

130. **B. Drinkwater and P. Cawley (1995)** *An ultrasonic wheel probe alternative to liquid coupling,* Review of Progress in Quantitative NDE, edited by D.O. Thompson and D.E. Chimenti, pp. 983-989.

131. **N. Guo, M.K. Lim and T. Pialucha (1995)** *Measurement of attenuation using a normalised amplitude spectrum,* Journal of Non-destructive Evaluation, vol. 14, pp. 9-19.

132. **T. Pialucha, C.C.H. Guyott and P. Cawley (1989)** *Amplitude spectrum method for the measurement of phase velocity,* Ultrasonics, vol. 27, pp. 270-279.